

Development of Novel Methodologies to Characterize Polyolefins using Multi-dimensional High Temperature Two Dimensional Liquid Chromatography

Vom Fachbereich Chemie
der Technischen Universität Darmstadt

zur Erlangung des akademischen Grades eines

Doktor-Ingenieurs (Dr.-Ing.)

genehmigte
Dissertation

vorgelegt von

M. Tech. K N Prabhu

aus Tamil Nadu, Indien

Referent:	Prof. Dr. Matthias Rehahn
Korreferent:	Prof. Dr. Markus Busch
Tag der Einreichung:	08. April 2016
Tag der mündlichen Prüfung:	23. Mai 2016

Darmstadt 2016

D 17

Diese Arbeit wurde unter der Leitung von Herrn Prof. Dr. Matthias Rehahn und Dr. Robert Brüll am Bereich Kunststoffe des Fraunhofer LBF in der Zeit von Juli 2012 bis November 2015 durchgeführt.

Dieses Forschungsprojekt wurde von der Firma SABIC finanziert. Es war Teil der Zusammenarbeit zwischen der Gruppe Materialanalytik des Fraunhofer LBF in Darmstadt, Deutschland und der Abteilung „Technology and Innovation“ der Firma SABIC in Geleen, Niederlande.

This study is a result of the work carried out from July 2013 to November 2015 at Plastic Division, Fraunhofer LBF (previously DKI) under the supervision of Prof. Dr. Matthias Rehahn and Dr. Robert Brüll.

This research was funded by SABIC and formed part of a joint collaboration between the Material Analytics Group from *Fraunhofer LBF* and the Technology and Innovation, STC Geleen, SABIC, The Netherlands.

-Dedicate this to all my Teachers and Chromatographic researchers

-Dedicate this to Kannan, Neela, Siva, Sharmi and Vinay for all the love and encouragement

Acknowledgements

It is my pleasure to thank all the people who have contributed, complemented, and supported me during the course of this scientific work. I am privileged to pay my sincere thanks to my research supervisors Prof. Dr. Matthias Rehahn, Dr. Robert Brüll for giving me this unique opportunity to work with their group in Fraunhofer Institute, Darmstadt.

I wish to extend my sincere appreciation to Dr. Robert Brüll, Dr. Tibor Macko, Dr. Klaas Remerie, Dr. Jacques Tacx, Dr. Priya Garg, and Dr. Anton Ginzburg for providing this very interesting and challenging topic for my PhD and also for all their inputs throughout. I would like to express my gratitude to Dr. Linda Havermans, Dr. Mark Boerakker, Dr. Haika Hildebrandt, Dr. Frank Malz, and Dr. Desiree Seegers for always providing me with excellent guidance, which was instrumental to the success of this research. I gratefully acknowledge SABIC, T & I, Geleen, The Netherlands for funding this PhD, as well as for the interesting symposia. I am also thankful to SABIC and Fraunhofer LBF for the necessary freedom that I had during my present research work. I deeply thank Dr. Olivier Guise (SABIC, Bergen op Zoom, The Netherlands) who encouraged and supported me to work on my thesis when needed, during my working time at SABIC. I also would like to thank my colleagues at SABIC, Bergen op zoom, The Netherlands, Dr. Christian Wold, Dr. Elena Uliyanchenko, Dr. Sebastien Pierrat, Dr. Johannes Gunther, Dr. Rolf Koevoets, Dr. Chanjuan Liu, Dr. Lanti Yang, Dr. Vaidyanath Ramakrishnan, Dr. Rajan Eben Solomon, Dr. Thambi Joel, Frits, Omid, Stijn, Barry, Jos, Eric, Han, Ed, Bianca, Toob, Menno, Julia, Dolinda and Mirte for making me feel more comfortable and for all their fruitful discussion. My heartily thanks to my colleagues and friends Roberto, Alban, Danny, Mathilde, Mathilde tall, Mylène, Marie, Marion, Carole, Jessica, Thomas, Raul, Sylvia, Joanna, Rajan, Preeti, Gabi and Joel who made me feel home.

I would like to specially thank from by bottom of my heart to my scientific co-worker Dr. Tibor Macko for all his molar support, love, and concern and for being a fatherly person. I also thank him for teaching me from basics to an expert level knowledge on chromatography. Thanks Dr. Tibor Macko and Robert Brüll for teaching me certain things, which can't be learnt from books, but by experience.

I want to express my gratitude for all my colleagues from Fraunhofer LBF for the pleasant working atmosphere and the cooperativeness in everyday matters. I would like to thank Dr. Anton Ginzburg, Dr. Rajesh Chitta and Dr. Dibyaranjan Mekap and Dr. Jan Hendrik Arndt, who helped me in getting the basic knowledge of the instruments and the techniques. My special thanks to Jan Hendrik Arndt for helping me in all German translations. I would like to thank my friends Priya, Subin, Mahesh, Dib, Sampat, Hansika, Abhishek, Nilesh, Sandeep, Biswas and Tarini who made me feel home.

Most importantly, I am ever so grateful to my dearest Mom (Neela), Dad (Kannan), Brother (Siva), Sister-in-law (Sharmi), nephew (Vinay) and all my family members for their moral support, endless love, trust, and uncountable sacrifice and constant motivation during my study. Their motivational nature and enthusiasm in both good and difficult times will remain in my memory forever. I also thank each and every soul, who prayed for me to get succeeded in life. Without you all this is never feasible. Thanks!

Publications:

1. “Separation of bimodal high density polyethylene using multi-dimensional high temperature liquid chromatography”
K N Prabhu, R. Brüll, T. Macko, K. Remerie, J. Tacx, P. Garg, A. Ginzburg
Journal of Chromatography A, 1419 (2015) 67-80.
2. “Separation of polypropylene grafted maleic anhydride using multi-dimensional high temperature liquid chromatography”
K N Prabhu, T. Macko, R. Brüll, K. Remerie, J. Tacx, P. Garg, A. Ginzburg
Journal of Chromatography A, (2016), Article in press
3. “Studying the interaction of graphite and polyethylene at high temperature in solution using Raman spectroscopy”
K N Prabhu, A. Sanoria, D. Fischer, R. Brüll, K. Remerie, J. Tacx, P. Garg, A. Ginzburg
RCS analytical submitted.

Oral presentations

1. “Multi-dimensional liquid chromatography of bimodal high density polyethylene”
High Performance Liquid Phase Separations and Related Techniques (HPLC),
Amsterdam, The Netherlands, June 16th, **2013**.
2. “Improving resolution in High temperature Liquid Chromatography (HT-LC) of polyolefins”
4th International Conference on Polyolefin Characterization (ICPC), Valencia,
Spain, September 21st, **2014**.

Conference posters

1. “High temperature two dimensional liquid chromatography of linear low density polyethylene”
Chemelot International Polyolefins Symposium (CIPS), Maastricht, The Netherlands,
October 7th, **2012**
2. “Multi-dimensional liquid chromatography of bimodal high density polyethylene”
High Performance Liquid Phase Separations and Related Techniques (HPLC),
Amsterdam, The Netherlands, June 16th, **2013**.
3. “Improving resolution in High temperature Liquid Chromatography (HT-LC) of polyolefins”
4th International Conference on Polyolefin Characterization (ICPC), Valencia,
Spain, September 21st, **2014**.

Your time is limited, don't waste it living someone else's life.

– **Steve Jobs (1955-2011)**

Contents

Acknowledgements	3
Contents	6
1. Abbreviations	8
2. Summary in German	10
3. Introduction and Preface	11
4. Theoretical Considerations	12
4.1. Introduction to Polyolefins	12
4.2. Types of Polyolefins	12
4.2.1. Polyethylene (PE)	12
4.2.2. Polypropylene (PP)	13
4.3. Polyolefin Synthesis: Catalyst Driven Process	14
4.4. Development of Polyolefins Driven by Application Demand	22
4.4.1. HDPE for Pipe Applications	22
4.4.2. Functionalized Polyolefins	25
4.5. Polyolefin Processing	27
5. Characterization of Polyolefins	29
5.1. Fractionation Techniques Based on Crystallinity	30
5.1.1. Temperature Rising Elution Fractionation (TREF)	31
5.1.2. Crystallization Analysis Fractionation (CRYSTAF)	32
5.1.3. Crystallization Elution Fractionation (CEF)	33
5.2. High Performance Liquid Chromatography (HPLC)	34
5.2.1. Size Exclusion Chromatography (SEC)	36
5.2.2. Liquid Adsorption Chromatography (LAC)	37
5.2.3. Cross-Fractionation Techniques	42
5.3. Raman Spectroscopy	45
5.4. Nuclear Magnetic Resonance (NMR) Spectroscopy	45
5.4.1. NMR of Polyolefins	46
6. Experimental	48
6.1. Column Packings	48
6.2. Samples	48
6.3. Solvents	50
6.4. High Temperature Size Exclusion Chromatography	50
6.5. Analytical SEC (ASEC) – LC-Transform – FTIR Off-line	51
6.6. Steps for Preparative Fractionation of HT-SEC Coupled with ¹ H NMR Off-line (Off-flow HT-SEC→ ¹ H NMR)	51
6.7. Calculations to Collect Sufficient Amount of Sample for Off-flow HT-SEC→ ¹ H NMR	52
6.8. Crystallization Analysis Fractionation (CRYSTAF)	52
6.9. Preparative CRYSTAF	52
6.10. High Temperature High Performance Liquid Chromatography (HT-HPLC)	53
6.11. Preparative HT-HPLC→FTIR	54
6.12. High Temperature Two Dimensional Liquid Chromatography (HT 2D-LC)	54
6.13. Calculation of Resolution and Column Efficiency of HT-SEC	56
6.14. Raman Spectroscopy	57
6.15. NMR Spectroscopy	58
7. Results and Discussion	59
7.1. Development of Separation of Bimodal HDPE using HT 2D-LC→IR	59
7.1.1. Introduction	59

7.1.2.	CRYSTAF→IR and HT-SEC→IR of HDPE, LLDPE and BiHDPE	60
7.1.3.	HT-HPLC→ELSD of Polyethylene and Ethylene/1-Butene Copolymers.....	61
7.1.4.	HT-HPLC→ELSD of HDPE, LLDPE and BiHDPE	64
7.1.5.	HT-HPLC→ELSD of Oligomers in HDPE and BiHDPE	64
7.1.6.	Effect of Temperature on HT-HPLC Separation	68
7.1.7.	HT 2D-LC→ELSD of HDPE, LLDPE and BiHDPE	68
7.1.8.	Conclusion.....	78
7.2.	Preparative Fractionation of Bimodal HDPE using Off-flow HT-SEC→NMR	79
7.2.1.	Introduction	79
7.2.2.	Manual Fraction Collection from HT-SEC	80
7.2.3.	Portable Automatic Fraction Collector (PAFC)	81
7.2.4.	Steps for Preparative Fractionation of Off-flow HT-SEC→NMR	84
7.2.5.	Preparative Fractionation of BiHDPE using Off-flow HT-SEC→NMR.....	84
7.2.6.	¹ H NMR Analysis on all Fractions.....	86
7.2.7.	Conclusion.....	88
7.3.	Development of Separation of Functionalized Polyolefins using HT 2D-LC→IR.....	
7.3.1.	Introduction	88
7.3.2.	Determination of Grafting Content across the MMD using HT-SEC→IR.....	89
7.3.3.	Determination of Compositional Heterogeneity using CRYSTAF→FTIR	90
7.3.4.	HT-HPLC and HT-HPLC→FTIR on PP-g-MA	92
7.3.5.	HT 2D-LC→ELSD-IR of PP-g-MA	94
7.3.6.	Conclusion.....	97
7.4.	Investigating Interactions of Polyethylene with Graphite in the Presence of Solvent	
7.4.1.	Introduction	99
7.4.2.	Interaction Study between Graphite and Alkanes	100
7.4.3.	Effect of Chain Length and Branching in the Interaction with Graphite	103
7.4.4.	Interaction of PE with Graphite using Raman Spectroscopy	105
7.4.5.	Conclusion.....	108
8.	Summary and Conclusions.....	109
9.	Bibliography.....	112

1. Abbreviations

2D-LC	Two Dimensional Liquid Chromatography
HT 2D-LC	Two Dimensional High Temperature Liquid Chromatography
<i>a</i> -PP	Atactic Polypropylene
CCD	Chemical Composition Distribution
CEF	Crystallization Elution Fractionation
CRYSTAF	Crystallization Analysis Fractionation
ELSD	Evaporative Light Scattering Detector
FTIR	Fourier Transform Infrared
G-10min	Linear Gradient of 10 min
GC	Gas Chromatography
HDPE	High Density Polyethylene
HPLC	High Performance Liquid Chromatography
HT-HPLC	High Temperature High Performance Liquid Chromatography
HT-LAC	High Temperature Liquid Adsorption Chromatography
HT-LCCC	High Temperature Liquid Chromatography at Critical Conditions
HT-SEC	High Temperature Size Exclusion Chromatography
HT-SGIC	High Temperature Solvent Gradient Interactive Chromatography
HT-TGIC	High Temperature Thermal Gradient Interactive Chromatography
IR	Infrared Spectroscopy
<i>i</i> -PP	Isotactic Polypropylene
LCB	Long Chain Branch
LDPE	Low Density Polyethylene
LLDPE	Linear Low Density Polyethylene
MMD	Molar Mass Distribution
N	Number of Theoretical Plates
NMR	Nuclear Magnetic Resonance
ODCB	1,2-Dichlorobenzene
PE	Polyethylene
PGC	Porous Graphitized Carbon
PP	Polypropylene
PP- <i>g</i> -MA	Polypropylene Grafted Maleic Anhydride
PMMA	Poly Methyl Methacrylate
Prep.	Preparative

Abbreviations

PS	Polystyrene
R	Resolution
RI	Refractive Index
SCB	Short Chain Branch
SEC	Size Exclusion Chromatography
TCB	1,2,4-Trichlorobenzene
TG-NMR	Thermal Gradient Nuclear Magnetic Resonance
TREF	Temperature Rising Elution Fractionation

Symbols

ΔG	Gibbs free energy difference
ΔH	Change in interaction enthalpy
ΔS	Change in conformational entropy
\bar{D}	Dispersity
K_d	Distribution coefficient
M_n	Number average molar mass
M_w	Weight average molar mass
R	Universal gas constant
T	Absolute temperature
T_c	Crystallization temperature
T_{mp}	Peak melting temperature
V_1	Molar volume of the diluent
v_1	Volume fraction of the diluent
mol %	Mole percent
wt. %	Weight percent
χ_1	Flory Huggins thermodynamic interaction parameter

2. Summary in German

Die Entwicklungen im Bereich der übergangsmetallkatalysierten Olefinpolymerisation während der letzten 50 Jahre haben es ermöglicht Polyolefine bei deutlich verbesserter Kontrolle der Regio- und Stereoselektivität, der Verzweigungen (ihre Anzahl und Länge) und der Abfolge in der Monomere in die Polymerkette inkorporiert werden, zu synthetisieren. Damit einhergehend wurde wuchs der Bedarf nach umfassenden analytischen Methoden für die molekulare Charakterisierung. Die molekularen Heterogenitäten in Polyolefinen können zu einem Großteil auf Basis der Molmassenverteilung (*Molar Mass Distribution*, MMD), der Verteilung der chemischen Zusammensetzung (*Chemical Composition Distribution*, CCD) und der Verteilung der Stereoregularitäten (*Stereo-Regularity Distribution*, SRD) definiert werden. In jüngster Zeit hat die Hochtemperatur-Wechselwirkungschromatographie mit Lösungsmittelgradienten (*High Temperature Solvent Gradient Interaction Chromatography*, HT-SGIC) große Bedeutung zur Bestimmung der CCD von Polyolefinen gewonnen. Die Wechselbeziehung zwischen den Verteilungen in Hinblick auf die Zusammensetzung und die Molmasse kann durch die Kopplung von HT-HPLC und HT-SEC in der multidimensionalen Chromatographie (HT 2D-LC) untersucht werden. Das Ziel der in dieser Dissertation präsentierten Arbeiten war es verbesserte quantitative HT 2D-LC Methoden zur Trennung komplexer Polyolefine, die im Hinblick auf ihre Zusammensetzung wie auch die Molmasse breit verteilt sind, zu entwickeln. Die Forschungsergebnisse sind in vier Teile unterteilt: Zunächst wird eine prägnante Zusammenfassung des Stands der Technik und der Ergebnisse geliefert, dann werden die gezogenen Schlussfolgerungen für jeden der Teile einzeln zusammengefasst.

Im ersten Teil wurde eine Methode entwickelt, um bimodales Polyethylen hoher Dichte (BiHDPE) (unpolare Polyolefine) mittels HT-SGIC in seine Bestandteile, HDPE und LLDPE, zu trennen. Eine schrittweise Optimierung der chromatographischen Parameter der HT-HPLC, einschließlich der Gradientensteigung und der Temperatur, wurde unter Verwendung von Modellschubstanzen (Homo- und Copolymeren von Ethylen) durchgeführt. Dabei war es das Ziel den Einfluss der Molmasse auf die Trennung nach Zusammensetzung (HT-HPLC) zu minimieren. Die mit der entwickelten HT-HPLC Methode erreichte Trennung wurde durch Kopplung mit der HT-SEC weiter optimiert: Der Einfluss der Säulentemperatur, des Volumens der HT-HPLC-Fractionen die in die HT-SEC injiziert wurden und der Trenneffizienz der HT-SEC wurden dabei untersucht. Erstmals wurde für BiHDPE Bimodalität sowohl in der HT-HPLC- wie auch in der HT-SEC-Dimension der HT 2D-LC beobachtet. Dies wurde durch die Verwendung eines geringen Transfervolumens von 100 μL , einer HT-SEC-Säule mit hoher Zahl theoretischer Böden (N_{11000}) und dadurch, dass für jede HT-SEC-Analyse genug Zeit gelassen wurde, erreicht.

Um quantitative Informationen über die aus der Chromatographie eluierenden Fractionen zu gewinnen, wurde der Verdampfungslichtstreuungsdetektor (*Evaporative Light Scattering Detector*, ELSD) durch einen Infrarot (IR)-Detektor ersetzt, und BiHDPE so mittels HT 2D-LC analysiert. Hierzu war eine sorgfältige Optimierung der chromatographischen Parameter erforderlich: Mit jedem Fractionstransfer aus der HT-HPLC in die HT-SEC-Dimension wird bei der HT 2D-LC eine kleine Menge 1-Decanol (Lösungsmittelpfropf) mitinjiziert, wobei die Menge von der jeweiligen Position im Gradienten abhängt. Da der hier verwendete IR-Detektor auf die Detektion der Streckschwingungen von Methyl- und Methylengruppen eingestellt ist, verursacht 1-Decanol einen intensiven und breiten Peak im Chromatogramm, der deutlich mit dem Polymerpeak überlappen kann, wenn eine Säule mit geringer Zahl theoretischer Böden (N_{4500}) verwendet wird. Um eine Trennung des Polymerpeaks vom Lösungsmittelpeak über den gesamten Molmassenbereich zu erreichen, wurde eine SEC-Säule mit hoher Zahl theoretischer Böden (N_{11000}) benötigt. Ebenfalls wurden ein optimales Transfervolumen zwischen der HT-HPLC- und der HT-SEC-Dimension und ein optimales Volumen für eine einzelne HT-SEC-

Analyse identifiziert. Unter Verwendung dieser Bedingungen wurden der Lösungsmittelpeak und der Polymerpeak in allen HT-SEC-Chromatogrammen vom BiHDPE Basislinien-getrennt. Im Ergebnis zeigte der Kontourplot der HT 2D-LC→IR zwei Areale, welche die Trennung des BiHDPE in die HDPE und LLDPE-Komponente widerspiegeln. Es wurde eine umfassende Kalibration des HT 2D-LC-Systems in Hinblick auf Molmasse, Zusammensetzung und Konzentration durchgeführt. Dies zeigte die Anwesenheit von Oligomeren (bis zu 500 g/mol) welche aus HDPE stammten und die Anwesenheit von Polymerfraktionen mit einem 1-Butengehalt in einem Bereich von 0 bis 6,5 mol %.

Um umfassende Kenntnisse über die molekularen Heterogenitäten in Polyolefinen zu gewinnen, kann eine chromatographische Trennung (HT-HPLC/HT-SEC) offline mit der ^{13}C -NMR (off-flow HT-HPLC/HT-SEC→ ^{13}C NMR) gekoppelt werden. Im Falle von BiHDPE ist der Comonomergehalt sehr gering. Dies kann auf Grund der erforderlichen Lösungsmittelunterdrückung eine HT-LC→ ^{13}C NMR Kopplung im online Modus sehr komplizieren. Daher wurde der Weg der offline HT-LC→ ^{13}C NMR gewählt. Zu diesem Zweck wurde ein tragbarer automatischer Fraktionssammler (*Portable Automatic Fraction Collector*, PAFC) entwickelt, der in einem weiten Temperaturbereich (20 – 220 °C) und mit einem weiten Spektrum von HT-LC-Geräten gekoppelt werden kann. Mit Hilfe des PAFC wurden Fraktionen von HT-SEC-Trennungen von BiHDPE gesammelt und offline mittels ^1H -NMR analysiert. Die Fraktionen, die mittels des PAFC aus der HT-SEC erhalten wurden, wiesen enge Dispersitäten mit Werten von 1,08 – 1,5 auf. Die ^1H -NMR-Untersuchungen der Fraktionen zeigten, dass der Comonomergehalt in der mittleren und hohen Molmassenregion höher ist. Der PAFC kann in Hinblick auf Temperatur und Zahl der Fraktionen an eine Vielzahl von Betriebsbedingungen angepasst werden. Perspektivisch wäre es möglich den entwickelten PAFC (Arbeitstemperatur 20 – 220 °C) für eine offline Kopplung von LC-Techniken (SGIC, TGIC, 2D-LC) mit der ^{13}C -NMR zu verwenden, um auf diese Weise eine eingehende und quantitative Untersuchung der strukturellen Heterogenitäten von Polyolefinen durchzuführen.

Polyolefine sind bei zahlreichen Anwendungen beschränkt durch ihre geringe Oberflächenenergie und ihre geringe Kompatibilität/Reaktivität mit anderen polaren Polymeren. Analog bedarf ihre Adhäsion an Materialien wie Holz, Metallen oder verstärkenden Fasern besonderer Beachtung. Die meisten dieser Schwierigkeiten können durch die Einführung polarer Funktionalitäten oder durch das Pfropfen passender polarer Monomere auf Polyolefine überwunden werden. Mit diesem Ziel ist die chemische Modifizierung von Polypropylen durch reaktive Extrusion von großem Interesse, und das Pfropfen von Maleinsäureanhydrid (MA) auf Polypropylen (PP) ist von hoher kommerzieller Relevanz. Die Anwendungseigenschaften solcher Produkte sind, bei gegebener Gesamtzusammensetzung, abhängig von der Molmassenverteilung (MMD) und der Verteilung der chemischen Zusammensetzung (CCD).

Unabhängig von der Tatsache, dass verschiedene analytische Techniken in der Vergangenheit zur Charakterisierung funktionalisierter Polyolefine eingesetzt wurden, bleibt die Herausforderung, die bivariate Zusammensetzung solcher Reaktionsprodukte zu bestimmen, ungelöst. Damit besteht Bedarf für eine analytische Technik, die funktionalisierte Polyolefine nach ihrem Funktionalisierungsgrad trennen kann. Zwei mit Maleinsäureanhydrid gepfropfte Polypropylenproben, PP-g-MA¹ und PP-g-MA^{1,7} mit einem mittleren MA-Gehalt von 1 bzw. 1,7 mol %, wurden für die Untersuchungen ausgewählt. Unter Verwendung von HT-SEC→FTIR mittels der LC-Transform-Technik konnte gezeigt werden, dass bei beiden Proben die Pfropfung des Maleinsäureanhydrids (MA) bevorzugt im niedrigen Molmassenbereich des Polypropylens (PP) stattfand. Mittels CRYSTAF konnte zwar eine Trennung nach Zusammensetzung erreicht werden, jedoch ist die Selektivität dieser Kristallisations-basierten Methode nicht ausreichend eine quantitative Analyse. Unter

Verwendung der HT-HPLC mit Silicagel als stationärer Phase und einem Lösungsmittelgradienten Decalin→Cyclohexanon^{G-10 min} bei 140 °C konnten jedoch beide PP-g-MA-Proben in einen funktionalisierten und einen nicht funktionalisierten Anteil getrennt werden. Analysen der Fraktionen mittels FTIR-Spektroskopie bestätigten die Trennung. Aufbauend auf diesen Ergebnissen ermöglichte es HT 2D-LC→IR erstmals die bivariate Verteilung von PP-g-MA zu untersuchen. Der erhaltene Kontourplot zeigte zwei Basisliniengetrennte Regionen, welche die Trennung in eine gepfropfte und eine nicht-gepfropfte Komponente widerspiegeln. Anhand des Kontour-Plots konnte gezeigt werden, dass die zwei PP-g-MA-Proben in Bezug auf die in ihnen enthaltene Menge an gepfropftem Material vergleichbar sind. Allerdings geht ein höherer Pfropfgrad mit einer geringeren Molmasse des gepfropften Anteils einher. Im Gegensatz dazu war die MMD des Polypropylenanteils der beiden Proben sehr ähnlich, wurde also kaum von der Pfropfreaktion beeinflusst. Die analytische Methode, die entwickelt wurde, ist potentiell sehr nützlich für die Entwicklung effizienterer Funktionalisierungsprozesse und liefert Informationen, um Struktur↔Eigenschafts-Beziehungen für funktionalisierte Polyolefine zu erarbeiten.

Alle der obigen Untersuchungen zu HT-SGIC und HT 2D-LC waren auf die Kontrolle der Trennung der Makromoleküle unter Verwendung porösen graphitischen Kohlenstoffs als stationärer Phase und eines Lösungsmittelgradienten bei konstanter Temperatur ausgerichtet. Um die Selektivität der Trennung und den Trennmechanismus zu verstehen, und um dieses Wissen zur Verbesserung der Auflösung der Trennung bei der HPLC von Polymeren zu verwenden, ist es essentiell Einblick in die Natur der Wechselwirkung zwischen Polymer und Sorbens zu gewinnen. Raman-Spektroskopie, die empfindlich für die Morphologie von Kohlenstoffmaterialien ist, wurde hier zum ersten Mal eingesetzt, um einen direkten Beleg für die Wechselwirkung zwischen einem Kohlenwasserstoff und der Oberfläche porösen Graphits (HypercarbTM) bei Raumtemperatur und hoher Temperatur zu liefern. Die charakteristischen Banden von Graphit (G-, D- und 2D-Bande) wurden gründlich in Hinblick auf ihre Empfindlichkeit gegenüber der Wechselwirkung zwischen Kohlenwasserstoff und der Oberfläche von HypercarbTM untersucht. Die wesentlichen Kriterien für die Auswahl des Analyten/Lösungsmittels waren geringe Flüchtigkeit und Abwesenheit von Lösungsmittelbanden im Bereich der G-Bande. Alkane (n-Decan, n-Dodecan und 2-Methylundecan) wurden als Modellanalyten ausgewählt, da sie Oligomere von PE und zudem löslich bei Raumtemperatur sind. Es wurde beobachtet, dass ein Anstieg der Kettenlänge zu einer erhöhten Verschiebung der G-Bande führte, also zu stärkeren Wechselwirkungen (HypercarbTM/n-Decan vs. n-Dodecan). Analog reduzierte die Einführung von kurzen Alkylverzweigungen die Wechselwirkung (HypercarbTM/n-Decan vs. 2-Methylundecan).

Der Ansatz wurde um das System HypercarbTM/n-Decan/PE bei 155 °C erweitert. Bei 155 °C zeigt das Raman-Spektrum von HypercarbTM/n-Decan/PE in Lösung eine Verschiebung der G- wie auch der 2D-Banden-Position um 13 cm⁻¹ bzw. 19 cm⁻¹. Diese Verschiebung bestätigt das Vorhandensein von van-der-Waals-Wechselwirkungen zwischen dem Analyten (PE) und HypercarbTM. Das Prinzip scheint dazu geeignet in Zukunft die Wechselwirkungen in verschiedenen Sorbens/Lösungsmittel-Systemen zu verstehen und einzustufen. Auf lange Sicht könnte die Raman-Spektroskopie zum Screening von geeigneten mobilen Phasen für wechselwirkungsbasierte chromatographische Trennungen unter Verwendung von porösem Graphit als stationäre Phase auszuwählen.

Durch die zuvor geschilderten Arbeiten wird das Verständnis von HT-HPLC-Trennungen von Makromolekülen nach Zusammensetzung unterstützt, und es werden neue Möglichkeiten für die Trennung nach Zusammensetzung von komplexen Makromolekülen eröffnet. Die Entwicklung einer Trennung von bimodalem HDPE unter Verwendung von HT 2D-LC→IR unterstützt die Bestimmung der molekularen Heterogenitäten von BiHDPE. Die Entwicklung

eines PAFC (Arbeitstemperaturbereich: 20 – 220 °C) erweitert den Anwendungsbereich der Chromatographie zur Aufklärung der Struktur komplexer Polymermaterialien. Die neu entwickelten HT-SGIC-Trennungen für funktionalisiertes PP könnten auf andere funktionalisierte Polyolefine weiter ausgedehnt werden, um auch für diese Trennungen in einen gefropften und einen nicht gefropften Anteil zu erreichen. Die Raman-Untersuchungen verbesserten das Verständnis der Wechselwirkungen im System PE/Graphit/Lösungsmittel in Lösung bei hoher Temperatur (155 °C). Dieses Wissen könnte verwendet werden um Trennungen mittels Wechselwirkungsbasierter Chromatographie besser zu kontrollieren.

3. Introduction and Preface

Polyolefins are, by volume, the most important polymers with a global demand in 2010 of more than 130 million metric tons [1] and with a forecasted to reach more than 200 million metric tons by the year 2020. Polyolefins continue to find acceptance in many novel and diverse applications due to their versatile properties combined with an excellent cost/performance ratio. This versatility arises from the ability to control the molecular heterogeneities, microstructure, and architecture of the macromolecules through advances in catalyst and process technology. At the same time, this infers the need to develop appropriate analytical methodologies for molecular characterization. The molecular heterogeneities in polyolefins are primarily defined by their distribution with regard to molar mass, chemical composition and stereo-regularity, which are interrelated.

Currently, crystallization based techniques like Crystallization Analysis Fractionation (CRYSTAF) and Temperature Rising Elution Fractionation (TREF) and, more recently, Crystallization Elution Fractionation (CEF) are used to deformulate semi-crystalline olefin copolymers according to their chemical composition. These techniques use the fact that the crystallization temperature is directly related to the content of comonomer. However, all crystallization based techniques are limited to samples that exhibit a sufficient degree of crystallinity. Moreover, they also suffer from co-crystallization i.e., components having similar crystallization temperature co-crystallize at the same temperature. As a consequence, High Temperature High Performance Liquid Chromatography (HT-HPLC) was developed, which separates macromolecules irrespective of crystallinity of a polymer. High temperature liquid adsorption chromatography, HT-LAC, which is a category under HT-HPLC, has emerged as a new technique for the compositional separation of polyolefins in 2009 and is currently experiencing immense attention in academia and industry as an alternative to traditional methods used for this purpose. The aim of the work presented in this thesis was to develop methods which are capable to unravel the chemical heterogeneities of non-polar olefin copolymers as well as polar modified ones using High Temperature Two Dimensional Liquid Chromatography (HT 2D-LC) with quantitative Infrared (IR) detection (HT 2D-LC→IR).

This thesis is divided into three parts. The first part comprising chapter 3-5 provides a general overview on synthesis, processing and properties of different polyolefins as material and the state of the art in characterization techniques, which are applied to study the different molecular heterogeneities present in polyolefins. The second part, represented by chapter 6, covers the results and discussion, which is subdivided into four sections: 1) Separation of non-polar polyolefins (BiHDPE) using HT 2D-LC→IR; 2) Fractionation of BiHDPE using HT-SEC coupled with NMR off-line; 3) Separation of polar polyolefins (PP-g-MA) using HT 2D-LC→IR; 4) Studying the interaction between graphite and polyolefin using Raman spectroscopy. Finally, chapter 7 summarizes the conclusions from the research conducted as part of this thesis.

4. Theoretical Considerations

4.1. Introduction to Polyolefins

Polyolefins are the plastics of choice for a wide range of applications, and polypropylene and polyethylene are almost a synonym for thermoplastics. For many decades polyolefins occupy the first position among all thermoplastics, where they account, by volume, for more than 60 % of the market. The accumulated annual production stood at 147 million tons in 2011, with a forecasted growth to 170 million tons by 2017 [2]. Polyolefins compete in many applications very successful with traditional materials like metals or ceramics, where their light weight or durability is often superior. Even more, beating forecasts from the 3rd quarter of the last century, they achieve success in the competition with engineering polymers, like polyamides or polyesters, due to their cost advantage. The underlying reasons for these trends are their excellent and widely adaptable properties, which can be adapted to a wide range of applications, and secondly their favorable cost/performance ratio. The last advantage arises from the fact that the feedstock for polyolefins is readily available from cracking of naphtha or natural gas and, more recently, also from biomass.

4.2. Types of Polyolefins

The most commonly used representatives are polyethylene (PE) and polypropylene (PP), which again can be subdivided into several grades for different applications.

4.2.1. Polyethylene (PE)

Polyethylenes are semi-crystalline thermoplastics and can be further classified based on their density and branching. The density of PE depends on the type and amount of branching [3], and using density as criterion the American Society for Testing and Materials (ASTM) has defined various types of PE [4].

-
- High density polyethylene (HDPE): $> 0.941 \text{ g/cm}^3$
- Linear medium density polyethylene (LMDPE): $0.926 - 0.940 \text{ g/cm}^3$
- Medium density polyethylene (MDPE): $0.926 - 0.940 \text{ g/cm}^3$
- Linear low density polyethylene (LLDPE): $0.919 - 0.925 \text{ g/cm}^3$
- Low density polyethylene (LDPE): $0.910 - 0.925 \text{ g/cm}^3$

These classifications have been further subdivided to convey additional information, such as molar mass or comonomer employed [5].

Low Density Polyethylene (LDPE) Chronologically, LDPE was the first of the PE family to be discovered and developed. In 1933 Gibson and Fawcett at Imperial Chemical Industries accidentally produced LDPE upon applying very high pressures (200 MPa) and temperatures ($> 200 \text{ }^\circ\text{C}$) to a mixture of ethylene and benzaldehyde, and only 6 years later ICI commenced commercial production [6]. LDPE is produced by polymerization of ethylene via a free radical mechanism at high temperatures ($> 200 \text{ }^\circ\text{C}$) and pressures (200 – 300 MPa). Process wise this can be realized in batch- or continuous mode, using autoclave or tubular reactors, respectively. The free radical process leads to significant amounts of long chain branching, resulting from chain transfer reactions [7,8]. LDPE also contains low amounts of short chain branches ($> \text{C}_3$) which result from backbiting reactions [8-10]. LDPE is a preferred material for blown film, shrink film, and extrusion coatings due to the enhanced strength and elasticity of the melt imparted by the content of LCB. Due to its clarity LDPE finds application for films where

transparency is a selector, like food and display packaging. The main disadvantages of LDPE are its low mechanical strength, stiffness, and susceptibility to environmental stress cracking.

Linear Low Density Polyethylene (LLDPE) LLDPE is produced by copolymerizing ethylene with α -olefins using Ziegler-Natta (Z-N) [11] or single site catalysts. Slurry and gas-phase process at low temperatures (80 – 110 °C) and pressures (~2 MPa) are commonly used for the production of LLDPE. The most widely used α -olefins are 1-butene, 1-hexene, and 1-octene. Their incorporation into the polymer chain decreases the density and crystallinity of the polymer. This is also a strategy to modify many macroscopic properties, for example mechanics (toughness, tensile strength), environmental stress cracking resistance (ESCR), and gloss, thus adapting the material to countless applications [12]. The primary advantages of LLDPE compared to LDPE, arising from its backbone linearity and the presence of SCB, are high tensile and impact strength and film gloss at low film thickness.

High Density Polyethylene (HDPE) HDPE is produced by polymerization of ethylene using Z-N or supported chromium ("Phillips") catalysts [13] in slurry and gas phase at low temperatures (80 – 110 °C) and pressures (2 – 4 MPa). Low amounts (< 1 mol %) of α -olefin comonomers are incorporated in many of the commodity grades. The introduction of low concentrations of short chain branching (SCB) enhances the processability, toughness, and ESCR. High molar mass HDPE is used in the manufacture of heavy duty bags, drums, and pipes, whereas the medium molar mass varieties find applications in packaging. A major market of HDPE is the production of pipes, used for transportation of various liquid media, including potable water, and gas because of its superior toughness and ESCR.

Ultra High Molecular Weight Polyethylene UHMWPE is produced using heterogeneous Z-N catalysts in a slurry process. UHMWPE contains long chains with higher molar mass than HDPE and exhibits high impact strength. UHMWPE fibers (Dyneema® and Spectra®) are light weight high strength fibers commonly used in ballistic protection, yachting, and skis and snowboards. UHMWPE is also widely used as material for endoprothetics in hip, knee and for spine implants and to produce abutments for bridges.

4.2.2. Polypropylene (PP)

PP is widely produced using Z-N catalysts, with metallocene catalysts steadily gaining importance. Slurry and gas phase processes are most often used at low temperatures (60 – 80 °C) and pressures (~2 – 4 MPa). Taking composition as a criterion, PP materials can be classified into [14].

- Homopolymer (HP – e.g., isotactic polypropylene (*i*-PP)),
- The random copolymer (RCP – e.g., ethylene-propylene copolymer (E/P)) and the
- Impact copolymer (PP-HI also called heterophasic copolymer).

HP accounts for roughly 78 % of the industrial PP market followed by PP-HI and RCP with 16 % and 6 %, respectively [14]. Generally, the homopolymer is characterized by high rigidity, while the incorporation of the comonomer leads to increased flexibility and higher transparency for RCP. PP-HI is the material with the highest flexibility and impact strength in the PP family [15,16]. HP and RCP can be produced in a single reactor process, while PP-HI is produced in a cascade process, where the HP or RCP are produced in the first step, and the ethylene-

propylene (EP) copolymer, which imparts the impact resistance to the final product, in the second reactor.

4.3. Polyolefin Synthesis: Catalyst Driven Process

The success story of polyolefins is to a large extent the result of a trail of serendipitous discoveries and systematically following up on these. Polyolefins were first discovered in 1898 by the German Chemist von Pechmann who decomposed diazomethane to produce *polymethylene*. Decades later, in 1930 Marvel and Friedrich synthesized a low molar mass polyethylene using lithium alkyls and an arsonium compound, but did not follow up on this finding. Gibson, a physical chemist who had worked with Michels in Amsterdam, and Fawcett, an organic chemist who became interested in polymerizations through his friendship with Carothers, were the key scientists in the discovery of LDPE. Michel's support was also crucial for setting up the infrastructure for high pressure experimentation at ICI in Winnington [1]. Then, in 1933 Gibson and Fawcett discovered a white waxy solid which was produced in a reaction involving ethylene gas and benzaldehyde at 200 MPa temperatures $> 200\text{ }^{\circ}\text{C}$. Subsequent work with ethylene alone at high pressures led to explosions bringing the experimentation to a halt. M. Perrin resumed the experiments and noted that oxygen functioned as a catalyst, and that the dose of oxygen plays a critical role in the course of the direction. After optimizing the conditions, LDPE production was piloted in 1937 and the first 100 tons were sold in 1939 [6,17].

Serendipity also played a crucial role in the next stages of olefin polymerization. This time it was the transition metal catalyzed polymerization, which started with the discoveries of Hogan and Banks from Phillips Petroleum and Ziegler at the Max Planck Institute in the early 1950s [13]. Hogan and Banks discovery was in fact serendipitous, but it was not accidental. In 1925, Oberfell convinced company founder Frank Phillips to investigate additional uses for natural gas liquids. That's when Hogan and Banks were came into picture and where attempting to convert propylene into components for gasoline and discovered polypropylene in 1951. By using a nickel catalyst in combination with a small amount of chromium oxide low molar mass hydrocarbons were expected. However, chromium oxide catalyst produced a crystalline material, polypropylene. Applying the same chromium catalyst to ethylene produced HDPE at much milder conditions ($80\text{ }^{\circ}\text{C}$, 2 – 3 MPa) than the ICI process. In 1953, Ziegler during his research on the *aufbau* (growth) reaction discovered the dimerization of ethylene to butene, which was caused by a nickel impurity in an autoclave. In systematic experiments following up on this observation Ziegler discovered a catalytic system based on titanium halides and triethyl aluminum that was capable of polymerizing ethylene at mild conditions ($60\text{ }^{\circ}\text{C}$ and 0.1 – 0.5 MPa). In the research sparked by this discovery it was also discovered that this system was capable of copolymerizing ethylene and higher α -olefins.

In 1957 Breslow et al. [18] investigated the homogeneous polymerization of ethylene using bis(cyclopentadienyl)-titanium or zirconium dialkyls in combination with methyl aluminum chloride ($\text{Cp}_2\text{TiCl}_2/\text{Me}_2\text{AlCl}$). Later, in 1976 Kaminsky and Sinn experimented with bis(cyclopentadienyl)-zirconium dichloride (Cp_2ZrCl_2) and trimethyl aluminum (AlMe_3) for ethylene polymerization, and accidentally discovered that addition of small amounts of water increased the polymerization activity of the system by a factor of 100 [19,20].

Later in 1996 Brookhart et al. [21] reported nickel diimine complexes which are comparable to the metallocene catalysts in terms of catalytic activity and molar mass of the produced polymer.

Then in 1998 Brookhart [22] and Gibson [23] reported that iron or cobalt complexes containing diimine-pyridine ligands exhibited very high activities for ethylene polymerization. These catalysts are nowadays referred to as post metallocene catalysts.

The chronology of the four families of transition metal based olefin polymerization catalyst is summarized as in Table 1.

Table 1 Catalyst types [24]

Type of catalyst	Physical state	Examples*
Phillips	Heterogeneous	CrO ₃ /SiO ₂
Z-N	Heterogeneous	TiCl ₃ , TiCl ₄ /MgCl ₂
	Homogeneous	VCl ₄ , VOCl ₃
Metallocene	Homogeneous	Cp ₂ ZrCl ₂
	Heterogeneous	Cp ₂ ZrCl ₂ /SiO ₂
Late transition metal	Homogeneous	Ni, Pd, Co, Fe with diimine and other ligands

*This is not a comprehensive list. These are simply representative examples.

Phillips catalysts: (Figure 1). The precatalyst is prepared by impregnating silica with CrO₃ (or chromium precursors) and then calcined at high temperatures (200 – 900 °C). During calcination the Cr species links to the silica (200 – 300 °C) via reactions with surface silanol groups and eliminating neighboring silanol groups (> 500 °C). The thermal treatment impacts the polymerization activity as well as the MMD and LCB content of the polymer. Phillips catalysts display significantly lower reactivity towards α -olefin incorporation and are thus not used for the production of LLDPE. Yet, they produce HDPE with ultra-broad MMD containing low levels of SCB and LCB [25]. These features contribute to some unique features (improved processability and high impact strength) of the produced resins for applications like pipes and films.

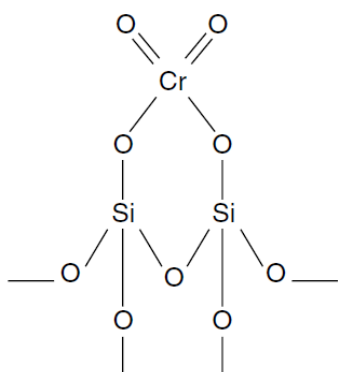


Figure 1 Chromium catalyst for olefin polymerization

Ziegler-Natta (Z-N) catalysts: Heterogeneous Z-N catalysts have been the workhorse of the polyolefin industry since their discovery. Typically, these include a titanium halide (TiCl_4) (Figure 2), a co-catalyst, usually a trialkyl aluminium compound (AlR_3) and magnesium dichloride as a support.

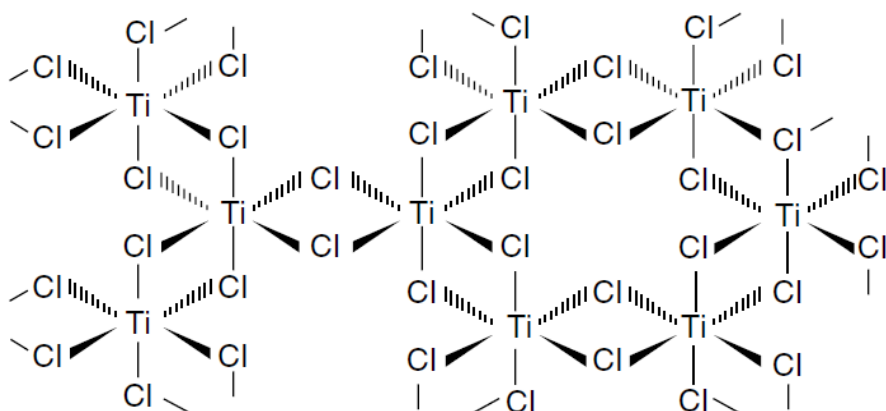


Figure 2 Structure of TiCl_4 [24]

Since the first mentioning of Z-N catalysts by Ziegler various generations of Z-N catalysts have been developed to produce polyolefins at high activity. The first generation Z-N catalyst (early 1960) was generated by reducing TiCl_4 with metallic aluminum, yielding AlCl_3 dispersed in titanium trichloride matrix ($\text{TiCl}_3/3\text{AlCl}_3$) [14]. The activity of this catalyst was poor (200 g polymer/ g catalyst) which led to the discovery of a second generation of catalysts. The latter used complexing agents (ether) for the preparation of catalytically active complexes based on TiCl_3 which increased the activity to 5000 g polymer/g catalyst [26]. In the following supported Z-N catalysts (using anhydrous MgCl_2 as support) in combination with titanium tetrachloride and triethyl aluminum (co-catalyst) are regarded as the third Z-N catalyst generation (activity 10,000 g polymer/ g catalyst) [27]. Further improvements for these supported catalysts (fourth and fifth generation Z-N catalyst) resulted in activities of 50,000 – 100,000 g polymer/g catalyst [14,28].

The pathway of α -olefin insertion underlying the polymerization in all Z-N catalysts has been formulated by Cossee and Arlman [29] (Figure 3).

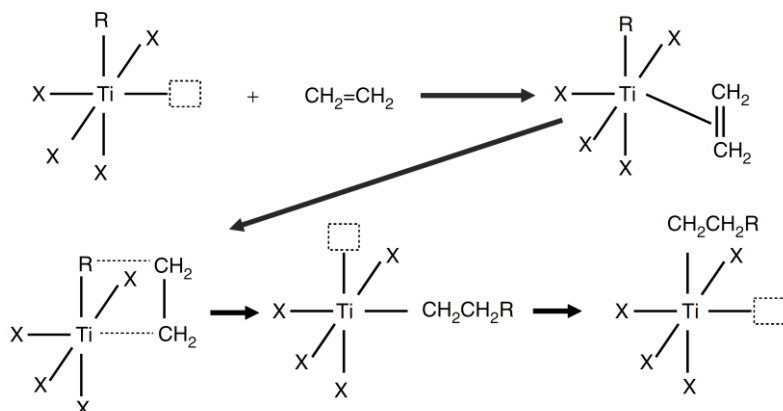


Figure 3 Cossee-Arlman mechanism: X are ligands and R is the growing polymer chain [24]

The active site is formed by an octahedrally co-ordinated transition metal ion with a vacant co-ordination position and one alkyl group in its co-ordination sphere. The role of the co-catalyst is to alkylate the active site and act as a scavenger. The π -bond of the olefin monomer co-ordinates to the vacant position, weakening the transition metal–carbon σ -bond. The polymerization occurs on the transition metal (titanium). In the next step the olefin is inserted into the σ -bond via a migratory insertion (cis-migration) according to Cossee and Arlman [29] (Figure 3). The polymer chain then grows through successive monomer insertion until transfer to hydrogen and β -hydride elimination takes place, during which a hydride is transferred to the titanium or the co-ordinated olefin. In either case, the catalyst center is not deactivated, since insertion of ethane into the Ti-H or Ti-C bond allows a new chain to start.

Z-N catalysts are characterized by the presence of several different active sites, each with its own rate of polymerization and chain termination, stereo-selectivity, comonomer incorporation, and chain transfer reaction. As a result, the polymers produced show broad distributions with regard to molar mass and short chain branch content, which makes them interesting for applications that require stiff, tough and yet processable material [30]. However, a substantial amount of empirical optimization is necessary before polymers of desired molecular parameters can be obtained. The majority of commercial HDPE and LLDPE resins are produced with heterogeneous Z-N catalysts.

Metallocenes: In metallocene catalysts a transition metal atom is “sandwiched” between two cyclopentadienyl (derivative) rings as depicted in Figure 4, which may be connected via a bridge (ansa metallocenes [31]). This makes the structure more rigid thus allowing better stereo control in the polymerization. By altering the electronic and steric environment around the active site its accessibility and reactivity can be modified to produce polyolefins with a wide range of microstructures, which are not accessible by using Z-N catalysts. Metallocene catalysts in combination with the conventional aluminum alkyl co-catalysts (AlMe_3 , AlEt_3) as used in Z-N systems are capable of polymerizing ethylene, but only at a very low activity [32].

With the discovery of methyl aluminoxane (MAO) it became possible to boost the activity by a factor of 10,000 [33,34]. Interestingly, despite its significant influence on catalytic performance, the role of the aluminoxane component is still not fully understood: It has been generally accepted that MAO acts as alkylating agent that facilitates the formation of an electron deficient co-ordinatively unsaturated cationic alkyl species. In addition it also serves as a scavenger for impurities. Its structure is still controversially discussed and experimental evidence exists for an oligomeric nature with a degree of oligomerization varying approximately from 6 to 20 [35]. Figure 4 shows representative metallocene catalysts used for olefin polymerization and Figure 5 shows the polymerization of PP using metallocene catalyst.

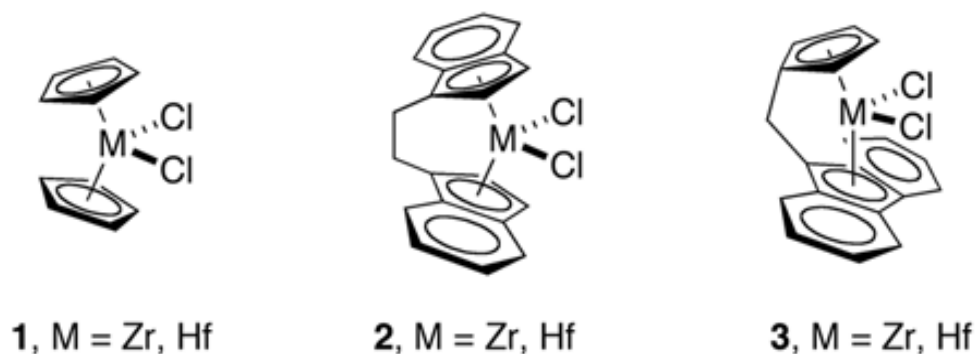


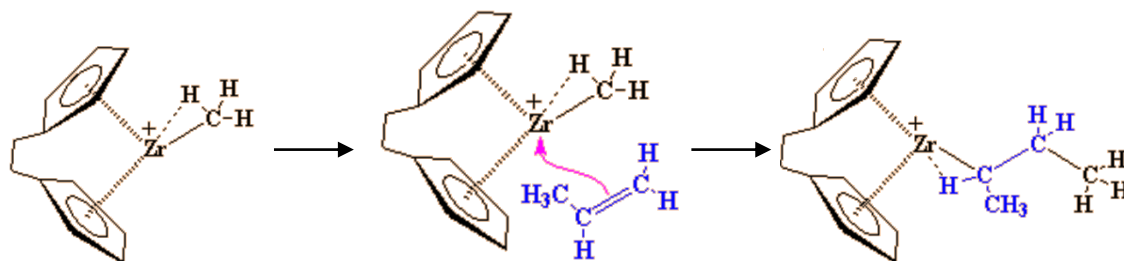
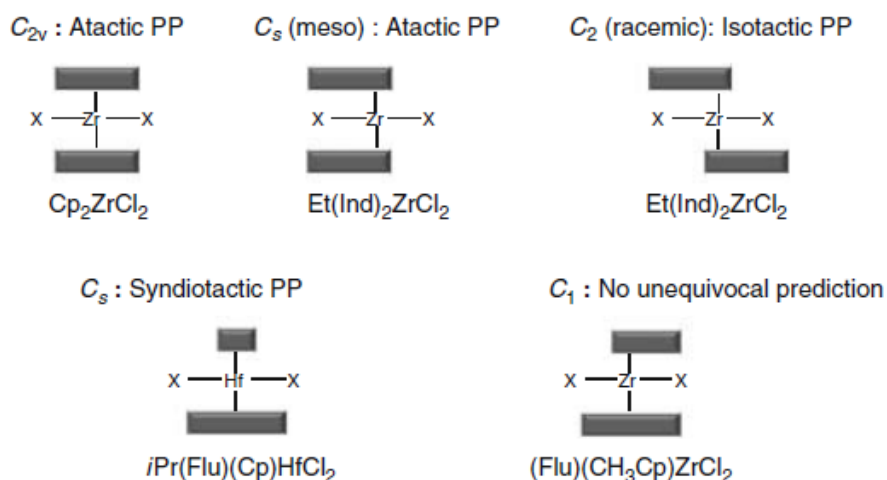
Figure 4 Metallocene catalysts for olefin polymerization**Figure 5** Mechanism of propylene polymerization by metallocene catalysts [36,37]

Figure 5 shows that the electrons in the zirconium-methyl carbon bond shift to form a bond with one of the propylene carbons. After the insertion of propylene, the zirconium ends up as it started, lacking a ligand. The polymer chain then grows through successive monomer insertion and results in polypropylene. An important characteristic of metallocene catalysts is that the stereo-selectivity of the polypropylene is determined by their ligand structure.

Figure 6 illustrates how different ligand structures enable to produce PP with various stereo-microstructures. Beyond the three “classical” types of polypropylene stereo-regularity, *i*-PP, *s*-PP, and *a*-PP, novel chain architectures are also accessible from other metallocene types, as illustrated in the Fischer projections in Figure 7.

**Figure 6** Different structures of ligand

Notice: C_p , cyclopentadienyl; Ind, indenyl; Flu, fluorenyl; NM, neomenthyl.

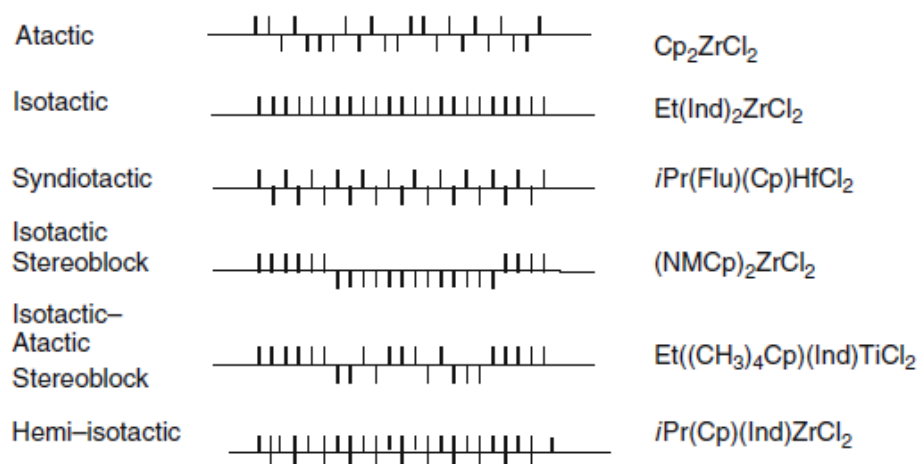


Figure 7 Types of PP chain configurations produced with metallocene [31,38]

After more than three decades of research single site catalysts are now available that can control the polymerization with regard to chain growth and stereo- as well as regio-chemistry of the monomer insertion in a way which is often impossible using Z-N catalysts. Metallocene catalysts have opened new perspectives due to the possibility to copolymerize ethylene or propylene with α -olefins, with olefin macro monomers or cyclic olefins, or with sterically hindered or functional monomers [39-41]. Copolymers of ethylene with a wide variety of monomers, among them 1-octene, 1-hexene (LLDPE), norbornene and styrene, olefin based elastomers and long chain branched PE with tailored rheological properties are already produced on an industrial scale [42,43]. PP made with metallocene catalysts exhibits distinct advantages over conventionally produced PP, higher stiffness and greater tensile strength [42].

Late transition metal catalysts: Compared to the early transition metals, the lower oxophilicity and, therefore, greater tolerance towards functional groups make late transitional metals based catalysts potential candidates for the industrial production of functionalized polyolefins. A major breakthrough in this direction was achieved by Brookhart et al. [44] who reported a set of catalysts based on Ni(II) and Pd(II) α -diimine complexes (Figure 8) [45-47]. These were remarkably active for the copolymerization of non-polar olefins with polar vinyl monomers such as acrylates, methyl vinyl ketones, and silyl vinyl ethers [47,48]. Brookhart, Gibson, and Bennett [22,23,49] reported cationic iron and cobalt catalyst systems for the polymerization of ethylene to highly linear PE.

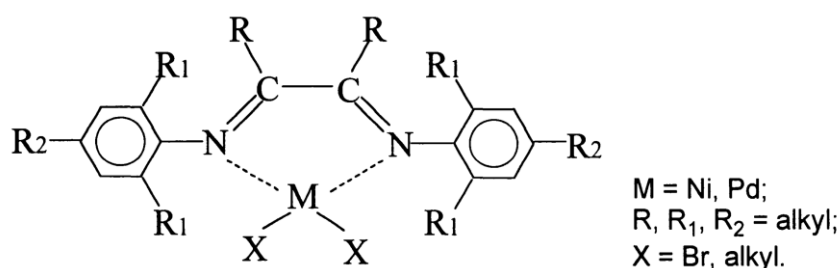


Figure 8 Structure of Ni(II)/Pd(II) α -diimine catalysts [50]

Concurrent Tandem Catalysts (CTC): Concurrent tandem catalysis (CTC) is an approach in which multiple catalysts are applied on a set of monomers in a single process to yield

microstructures otherwise impossible to obtain with a single catalysts system. One of the outcomes of tandem catalysts is the development of olefin block copolymers via the chain shuttling polymerization [51,52]. The latter is a dual catalyst method for producing block copolymers with alternating or variable blocks which combine the properties of both polymers. The evolution for the synthesis of PE and PP is shown as a timeline (Figure 9 and Figure 10).

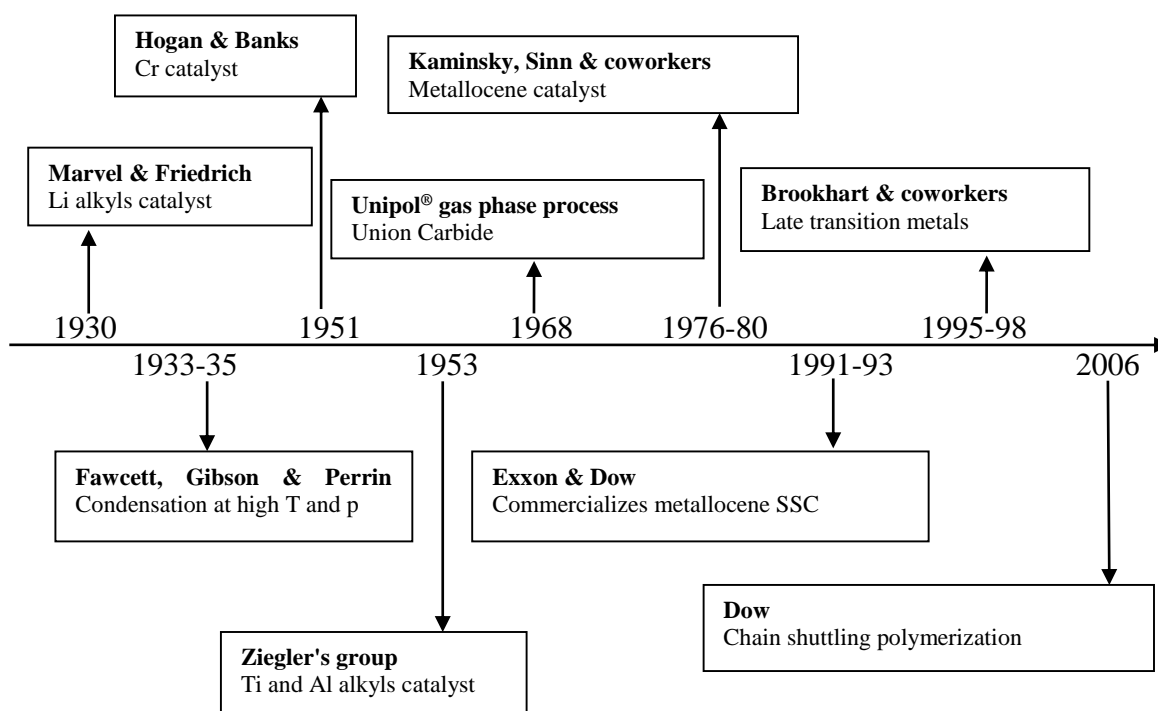


Figure 9 Timeline for the synthesis of PE

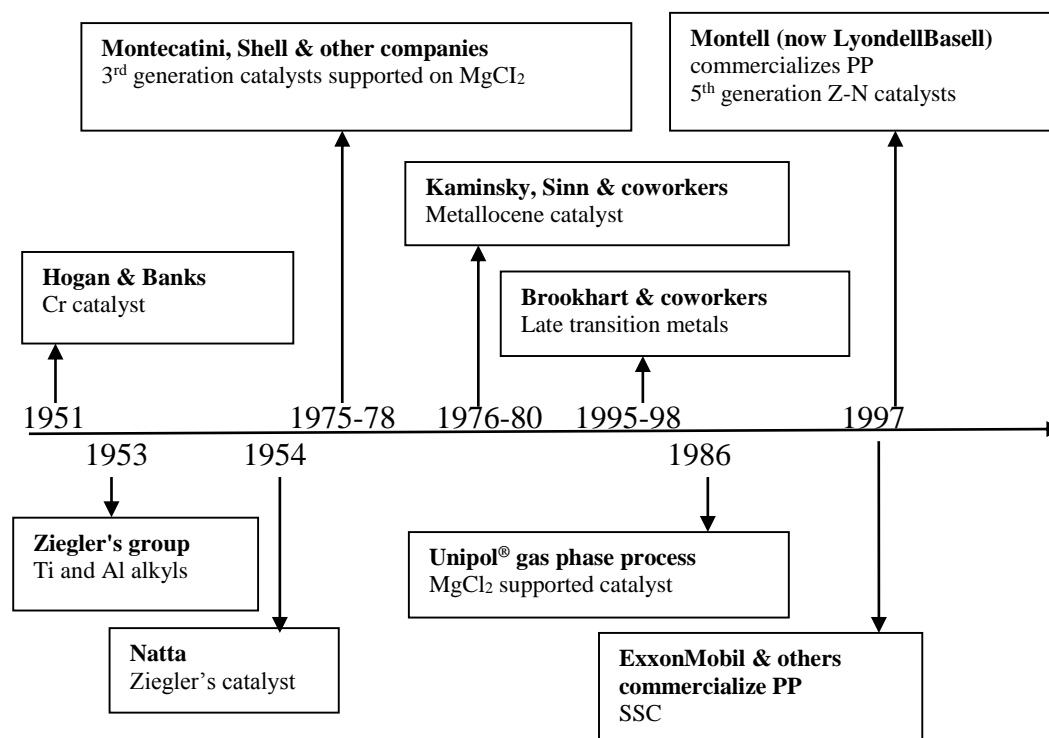


Figure 10 Timeline for the synthesis of PP

Notice: T- temperature, p- Pressure, SSC- single site catalyst.

4.4. Development of Polyolefins Driven by Application Demand

Without doubt the rise of polyolefins to the most important class of thermoplastics would not have been possible without the discoveries on the catalytic side, which made access to these materials on a constantly increasing scale possible. But at the same time it has to be kept in mind that this would not have happened without the demand from markets, which gave thrust to the development of new types of PE resins. Thus, the request for insulation of telecommunication cables in World War II spurred the development of polyethylene. Although not fit for this purpose at that time, the demand for insulation of cables for the newly developed radar then was a very suitable application for the brand LDPE. Ziegler's discovery fell in the post war period with a strong demand for new materials from many growing industrial sectors in the recovering and then growing economies. Nowadays, the applications of PE are highly diverse, and can be broadly divided into such of durable and non-durable nature. The last ones can be exemplified by film applications for various markets. Durable applications with varying lifetime expectation are found in the sectors of mobility or construction and civil engineering. One of particular relevance, which is responsible for a very significant share of the PE consumption, is the production of pipes, which serve for transportation of various liquid or gaseous media. In the following the development of HDPE resins for pipe applications shall be inspected more closely.

4.4.1. HDPE for Pipe Applications

In pipes the resistance towards environmental stress cracking (ESCR) and Rapid Crack Propagation are crucial properties [24,53]. ESCR describes the resistance of a material towards failure in the presence of surface active agents, and is a well investigated type of slow crack

growth [54-56]. RCP refers to the rapid propagation of a crack when the product is subjected to an intense impact. Due to the significance of these properties various tests have been developed for their measurement The bent strip test, Polyethylene Notch Tensile test (PENT), Single Point Notched Constant Tensile Load (NCTL) and the Full Notch Creep Test (FNCT) rank PE resins with regard to their ESCR [57]. Reproducibility and time requirements are important criteria for such tests, and recent research efforts have led to the development of the strain hardening test [58], which is simpler to conduct and less time consuming. The Full Scale (FS) test and the Small Scale Steady State (S4) tests are used to determine RCP [59]. Hydrostatic pressure tests [60] are commonly used to determine the lifetime of polyolefin pipes and according to their long term behavior PE resins are commonly classified as PE X, where X stands for the minimum hoop stress the material has to withstand at 20 °C for 50 years without failure [61]. The evolution of pipe grade PE resins from that point of view is presented in Table 2.

Table 2 Time line for pipe grade PE resins [62]

Designation of material	MRS at 50 years and 20 °C MPa (*bar)	Commercialized	Applications
PE 32 (LDPE)	3.2 (*32)	1950's	low pressure piping
PE 40 (LDPE)	4 (40)	1950's	low pressure piping
PE 63 (HDPE)	6.3 (63)	1960's	medium pressure piping, irrigation systems, and drinking water systems
PE 80 (HDPE)	8 (80)	1980's	gas pipes, drinking water pipes, sewers, outfall pipes, and industrial pipes
PE 100 (HDPE)	10 (100)	1990's	high demand piping

4.4.1.1. Unimodal HDPE

Generally, unimodal PE resins can be produced with a wide range of molar mass characteristics, depending on the catalyst system and process technology used. Unimodal HDPE resins [63,64] for pipe applications are produced using one catalyst (either Z-N or chromium based) in a single reactor. The result is a polymer with a broad MMD and low amounts of comonomer incorporated in a gradient over the MMD, preferentially in the low molar mass segment. The short chain branches (SCB) disrupt the crystalline structure of the polymer and as a result lower the density. As the short chain branches are concentrated in the low molar mass part, the high molar mass fractions are excluded from the amorphous tie molecules. Developments of PE resins for pipe applications in the 70s focused on broadening the MMD and increasing the branch length. These resins were developed to substantially improve the performance in pipes and were classified as PE 80. However, at certain applications (e.g., pipes in oil and gas production, mining, industrial chemicals, etc.,) this material doesn't withstand because of its pressure rating.

4.4.1.2. Bimodal HDPE (BiHDPE)

Consequently, the molecular characteristics which had to be addressed to improve the performance of PE resins in pipe applications was not the shape of the molar mass distribution (MMD) but the location of the short chain branches along the MMD. Specifically, an inversion of the comonomer incorporation along the MMD would be required, which cannot be achieved in a single polymerization process, as it contradicts the copolymerization behavior of all known catalysts. Thus, this goal can only be accomplished by blending resins with different molar mass and short chain branching characteristics. Technologically, this was accomplished by combining two polymerization processes in a cascade (Figure 11).

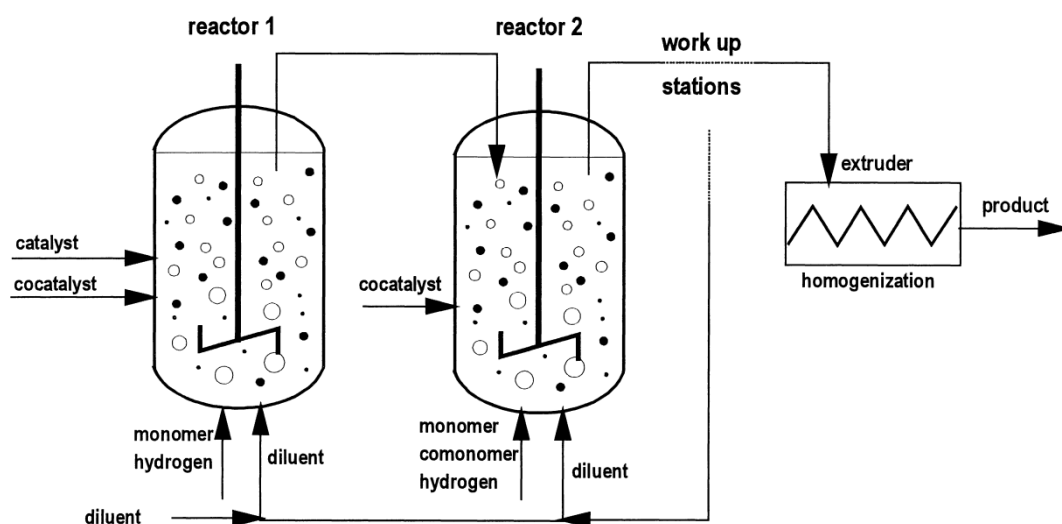


Figure 11 Scheme of a cascade slurry process for production of BiHDPE [24]

The first reactor is fed with ethylene and hydrogen to produce an unbranched PE of low molar mass. The hydrogen is then removed, and the resulting product transferred to a second reactor, where a α -olefinic comonomer (1-butene or 1-hexene) is added to the ethylene as comonomer to produce a high molar mass short chain branched copolymer [24,53]. Typically, this second reactor product is characterized by a comonomer distribution over the MMD such that the highest comonomer contents are found in the lower molar masses. As a result, BiHDPE exhibits a comonomer distribution such that the comonomer content decreases towards the low and high molar mass region. The crystalline regions are mainly formed by the low molar mass homopolymer PE as well as the ethylene sequences in the copolymer fractions as the comonomer is rejected from the growing crystals. High molar mass copolymers form the amorphous region and act as tie molecules that connect crystal lamella. Tie molecules improve the resistance of PE against environmental stress cracking resistance (ESCR) and rapid crack propagation (RCP) [24].

The ESCR and the resistance towards RCP of bimodal resins are higher than that of many unimodal grades [24,58,63]. Due to this substantial leap in mechanical and physical properties BiHDPE surpasses the performance of unimodal resins in pipe/film/blow molding applications [64]. The MMD and the comonomer distribution along the MMD with functions assigned to various molar mass fractions are compared for a BiHDPE and a unimodal resin in Figure 12.

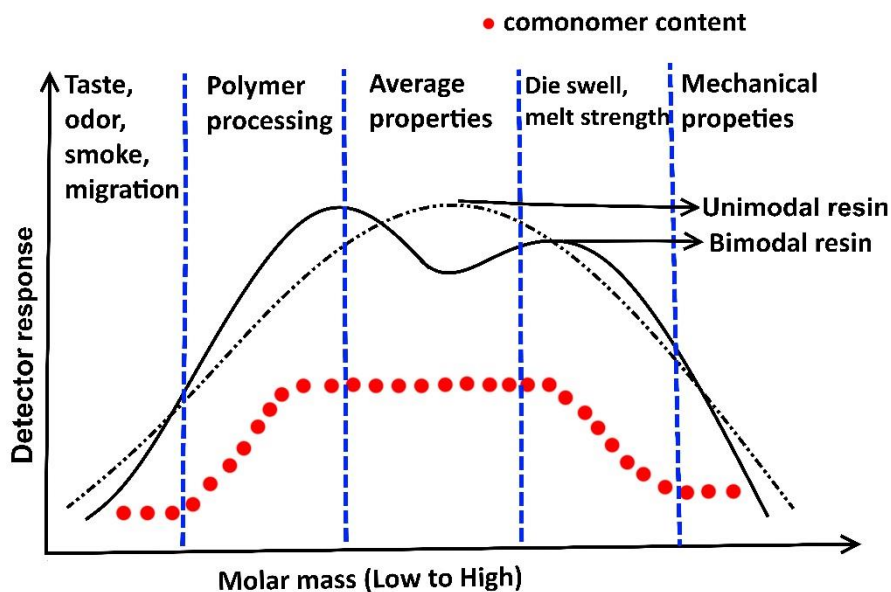


Figure 12 Comparison of unimodal and bimodal resin with macroscopic properties assigned to individual molar mass regions and the distribution of comonomer across the MMD

4.4.2. Functionalized Polyolefins

Polyolefins are limited in certain applications due to their low surface energy and poor compatibility with other (polar) polymers. In the same sense, their adhesion to materials like wood, metals, or reinforcing fibers requires special attention [65]. Most of these difficulties should be resolved by the incorporation of polar monomers. Generally, there are three possible approaches to functionalize polyolefins, namely (a) copolymerization of a α -olefin (ethylene, propylene, 1-butene, and 1-octene) with a functional monomer, (b) chemical modification of a preformed polymer and (c) a reactive copolymer approach, where a reactive comonomer is incorporated into the chain that can then be selectively and effectively converted to desired functional groups.

a) Copolymerization of an α -olefin with a functional monomer

Z-N and metallocene catalysts based on early transition metals are widely used in polyolefin synthesis. However, when monomers containing polar groups are added to the monomer feed the Lewis acid components (Ti, Zr, Hf, V and Al) of the catalyst tends to complex with the functional groups (-OH, -COOH, -NH₂- and halides) thus blocking the active sites and inhibiting the polymerization [66,67]. This can to some extent be prevented by protecting the polar functional groups and a following transformation. A more efficient alternative is the use of less oxophilic late transition metal catalysts based on Fe, Ni, Co, and Pd [68].

b) Chemical modification of a preformed polymer

Chemically modifying polyolefins is difficult due to the low reactivity of C-H bonds. A practical way [69,70] to overcome this is to break C-H bonds by abstracting hydrogen radicals and thus form free radicals along the polymer chain. The energy required for this step can be inferred for example by energy rich radiation or radical starters [68]. Since the stability of C-H bonds decreases in the order tertiary > secondary > primary the susceptibility towards hydrogen abstraction follows the same trend. Accordingly, PP is most susceptible among the polyolefins

towards attack by free radicals [71]. The polymeric (C*) radical formed after hydrogen abstraction can react with an unsaturated monomer in a graft reaction. The free radicals may also undergo other reactions as shown as shown in Figure 13 [68].

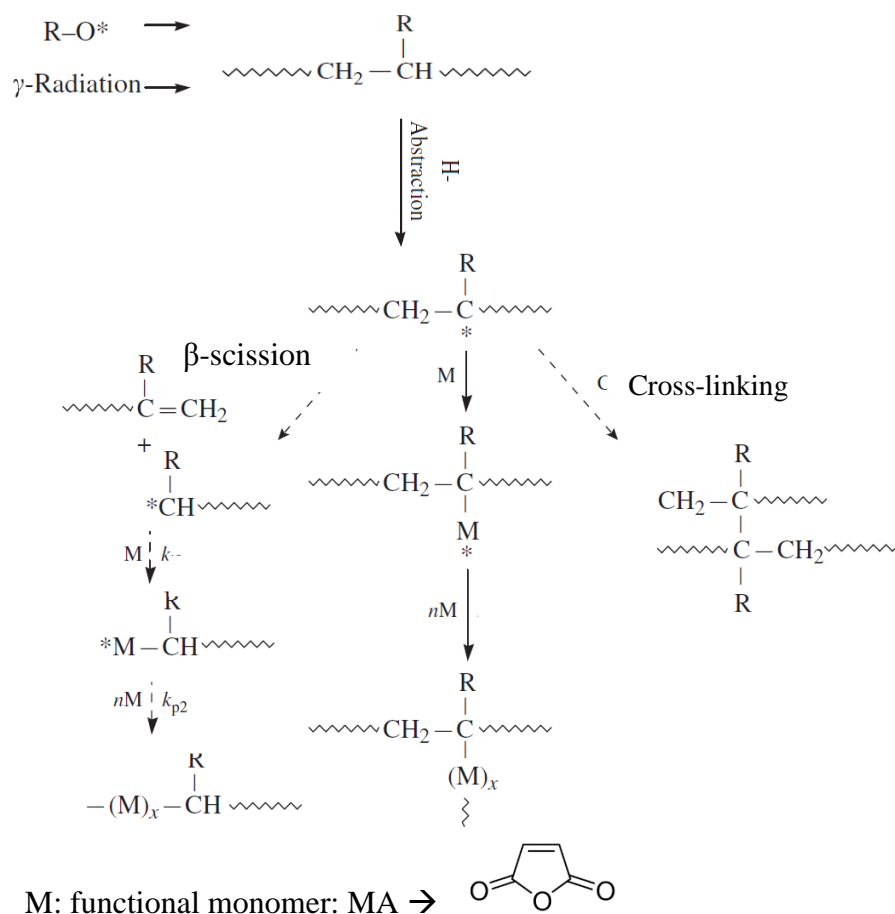


Figure 13 Possible reaction mechanisms for the grafting of maleic anhydride onto polypropylene in the melt state [66,72]

Figure 13 shows that the polymeric (C*) radical formed after abstraction can further react with other polymer chains resulting in cross-linking. Alternatively, as the susceptibility for hydrogen abstraction is higher for PP chain which contains higher tertiary carbon atom, β -scission may occur, which leads to a decrease in chain length. This can easily take place prior to the functionalization reaction. Chain scission reduces the polymer molar mass and transfers the C* radical to one of the newly generated chain ends. The terminal polymeric radical then engages in the grafting reaction by initiating and propagating with functional monomers to produce a graft copolymer. The overall outcome is strongly dependent on the reaction conditions. This post reactor modification of polyolefins is widely used in industry as the optimization of the processing parameters results in desired molecular characteristics which meets the desired set of properties.

c) Reactive polyolefins

To overcome the limitations of the above mentioned methods Chung [68] developed an approach to synthesize functional polyolefins with well-defined composition and molecular structure. The reaction involves two-steps: Firstly an α -olefin is copolymerized with a

comonomer containing a reactive group that can be effectively incorporated in the polyolefin. The comonomer can then in a second step be transformed into various functional groups, for example via reactive extrusion. Functional monomers containing borane [73], p-methylstyrene [74] and divinylbenzene [75], which are highly versatile in subsequent transformation reactions, are commonly used as comonomers. The reaction scheme for the synthesis of PP-g-MA using 9-BBN is described in Figure 14.

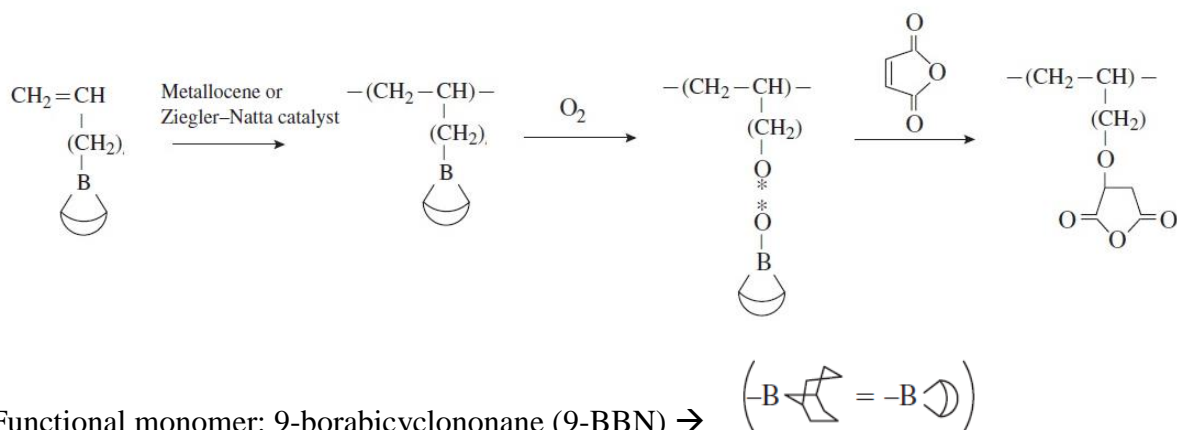


Figure 14 Synthesis of MA functionalized PP via reactive processing of PP containing 9-BBN as precursor [68]

4.5. Polyolefin Processing

The six by volume most relevant processing methods for polyolefins are injection molding, extrusion, rotational molding, blow molding, thermoforming, and structural foam molding [3].

Injection molding Injection molding is a cyclic process. The granules are placed in a hopper that continuously feeds the heated barrel of an extruder, where the polymer is plasticated. The molten material is injected under high pressure into a cold mold where it solidifies replicating the shape of the mold cavity. Low melt viscosity is required to ensure that the mold cavity is filled in a minimum possible cycle time. Bottle caps, automotive dashboards, plastic chairs, brushes are just a few examples for products manufactured by injection molding.

Extrusion Extrusion molding is a continuous process. The polyolefin granules or pellets are placed into a hopper that continuously feeds the heated barrel of an extruder where the polymer is plasticated. The molten material is then pressed through a die of roughly the same shape as the final product. High melt strength is required to avoid sagging of the extrudate leaving out of the die. The extruded product is drawn by take-off equipment, sized, and cooled until solidified. Sheets, pipes, films, and coatings for wires and cables are the commonly produced products by extrusion molding.

Rotational molding Rotational molding is a cyclic process. Finely ground thermoplastic powders or liquid resin or pellets are heated inside a rotating mold where the polymer melts and uniformly coats the inner surface of the mold. Low melt viscosity is required to ensure that the mold is uniformly coated. The mold is cooled in a special chamber prior to part removal. This process is used for the production of large complex polyolefin parts such as containers, storage tanks, water tanks, and portable sanitary facilities.

Blow molding Blow molding is a cyclic process. The blow molding process begins with melting down the plastic and forming it into a parison. The parison is a tube-like piece of plastic with a hole in one end through which compressed air can pass. The parison is then clamped into a mold and air is blown into it. The air pressure then pushes the plastic out to match the mold. High melt strength is required to avoid parison sag. Once the plastic has cooled and hardened the mold opens and the part is ejected. In general, there are three main types of blow molding: extrusion blow molding, injection blow molding, and injection stretch blow molding. Blow molding process is mainly used to produce hollow plastic parts. Smaller containers (< 1 liter) are produced by injection blow molding, whereas extrusion blow molding is suitable for larger containers and for containers with handles.

Thermoforming Thermoforming is a cyclic process, which involves the softening of polyolefin sheets by heat, followed by the application of vacuum or pressure (forming). The sheet may be stretched over a core (positive forming) or into a cavity (negative forming). When the polymer melt solidifies, its shape conforms to that of the mold. Low melt viscosity is required to ensure that the mold cavity is filled in a minimum possible cycle time. Thermoforming competes with blow molding and injection molding because of its relatively low cost machinery and molds, the ease of forming large areas and thin section parts. This process is mainly used to produce plastic cups, plates, tiffin boxes and several automobile parts.

Structural foam molding Structural foam molding is a cyclic process. In this process injection of nitrogen into the polymer melt or the use of chemical blowing agents causes the molding compound to expand after injection into the mold cavity. The foaming process starts when the polymer melt enters the mold cavity. Finally, a thin plastic skin forms in the mold and then solidifies in the mold wall. Low melt viscosity is required to ensure that the mold cavity is filled in a minimum possible cycle time. The uniqueness of this technique is that the final product exhibits excellent strength to weight ratio. This type of plastic molding is applicable to any thermoplastic that can be injection molded. It is usually used for parts that require thicker walls than standard injection molding. This technique is also capable of producing large structural parts at low process pressures.

5. Characterization of Polyolefins

Polyolefins, though constituted from simple hydrocarbons, show a large variety in their molecular heterogeneities, which lead to complexity in terms of characterization. Polymers can display various types of molecular heterogeneities which are interdependent. The most important distributions in polyolefins are those with regard to molar mass (MMD) and chemical composition (CCD); other molecular heterogeneities arise from unsaturation and microstructural features like inverse monomer insertion and comonomer sequence distribution. The different molecular heterogeneities in polyolefins and the common analytical techniques applied to determine these are illustrated in Figure 15.

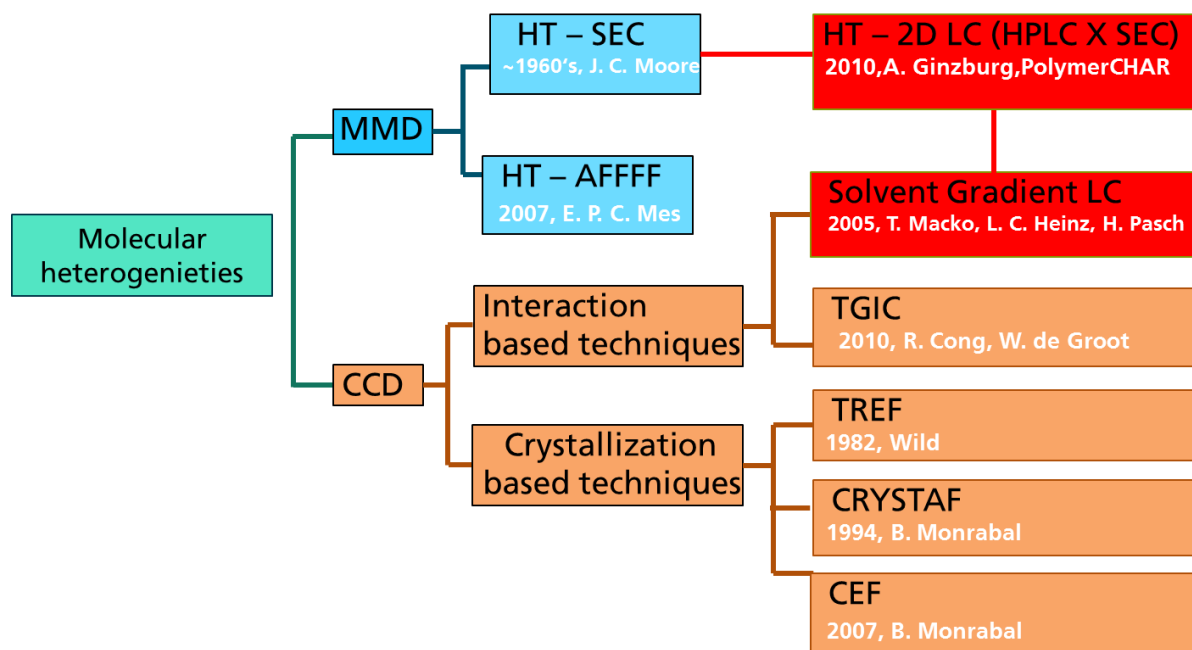


Figure 15 Molecular heterogeneities in polyolefins and analytical techniques to characterize them

(NMR: Nuclear Magnetic Resonance Spectroscopy, HT-SEC: High Temperature Liquid Adsorption Chromatography, HT-AF4: High Temperature Asymmetric Flow Field Flow Fractionation, DSC: Differential Scanning Calorimetry, FTIR: Fourier Transform Infrared Spectroscopy, TREF: Temperature Rising Elution Fractionation, CRYSTAF: Crystallization Analysis Fractionation, CEF: Crystallization Elution Fractionation, HT-LAC: High Temperature Liquid Adsorption Chromatography, HT-SGIC: High Temperature Solvent Gradient Interaction Chromatography, HT-TGIC: High Temperature Thermal Gradient Interactive Chromatography)

Measuring these heterogeneities is the key to develop structure↔property relationships, understand reaction mechanisms and kinetics of polymerization, and last but not least to develop processing↔property relationships. To sum up, the end-use properties of polyolefins depend largely on these molecular heterogeneities. Over the years, increased interest in synthesis of polyolefins with defined structure and tailored properties has led to the demand for accurate, reliable, and convenient methods of measuring microstructure.

5.1. Fractionation Techniques Based on Crystallinity

The chemical heterogeneity present in semi-crystalline olefin copolymers can be studied using various techniques. For polyolefins, other than MMD, the CCD is the most important factor impacting the end-use properties, and since the 1990s crystallization based techniques have been routinely used for its determination. The CCD of semi-crystalline polyolefins is commonly analyzed by Temperature Rising Elution Fractionation (TREF) [76], Crystallization Analysis Fractionation (CRYSTAF) or Crystallization Elution Fractionation (CEF) [77-79]. These techniques use the fact that the crystallization from dilute solution is related to the comonomer content.

The Flory–Huggins equation for the free energy of mixing can be used to describe the thermodynamic equilibrium of a polymer solution assuming a uniform distribution of solvent and polymer segments [80]. The depression in the equilibrium dissolution temperature of the homopolymer due to the presence of solvent and the number of chain segments is given by Eq. 1:

$$\frac{1}{T_m} - \frac{1}{T_m^0} = \left(\frac{R}{\Delta H_u} \right) \left(\frac{V_u}{V_1} \right) \left[-\frac{\ln(v_2)}{x} + \left(1 - \frac{1}{x}\right)v_1 - \chi_1 v_1^2 \right] \quad (1)$$

Where, T_m^0 = Melting temperature of the homopolymer,

T_m = Equilibrium dissolution temperature of the homopolymer in solution,

ΔH_u = Heat of fusion per repeating unit,

V_u and V_1 are the molar volumes of the homopolymer repeating unit and diluent, respectively,

v_1 and v_2 are the volume fractions of the diluent and homopolymer, respectively,

x = the number of segments, and

χ_1 = the Flory–Huggins thermodynamic interaction parameter.

However, in all crystallization based techniques the crystallization step occurs in dilute solution, and as increasing the dilution does not significantly impact the melting temperature [81] Eq. 1 is applicable over the entire range of concentration. Thus, for a homopolymer in a dilute solution the impact of chain length on the dissolution temperature can be quantified by rearranging Eq. 1 into Eq. 2:

$$\frac{1}{T_m} - \frac{1}{T_m^0} = \frac{R}{\Delta H_u} \frac{V_u}{V_1} (v_1 - \chi_1 v_1^2) - \frac{R}{\Delta H_u} \left[\frac{\ln(v_2)}{r} + \frac{v_1}{r} \right] \quad (2)$$

Where, r = number of repeating units per polymer.

In Eq. 2 the second term on the right hand side which accounts for the impact of chain length shows that the equilibrium dissolution temperature drops with decreasing molar mass [81,82]. However, this molar mass influence is significant only for lower values while at higher molar mass the dissolution temperature becomes independent of the chain length and hence Eq. 2 gets simplified to Eq. 3:

$$\frac{1}{T_m} - \frac{1}{T_m^0} = \frac{R}{\Delta H_u} \frac{V_u}{V_1} (\nu_1 - \chi_1 \nu_1^2) \quad (3)$$

From Eq. 3 it can be concluded that homopolymer of relatively high molar mass crystallize at the same temperature provided their composition and other experimental parameters remains same. This is in good agreement with experimental results obtained by CRYSTAF and TREF [83,84].

Copolymers in dilute solution present additional complications as the dissolution temperature also depends on the interactions between the different monomeric units apart from those with the solvent molecules. Taking into account the different interactions between the comonomers and the solvent molecules, the net Flory-Huggins thermodynamic interaction parameter can be defined as in Eq. 4:

$$\chi_1 = \nu_A \chi_{1A} + \nu_B \chi_{1B} - \nu_A \nu_B \chi_{AB} \quad (\text{For copolymer with two comonomers}) \quad (4)$$

Where, χ_1 = interaction parameter of a binary copolymer with pure solvent,

χ_{1A} and χ_{1B} are the interaction parameters of the corresponding homopolymer with the solvent,

χ_{AB} = interaction parameter between comonomers A and B in the copolymer chain,

ν_A and ν_B are volume fractions of comonomers A and B in the copolymer molecule, respectively.

For copolymers in dilute solution, the comonomer unit fraction is the most important factor that affects the crystallizability of the macromolecules. The comonomer units act as defect in the chain and interrupt its regularity, thereby lowering the crystallizability of the macromolecule. The crystallization behavior of copolymers in dilute solution was theoretically explained by Anantawaraskul et al. [85].

5.1.1. Temperature Rising Elution Fractionation (TREF)

TREF was first reported by Desreux and Spiegels in 1950 [86] and has been applied as a routine method to determine the CCD of polyolefins since the late 1980s [87]. TREF is based on a two-step separation process: In the first cycle the sample is dissolved in a thermodynamically good solvent at elevated temperature and the solution is then loaded into a column containing a support (e.g. sea sand or glass beads). Then a cooling cycle at a slow cooling rate with no flow is started, during which the polymer is fractionated by segregation of crystals with successively decreasing crystallinity. This is followed by a second cycle, during which fresh solvent is pumped through the column while the temperature is raised. The solvent dissolves polymer fractions of increasing crystallinity (i.e., decreasing content of SCB), as the temperature is raised. TREF can be performed either on an analytical or preparative (prep. TREF) scale. In a-TREF the concentration of the polymer in solution during the heating cycle is monitored using an infrared detector. In the prep. version fractions of the polymer are collected which can later be analyzed by e.g. HT-SEC, NMR or infrared spectroscopy. Crystallization is the most important step in TREF, and the cooling rate has been observed to have a strong influence on the quality of the separation with lower cooling rates resulting in a higher resolution [87]. The type of support has little to no influence on the fractionation process, and glass beads and

stainless steel shots are commonly used for this purpose. The solvent of choice for TREF of polyolefins are xylene, ODCB and TCB.

TREF has been reviewed by Wild [88], Glöckner [89], Fonseca and Harrison [90], Soares and Hamielec [91], Anantawaraskul [92] and Monrabal [93,94]. Soares et al. explained the broadening of the peaks in TREF observed with increasing comonomer content on the basis of Stockmayer's bivariate distribution [95]. Monrabal et al. [77] experimentally established a linear correlation between the temperature of elution and the SCB content in TREF separations of LLDPE. However, TREF based separations suffer from limitations with respect to throughput and long duration of experiments, which has led to the development of other techniques as given in the next sub-sections.

5.1.2. Crystallization Analysis Fractionation (CRYSTAF)

CRYSTAF was developed by Monrabal [96,97] in the early 1990s with an intention to develop a faster alternative to TREF by fractionating the polyolefin sample in a single crystallization step without the elution step common to TREF. Moreover, 5 samples can be simultaneously analyzed per run, which typically takes between 8 and 24 h. In CRYSTAF the polymer is dissolved in a thermodynamically good solvent (e.g., ODCB, TCB) at elevated temperatures inside a cylindrical reactor. The analysis is carried out stirred crystallization vessels with no support. Aliquots of the polymer solution are filtered out and analyzed with a concentration sensitive detector e.g., IR. The baseline is set from experimental data points taken above the crystallization temperatures. As the temperature is reduced at a fixed rate the polymer sample crystallizes out of the solution according to differences in their crystallizability or SCB/comonomer content. The portion of the sample that remains soluble even at room temperatures (30 °C) i.e., the soluble fraction (SF) represents the non-crystalline (amorphous) fraction of the sample. From CRYSTAF, a profile of concentration (w[%]) versus temperature is obtained. The first derivative of this curve, dW/dT , contains information about the CCD (Figure 16).

Brüll et al. showed the separations by CRYSTAF to be independent of the length of comonomer unit for different propene/ α -olefin [98] and ethylene/ α -olefin [99] statistical copolymers, varying in the type of α -olefins (1-octene, 1-decene, 1-tetradecene, and 1-octadecene). Sarzotti et al. [99] reported that MM influences on the crystallization temperature in CRYSTAF disappeared above the M_w value of 10,000 g/mol with the help of ethylene/1-hexene statistical copolymers. Analogous to TREF, the peaks in CRYSTAF also exhibit broadening with increasing comonomer content as explained theoretically with the help of Stockmayer's distribution. CRYSTAF has been applied to separate blends of HDPE/LDPE and PE/PP [100]. CRYSTAF separations show a linear correlation between the crystallization temperature and the comonomer content of LLDPE similar to TREF. However, although both TREF and CRYSTAF are based on the principle of crystallization TREF has been established to show better resolution as compared to CRYSTAF [87]. Thus, a necessity existed for a method which shows similar resolution as TREF and at the same time overcomes the bottleneck of long analysis time. This led to the development of crystallization elution fractionation (CEF) which is described next.

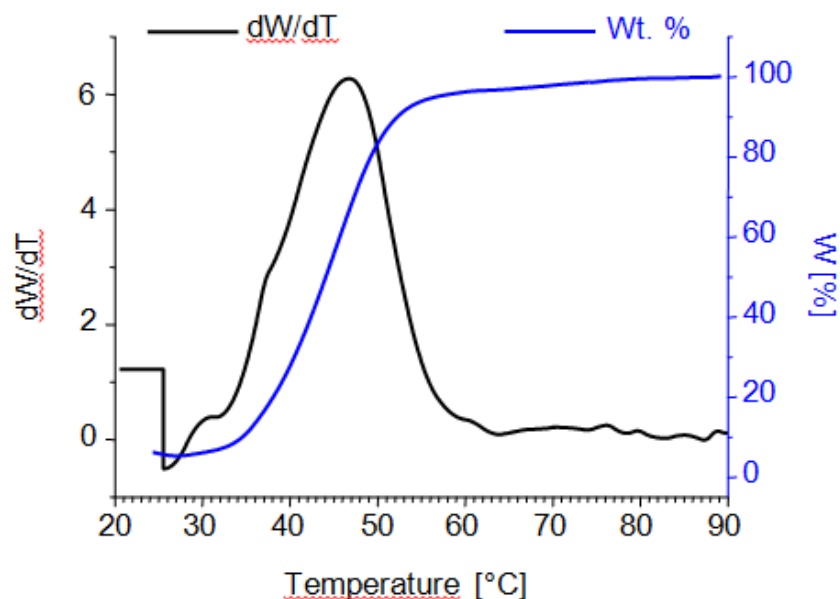


Figure 16 Concentration profile (wt. %) and its first derivative (dW/dT) of a CRYSTAF analysis

5.1.3. Crystallization Elution Fractionation (CEF)

Recently, Crystallization Elution Fractionation (CEF) has been introduced by Monrabal [101,102] to reduce co-crystallization and improve resolution. CEF involves the steps of crystallization and elution. This technique is based on a new separation principle referred to as Dynamic Crystallization. It separates fractions inside a column by crystallizability while a slow flow of solvent is passing through the column. CEF combines the separation power of Dynamic Crystallization in the crystallization step with the separation during dissolution of the TREF, consequently the resolution is improved. CEF achieves resolution comparable to TREF and enables faster analysis by applying the concept of *dynamic crystallization*. The separation in TREF and CEF is shown in Figure 17 as reported by Monrabal et al. [79]

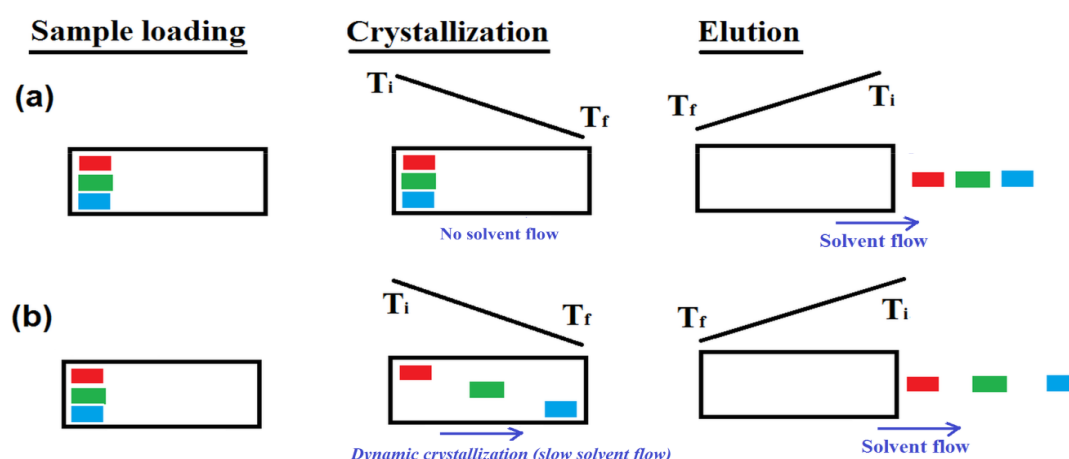


Figure 17 Separation diagram by crystallizability for a) TREF and b) CEF. Note: T_i and T_f are initial and final temperatures in the column [78]

In dynamic crystallization the different components of a sample are separated from each other in the crystallization step, during which a very slow flow of solvent is maintained [78] (Figure 17). This necessitates the usage of longer columns in CEF and also to optimize the flow rate for achieving the best separation. The application of dynamic crystallization enables the use of higher cooling rates which is the principle reason for faster analysis by CEF compared to TREF and CRYSTAF. Monrabal et al. [79,103] compared the CCD based characterization of polyolefins by CEF with that by adsorption based techniques like High Temperature Liquid Adsorption Chromatography (HT-LAC).

In summa, crystallization based techniques are being used routinely to determine the CCD of polyolefins. However, there are two major limitations of the technique that necessitate the finding of fundamental alternatives. The first limitation arises from co-crystallization which makes quantitative separations of blends difficult [85]. Secondly, as these techniques are based on the principle of crystallization, they cannot be applied to polymers with a lower degree of crystallinity. This was shown by Wild [76] and Kelusky [86] who analyzed the CCD of ethylene/vinyl acetate (EVA) statistical copolymers containing 9 – 42 wt. % VA by TREF and found that copolymers with higher VA content are fully amorphous and thus could not be separated by TREF or CRYSTAF. For statistical copolymers of ethylene and 1-octene the range of separation via CRYSTAF has been found to be in the range 0 – 27 wt. % (or 0 – 9 mol %) of 1-octene content [79,104]. This range may be increased by applying cryogenic techniques, but the freezing point of the solvent acts as a limiter. These limitations provided the driving force for the development of high temperature high performance liquid chromatography (HT-HPLC) as an alternative method for CCD determination of polyolefins.

5.2. High Performance Liquid Chromatography (HPLC)

HPLC has been applied as a fast and selective separation technique to determine the MMD and CCD of polymers soluble at room temperature for many decades. In HPLC the macromolecules are separated based on different retention times as they pass through a chromatographic system comprising of a specific stationary and mobile phase. Different retention times of the individual components are caused by differences in the partitioning equilibrium between the stationary phase and the mobile phase [105]. The equilibrium can be expressed by the partitioning coefficient, K_d , given by Eq. 5:

$$K_d = \frac{C_{SP}}{C_{MP}} \quad (5)$$

Where, C_{SP} and C_{MS} are the concentrations of the analyte in the stationary phase and mobile phase, respectively.

Thermodynamically, K_d is related to the difference in Gibbs free energy of the analyte in both the mobile and the stationary phase [106]. The difference between the enthalpic and entropic contributions results in a change of the Gibbs free energy (ΔG) as shown in Eq. 6:

$$\Delta G = \Delta H - T\Delta S = -RT \ln K_d \quad (6)$$

Eq. 6 rearranges into Eq. 7:

$$\ln K_d = \frac{-\Delta G}{RT} = \frac{-\Delta H + T\Delta S}{RT}$$

$$K_d = \exp(\Delta S / R - \Delta H / RT)$$
(7)

Where, R = universal gas constant,
 T = the absolute temperature,
 ΔH and ΔS are the changes in enthalpic and entropic contributions, respectively.

ΔH is the overall change in enthalpy from different attractive or repulsive interactions of the macromolecules with both the stationary and the mobile phase. ΔS is the overall change in entropy of the macromolecules arising from differences related to the hydrodynamic volume as they are excluded or enter the pores [107] of the stationary phase. The enthalpic and entropic contributions in a chromatographic separation can be controlled by the choice of the stationary and mobile phase and the temperature. Based on the enthalpic and entropic contributions, HPLC separations can be classified into size exclusion chromatography (SEC), liquid adsorption chromatography (LAC) and liquid chromatography at critical conditions (LCCC). Recently, LCCC for high temperature soluble polymers i.e., PE [108] and PP [109] was established.

In summa, depending on the mechanism three modes of chromatographic separation can be distinguished in the case of polymers, which differ with regard to their relationship between the molar mass and the elution volume (Figure 18).

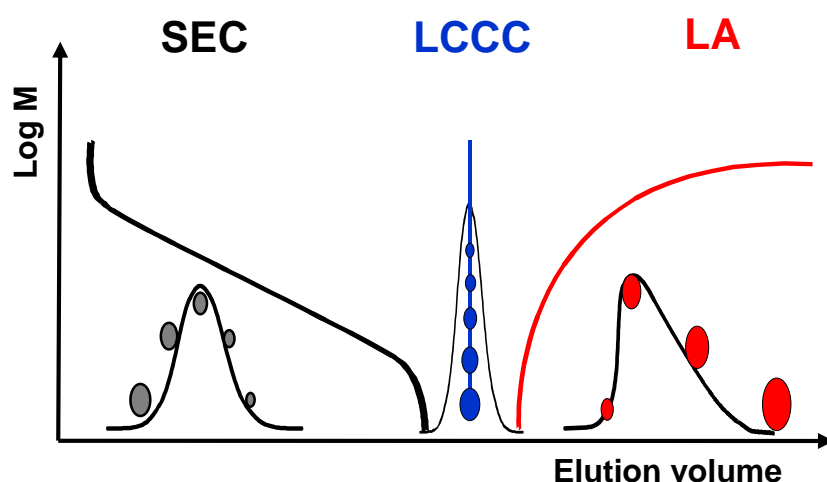


Figure 18 Three modes of chromatographic separation

5.2.1. Size Exclusion Chromatography (SEC)

SEC separates macromolecules based on differences in their hydrodynamic volume in a mobile phase. The parameter, which determines the separation i.e., the hydrodynamic volume is a function of the molar mass, the molecular architecture, and the chemical composition. Semi-crystalline polyolefins require elevated temperatures ($> 100\text{ }^{\circ}\text{C}$) for dissolving, and this led to the development of high temperature SEC (HT-SEC) [110]. A HT-SEC column set comprises multiple columns connected in series that fulfill the necessary pore size distribution according

to the sample being analyzed. The stationary phase of choice is cross-linked poly styrene divinylbenzene, whereas the routinely used mobile phase is TCB. The elution volume in HT-SEC can be converted to molar mass by using narrow disperse standards of known MM. This calibration can then be applied to extract information about MM, MMD and dispersity (\bar{D}) of unknown polymers samples. Since different polymers are extended to different sizes in different solvents, a calibration curve has to be created for every polymer/solvent system. However, in case the calibration standards are not chemically identical to the sample, the obtained MM, MMD, and \bar{D} of the sample can be expressed only as a relative value. This problem can be solved by attaching a MM sensitive detector e.g., multi-angle laser light scattering (MALLS) [111] which enables to determine the absolute MM.

Various detectors have been used with HT-SEC for the characterization of polymers. A refractive index (RI) detector has been preferred for measuring the concentration of polymer eluting from the columns (HT-SEC/RI). More recently, infrared (IR) spectroscopy has gained acceptance as concentration sensitive detector for HT-SEC (HT-SEC/IR). The main advantage IR shows over the RI detectors are a comparatively more stable baseline and lower sensitivity to temperature fluctuations which is particularly important for high temperature applications. Coupling HT-SEC with spectroscopic techniques, such as FTIR [112,113] or NMR [114,115] enables to determine average chemical compositions along the molar mass axis. HT-SEC→FTIR of polyolefins can be performed in two ways: either the eluent from the HT-SEC column is sprayed onto a rotating germanium disk and subsequently analyzed off-line by FTIR [116] or the columns are coupled to a heated flow cell placed in an FTIR spectrometer [117,118]. Hereby, profiles are obtained showing the MMD and, additionally, the content of SCB as a function of molar mass. Nowadays, besides IR spectrometers recording full spectra, IR detectors with fixed wavelengths using at least two different band filters are also available for compositional analysis [119]. TCB (or ODCB or tetrachloroethylene) can be used as mobile phase for flow through FTIR detection as it is sufficiently transparent between ca. 3500-2700 cm^{-1} , which corresponds to the $> \text{C-H}$ stretching region i.e., the region of interest for polyolefins. Typically, at least two bands associated to methyl ($-\text{CH}_3$) and methylene ($-\text{CH}_2-$) groups are measured and their ratio is calibrated against polymer standards [119,120]. This method is not applicable for very low degrees of branching ($< 2\text{-CH}_3/1000\text{C}$) due to signal to noise limitations.

HT-SEC has also been applied to analyze the distribution of LCB in polyolefins such as LDPE by coupling it to specific detectors. The presence of LCB makes the macromolecule more compact compared to a linear one i.e., the hydrodynamic volume is smaller for the LCB containing macromolecule compared to the linear equivalent. This effect may be observed by applying a viscometer (VISC) and/or light scattering (LS) detector. A viscometer detects the presence of LCB by comparing the resultant differences in their intrinsic viscosity, and a LS detector determines the LCB content by comparing the radius of gyration (R_g) of a branched and a linear macromolecule with similar MM. Both detectors can be coupled on-line to HT-SEC e.g., HT-SEC/RI-VISC, HT-SEC/LS, or HT-SEC/RI-VISC-LS, to analyze the LCB distribution along the MMD of polyolefins. The triple detector system HT-SEC/RI-VISC-LS is becoming increasingly common for unraveling the molecular heterogeneities of polyolefins [110]. HT-SEC has also been applied to determine the distribution of SCBs along the MMD in olefinic copolymers by coupling it with Fourier transform infrared (FTIR), off-line methods via a LC-Transform [121] or on-line with a heated flow cell [122].

5.2.2. Liquid Adsorption Chromatography (LAC)

LAC has been widely used to separate polymers which are soluble at ambient temperatures according to their composition. The separation is driven by enthalpic interactions between the macromolecules and the stationary phase in the presence of an appropriate mobile phase and temperature. The thermodynamics behind an ideal LAC separation can be represented by Eq. 8:

$$K_d = K_{LAC} = e^{\frac{-\Delta H}{RT}} \quad (8)$$

Since ΔH is negative the values of the distribution coefficient K_{LAC} are > 1 . In order to achieve enthalpic interactions between the dissolved macromolecules and the stationary phase, a thermodynamically poor i.e., adsorption promoting solvent is used as mobile phase. By adding a thermodynamically good (desorption promoting) solvent the enthalpic interactions between the macromolecules and the stationary phase can be reduced. Glöckner [123] noticed that there is a fundamental difference between the behavior of low molar mass compounds and macromolecules, which is called a molar mass effect. With increasing molar mass the number of interacting units and consequently the adsorption of the molecules on the stationary phase increase. The molar mass dependence in LAC is opposite to that in SEC. The strength of interaction between the analyte molecules and the stationary phase can be either controlled by the eluent composition (e.g. solvent gradient) and/or the temperature [124].

The majority of published HPLC separations of synthetic polymers has been realized at temperatures below 60 °C [123,125]. Dissolution and chromatographic separation of semi-crystalline polyolefins, however, require temperatures of up to 130 – 160 °C [126-128]. This led to the development of high temperature LAC (HT-LAC) to investigate semi-crystalline polyolefins. Macko et al. [129] were the first group to show the irreversible retention of linear PE and isotactic PP from dilute solutions in decalin on specific zeolites in 2003. Since the process is irreversible the approach was not a practical solution to the challenge. The first chromatographic systems for the separation of polyolefins according to their chemical composition (HT-HPLC) were published only recently [130-132]. They were based either on the selective precipitation/dissolution (PP is soluble in ethylene glycol monobutyl ether and PE non-soluble) or on the selective adsorption/desorption of PE or PP [133-135].

Heinz et al. [136] separated a blend of HDPE and *i*-PP by using silica-gel as stationary phase and a gradient of TCB→ethylene glycol monobutyl ether (EGMBE) by a mechanism of precipitation/dissolution. (EGMBE is a solvent for *i*-PP and non-solvent for PE) in 2005. However, the separation was significantly influenced by the MM of the polymer, which even overrides the effect of composition on the separation, and method was not robust and reliable. Möckel et al. [137] found that n-alkanes are retained on a carbon-based column (Hypercarb™) from methanol stronger than on a reversed phase silica gel. Adsorption isotherm studies by Kalies et al. [138] revealed that n-alkanes are preferentially adsorbed from alcohols on a carbon sorbent. Findenegg and Liphard observed that C₁₆-C₃₂ alkanes show affinity towards a graphite surface via adsorption isotherm measurements [139]. Yin et al. [140] also found that there were interactions between graphite and C₈-C₃₄ alkanes. Additionally, the strength of interaction increases with the chain length. This methodology was first extended and applied on non-polar polyolefins by Macko and Pasch in 2009 [141]. This breakthrough came with the discovery of porous graphitic carbon (PGC) as stationary phase [141,142].

The development of PGC for liquid chromatography, which is commercially available as Hypercarb™, is credited to Knox et al. [142]. PGC constitutes of porous spherical particles with a surface that is crystalline and devoid of micro-pores. At the molecular level PGC is made up of graphitic sheets of hexagonally arranged carbon atoms linked by conjugated 1.5 order bonds, which are stacked together on top of each other. The graphitic carbon atoms have fully satisfied valencies and hence in principle there are no functional groups on the surface of PGC. PGC is produced by first choosing a highly porous silica as template into which the carbon based material is impregnated with a phenol-formaldehyde mixture. This mixture is then heated to 80 – 160 °C to initiate polymerization. The size and porosity of the carbon particles produced depend upon the choice of the silica template. This is then pyrolyzed under inert atmosphere (nitrogen) at 1000 °C to produce a highly porous amorphous carbon. The silica template is then dissolved by passing a hot aqueous solution of sodium hydroxide. The porous amorphous carbon is next graphitized by thermal treatment at 2340 °C under inert atmosphere (argon) results in the removal of surface functional groups, rearrangements in the graphite structure and closing of micro-pores.

LAC can be conducted in two ways based on the type of gradient that drives the separation. When the separation is controlled by varying the mobile phase composition while keeping the temperature constant, the LAC method is termed as solvent gradient interactive chromatography (SGIC). On the contrary, if the separation is controlled by varying the temperature of the stationary phase at isocratic mobile phase composition the method is referred to as Thermal Gradient Interactive Chromatography (TGIC). For the purpose of the thesis only the high temperature gradient techniques will be described as the focus of the thesis is on polyolefins.

5.2.2.1. High Temperature Solvent Gradient Interaction Chromatography (HT-SGIC)

In HT-SGIC the macromolecules are separated by applying a gradient of mobile phase composition at isothermal conditions. Typical adsorption promoting solvents for polyolefins are 1-decanol and n-decane, while ODCB and TCB [143-145] are desorption promoting. In HT-SGIC the sample is first dissolved and injected in an adsorption promoting solvent to adsorb the macromolecules onto a column packed with graphitic sorbents. The adsorbed sample is then selectively desorbed by applying a gradient from adsorption to desorption promoting solvent. The adsorbed macromolecules elute depending on the strength of adsorption with the sorbent, which in turn is a function of their composition and, to a subordinate extent, their MM.

Various carbon sorbents like PGC, carbon-clad zirconia, activated carbon and exfoliated graphite were tested by Chitta et al. [146] with regard to their selectivity as stationary phase for HT-SGIC of PE and PP of varying tacticity. HT-SGIC has been applied to separate blends of linear PE and PP of varying tacticity [141]. Statistical copolymers of ethylene/ α -olefins as well as propylene/ α -olefins were also separated based on their α -olefins content by HT-SGIC [143]. The separation in HT-SGIC was shown to be independent of MM above ~20 kg/mol by Ginzburg et al. [145] for HDPE in a 10 minute linear gradient of 1-decanol \rightarrow TCB. The separation of polyolefins by HT-SGIC has been reviewed by Macko et al. [147].

The significant advantage of HT-SGIC over crystallization based techniques like TREF, CRYSTAF and CEF is the fact that it offers the capability to separate olefinic copolymers over the full range of comonomer content [143,148]. Yet, HT-SGIC is limited with regard to the choice of detectors with the evaporative light scattering detector (ELSD) being the only option.

The ELSD suffers from non-linear dependence of the detector signal on sample concentration as well as solvent composition [149]. Even with careful calibration of its response, it is extremely difficult to obtain quantitative results with the ELSD, and this was the driving force for the development of HT 2D-LC as an analytical tool for polyolefin separations.

5.2.2.2. High Temperature Two dimensional Liquid chromatography (HT 2D-LC)

In chromatography, the separation efficiency of any single separation method is limited by the efficiency and selectivity of the separation mode, that is, the number of plates of the column and the phase of the selected system. As discussed, polyolefins are distributed in more than one parameter of molecular heterogeneity. It is obvious that independent parameters require n-dimensional analytical methods for accurate (independent) characterization of the different structural parameters.

Comprehensive two dimensional liquid chromatography implemented by coupling two separations exists in three schemes: on-line; stop-and-flow; and off-line. Each approach has distinct features and drawbacks; particular approaches allow making use of one of them more advantageous than that of the other ones for some specific applications, as it was demonstrated by Fairchild et al. [150]. The resulting data is a matrix, usually represented as a contour plot, with each chromatographic separation along an axis. In the very first examples of 2D-LC separations of synthetic polymers, SEC was performed first [151] followed by HPLC in the second dimension. In these experiments, the heart-cut (off-line) approach was very frequently used; meaning, that only selected fractions were transferred into the second dimension. In recent years, the sequence of HPLC in the first dimension and SEC in the second dimension is favored. Owing the fact the fact that state of the art SEC experiments employing new small columns with improved separation efficiencies can be performed in a very short period of time (down to several minutes) [151-153], a complete transfer of all fractions from the first dimension into the SEC column became possible (Figure 19).

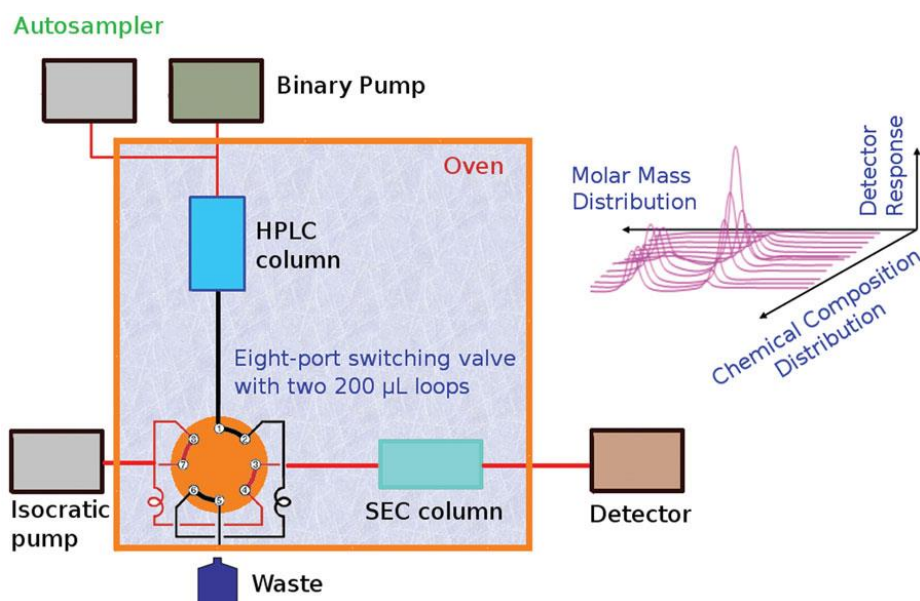


Figure 19 Schematic configuration of HT-HPLC × HT-SEC setup (HT 2D-LC) [145]

The advantages and disadvantages of using either HPLC \times SEC or SEC \times HPLC sequences were discussed in detail by van der Horst and Schoenmakers [154,155]. From the practical point of view, a preferred 2D-LC set-up is fractionation of a sample by HPLC and subsequent analysis of the fractions eluting from the HPLC column by SEC. Namely, HPLC was found to be less sensitive towards molar mass effects and yielded uniform fractions with respect to chemical composition. SEC is in the majority of publications used for the second dimension, which allows using different detectors [151]. In the case of using SEC in the first dimension, each fraction is dissolved in a thermodynamically good solvent when injected into HPLC and breakthrough peaks can occur [156]. If SEC is used in the second dimension, the injected solvent from the HPLC will simply be separated from the polymer fraction. In the present treatment, we will focus exclusively on the comprehensive mode, where the entire first dimension effluent is subjected into the second dimension separation.

An eight-port valve with matching sample loops is typically used for the coupling [151]. The valve is controlled electronically and allows a complete transfer of all eluting polymer fractions from the first to the second dimension by choosing the proper flow rates in both dimensions and by adjusting the sampling time. The configuration of such a transfer valve is depicted in Figure 20.

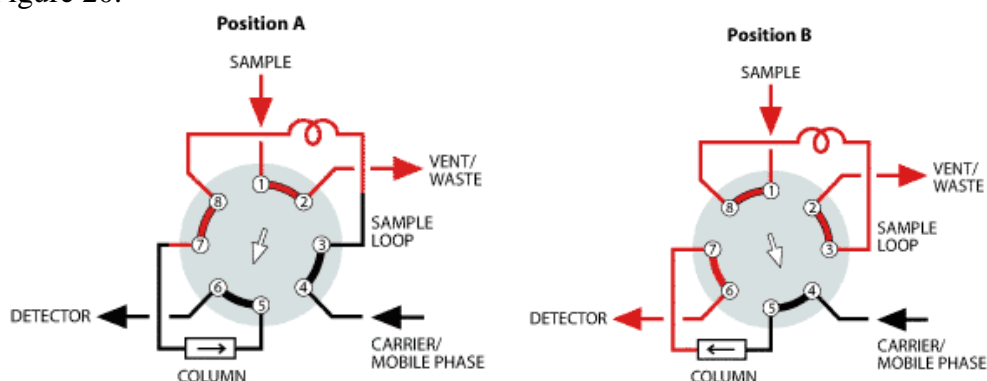


Figure 20 Configuration of an automatic fraction transfer valve (from vici.com)

However, such separations were realized at high temperature only recently for functionalized semi-crystalline polyolefins [157], ethylene/1-octene copolymers [158], and polyolefin blends [159,160]. Polymer samples undergo two fractionation steps in 2D LC, finally resulting in highly diluted analytes. Highly sensitive detectors are thus required for quantification.

5.2.3. Cross-Fractionation Techniques

The multitude of molecular heterogeneities in polyolefins has already been discussed. These heterogeneities with regard to various molecular parameters are as a rule inter-related and influence each other, and cross-fractionation techniques were developed to study these relationships. Coupling two orthogonal separations can also significantly enhance the separation efficiency as shown theoretically by Rittig et al. [161]. Various cross-fractionation techniques have been developed but only those applicable for polyolefins will be discussed as part of this thesis.

In polyolefins the two most important molecular heterogeneities are the CCD and the MMD, and, therefore, the majority of cross-fractionation techniques aim to couple different analytical techniques to determine the bivariate CCD \times MMD. Technically, the coupling may be realized

via stop-flow (off-line) or in a continuous mode (on-line). The advantages of both approaches were reviewed by Fairchild et al. [150]. HT-SEC is routinely applied to determine the MMD of polyolefins [110]. However, for determining the CCD different crystallization and, more recently, LC based techniques are used. Wild [76] first combined TREF and HT-SEC in an off-line manner (TREF x HT-SEC). Since 2007, Ortin et al. [162] have commercialized an automated TREF x HT-SEC instrument which has led to more consistent results compared to earlier constructed setups. Although TREF x HT-SEC offers the required comprehensive characterization a limitation is the fact that TREF can only be applied to well crystallizable samples [163]. This spurred the application of HT-LAC for the determination of CCD and the development of two dimensional liquid chromatography (2D LC) techniques. Several successful 2D LC separations have been reported for polymer at ambient temperatures [164-166]. However, for polyolefins the development of HT 2D-LC separations has been possible only recently [167,168], with the combination of HT-SEC and HT-LAC in an on-line mode. The results of a cross-fractionation experiment are usually represented in a color coded contour plot. Similarly, in 2D HT-LC, the two different chromatographic modes of separation are denoted by the two axes of the contour plot, and the intensity of the peaks is shown by a color scale.

BiHDPE and functionalized POs are commercially relevant materials. Their application properties are defined by their molecular heterogeneities, which are defined by the distributions with regard to molar mass, composition, and microstructure (stereo- and regio-regularity). These distributions are interrelated, and their analysis requires multi-dimensional separations, with a maximum degree of orthogonality. These bivariate distributed samples can be characterized by HT 2D-LC. However, in order to get the microstructural information hyphenation with ^{13}C hyphenation is required. Nevertheless, NMR needs sufficient amount of material for microstructural characterization. Thus portable fraction collector (explained elaborately in section 6.3) was employed to collect sufficient fraction from HT-SEC or HT-HPLC (first dimension) and then subsequently analyzed in ^1H NMR and ^{13}C NMR.

The complete timeline for the characterization of POs using liquid chromatography is shown in Figure 21.

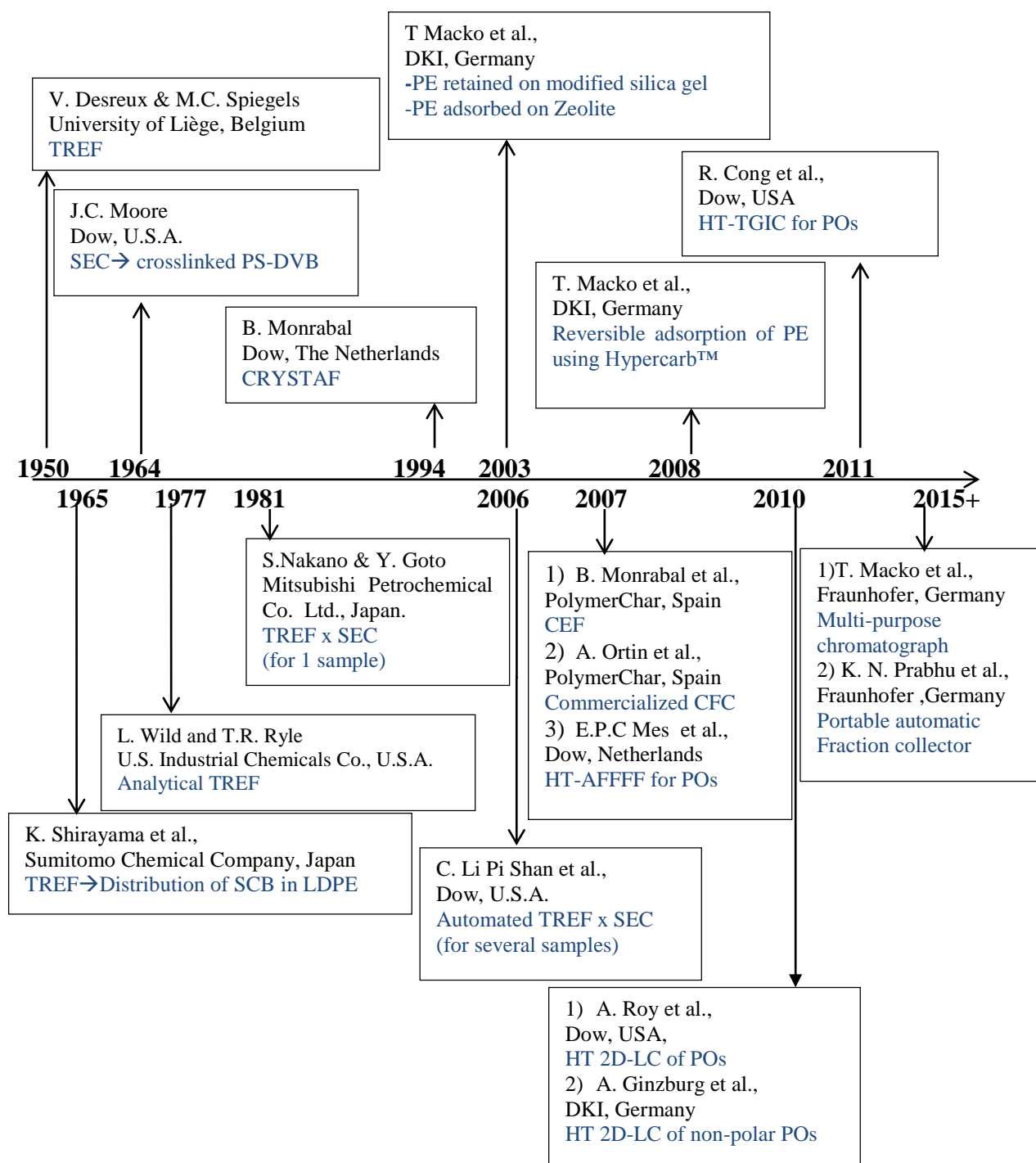


Figure 21 Timeline for the polyolefin characterization using liquid chromatography

5.3. Raman Spectroscopy

Raman spectroscopy is sensitive to structural changes of carbon materials [169-173]. Several researchers utilized Raman spectroscopy to characterize different carbon materials and focused on the origin of the D and G band [34-39]. The Raman spectrum of graphite exhibits three prominent bands, namely the G-band (graphite band), the D-band (disorder band), and the 2D band (overtone of the D-band) [169-172,174]. The G-band is the primary Raman active mode in graphite, and it provides a good representation of the sp^2 -bonded carbon that is present in the planar sheet configurations of graphite. The G-band originates from the tangential vibrations of the carbon atoms and these in-plane vibrations are Raman active [172,174-176]. The D-band, also known as the disorder or defect mode, originates from edge configurations in graphite where the planar sheet configuration is disrupted [172,174-176]. The 2D-band is an overtone of the D-band, but its intensity does not necessarily track with that of the D-band. Yet, the 2D-band is generally more sensitive to the changes in the environment of planar sheet configuration than the D-band [169,172]. The G-band which appears for the graphitic structures is characteristic of the C-C vibrations [174,177]. In case of interactions between an analyte and graphite in a solution this G-band can shift [169-172,174-176,178,179]. Hodkiewicz et al. [172] reported a G-band shift to higher wavenumber when comparing the spectrum of graphene with that of graphite. The interaction between the basal planes of graphite is largely dominated by long range van der Waals forces, which originate from the correlated motions of electrons in different planes [172]. Thus, Raman spectroscopy can be utilized to gain more insight into the interaction between graphite (Hypercarb™) and polyethylene (PE) in an organic solution (n-decane) at temperatures above the crystallization temperature of PE.

5.4. Nuclear Magnetic Resonance (NMR) Spectroscopy

NMR spectroscopy is a powerful technique for chemical analysis having extensive applications in inorganic and organic chemistry, biochemistry, as well as medical sciences. NMR is based on the interaction of the magnetic properties of nuclei with an external magnetic field. In the absence of an external magnetic field the nuclei are aligned in a way that the magnetic dipoles are randomly oriented. However, when an external magnetic field is applied, the dipoles orient in different energy states based on an energy difference, ΔE , governed by Eq. 9:

$$\Delta E = \left(\frac{h\gamma}{2\pi} \right) B \quad (9)$$

Where, γ = gyromagnetic ratio,

h = Planck's constant,

B = the strength of the external magnetic field.

The energy states with and without an external magnetic field for ^1H are shown in (Figure 22) as an example.

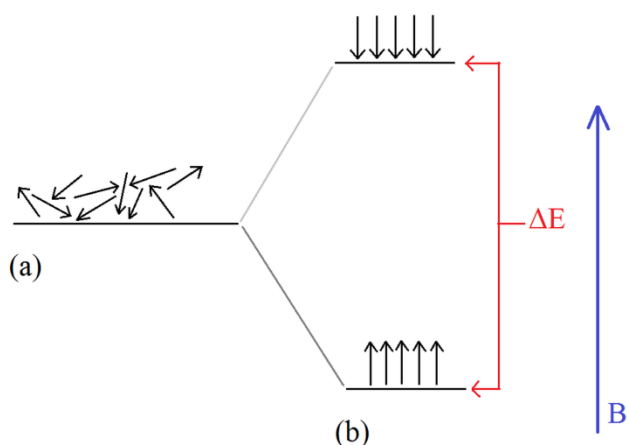


Figure 22 Representation of spins of ^1H atoms under (a) no magnetic field and (b) an external magnetic field B

Apart from the nucleus, the applied magnetic field also interacts with the electrons spinning around the nucleus. The spinning electrons induce a secondary magnetic field which also influences the total magnetic field experienced by the nuclei. As the electron cloud is distributed unevenly in a molecule, the magnetic field experienced by a specific nucleus depends on its environment, and this delivers vital information about the molecular structure of the sample. Different nuclei are chosen for NMR spectroscopy based on requirement. Examples of nuclei applied for NMR are ^1H , ^{13}C , ^{15}N , ^{19}F , ^{31}P etc. Among these ^1H and ^{13}C are most commonly applied in NMR spectroscopy of polyolefins and will be focused on in greater detail.

5.4.1. NMR of Polyolefins

For polyolefins NMR spectroscopy serves as an excellent technique for structure elucidation. A variety of structural information may be derived from a NMR spectrum with the help of *chemical shift* (ppm) which represents the ΔE relative to the reference proton (e.g., ^1H in Figure 22). A reference is commonly chosen, e.g., tetramethylsilane (TMS), whose chemical shift is assigned 0.00 ppm, and the different resonances are arranged according to the IUPAC recommended δ chemical shift scale [180]. The shielding effect from the surrounding electrons also influences the values of chemical shift. Even the same nucleus may exhibit different shifts based on differences in the electron cloud surrounding it, and this assists in deriving vital information about the microstructure of polyolefins. The factor that determines the position of the signal in an NMR experiment is the magnetic field created by the other nuclei and the electrons in the molecule.

NMR spectroscopy of polyolefins requires elevated temperatures and solvents which have to be chemically stable and that don't evaporate at elevated temperatures. Additionally, for quantitative analysis of polyolefins the experimental parameters of NMR like probe tuning and relaxation delay need to be optimized [181]. NMR spectroscopy has become a routine technique for the characterization of polyolefins, and a few common applications are covered in the next section.

^1H and ^{13}C are the commonly applied nuclei for NMR spectroscopy of polyolefins. ^1H NMR has significantly higher sensitivities compared to ^{13}C NMR and is commonly applied for determining the chemical composition e.g., functional groups [182], end-groups [183],

unsaturation [181-184] etc., that are present in too small quantities to be detected by ^{13}C NMR. ^1H NMR finds application as a great tool for quantification as it doesn't require additional calibration [181]. The area under the curve of each ^1H NMR signal is proportional to the number of equivalent protons creating the signal. Hence, by integrating the area under each curve the relative number of protons that constitute each curve can be quantified.

^{13}C NMR is the preferred technique for investigating the microstructure of polyolefins. The larger spectral width (~ 20 times) of ^{13}C NMR compared to ^1H NMR enables quantification of the microstructure of polyolefins. ^{13}C NMR has been successfully applied to determine microstructural information such as tacticity [185], inverse insertion [185] and comonomer sequence distribution [186]. ^{13}C NMR has also been applied to quantify SCB [187-189] and LCB [187-190] content in PE. The peak assignments for ethylene/1-octene copolymers (E/O) were reported by Qiu et al. [191].

6. Experimental

6.1. Column Packings

A Hypercarb™ column (Thermo Fisher Scientific, Dreieich, Germany) containing porous graphite particles with particle diameter 5 µm and column size 250 x 4.6 mm, L. x I.D. was used for HT-HPLC measurements.

A silica gel column (PerfectSil® 300 Å from MZ Analysentechnik, Mainz, Germany) with an average particle diameter of 5 µm and a column size of 250 x 4.6 mm L. x I.D. was used for HT-HPLC measurements.

Particles of Mica (muscovite) from Creations Couleurs, The Innovation Company, Dreux, France, with a particle diameter between 5 – 15 µm, were dry packed manually into a column of 150 x 4.6 mm L. x I.D. and was used for HT-HPLC measurements.

PLgel Olexis column (Polymer Laboratories, Church Stretton, England) containing particles of 10 µm diameter and a column size of 300 x 7.5 mm L. x I.D. was used for HT-SEC measurements

A PL Rapide H column (Polymer Laboratories, Church Stretton, England) containing particles of 10 µm diameter and a column size of 150 x 7.5 mm, L. x I.D. was used for HT-SEC measurements.

6.2. Samples

HDPE (1st reactor product) and LLDPE (2nd reactor product) were prepared using the same Z-N catalyst as used for synthesis of the BiHDPE sample and were obtained from SABIC, Geleen. A series of ethylene/1-butene (EB) copolymers, synthesized with a Z-N catalyst, was received from SABIC, Geleen and EB copolymers, synthesized with a metallocene catalyst as described in [192], were obtained from Dr. Y. Thomann (University, Freiburg, Germany).

A linear PE standard (500 – 126 kg/mol) from PSS, Mainz, Germany was used. Isotactic PP (*i*-PP) with different M_w (e.g., *i*-PP – 250 kg/mol (*i*-PP²⁵⁰)) was products of American Polymer Standards Corp. (Mentor, US). The weight average molar mass (M_w) and dispersity index (\bar{D}) were determined by HT-SEC using a calibration with linear PE standards in the range of 0.5 – 126 kg/mol and a \bar{D} range of 1 – 2 (PSS, Mainz, Germany). The average comonomer content was determined by ¹³C NMR spectroscopy and the average polar comonomer content was determined by titration method.

Two PP-g-MA samples with varying MA content i.e., PP-g-MA with 1 mol % MA (PP-g-MA¹) and PP-g-MA with 1.7 mol % MA (PP-g-MA^{1.7}) were also obtained from SABIC, Geleen.

The characteristics of the samples obtained are listed in Table 3.

Table 3 Characteristics of the polymer samples

Sample name	**Average amount of comonomer [mol %]	Comonomer	Catalyst	M _w [kg/mol]	Đ	MMD	Ref.
HDPE	*n.a.	n.a.	Z-N	34	7	monomodal	This work
LLDPE	1.2	1-butene		480	5.6	monomodal	
BiHDPE	0.80	1-butene		270	30	bimodal	
EB	5.8	1-butene	Metallocene	307	2.4	monomodal	[192]
	11.2	1-butene		304	2.5		
	19.1	1-butene		248	2.3		
	35.3	1-butene		198	2.4		
	56.1	1-butene		149	2.4		
	65.9	1-butene		175	2.5		
	77.8	1-butene		196	2.4		
EB	0.26	1-butene	Z-N	500	3.3	monomodal	This work
	0.28	1-butene		205	3.8		
	0.40	1-butene		115	4.1		
	0.42	1-butene		365	2.9		
	0.58	1-butene		440	2.8		
	0.96	1-butene		292	3.2		
	2.44	1-butene		245	3.7		
	3.48	1-butene		220	3.9		
	3.78	1-butene		150	3.1		
	4.10	1-butene		120	5		
<i>i</i> -PP ⁹⁵		n.a.	n.a.	95	3.4	monomodal	This work
<i>i</i> -PP ²⁵⁰		n.a.	n.a.	250	5.5	monomodal	
PP- <i>g</i> -MA	1	MA	n.a.	132	5.1	monomodal	
PP- <i>g</i> -MA	1.7	MA	n.a.	103	3.4	monomodal	

*n.a. - not applicable

The polymer solutions were prepared by dissolving the samples in the adsorption promoting solvent (1-decanol/decalin) at concentrations of about 1 – 1.5 mg/mL. The temperature of the dissolution was 160 °C/140 °C and the time of dissolution was in the range of 2 – 3 h.

6.3. Solvents

n-decane (boiling point: 174 °C), n-dodecane (216 °C), 2-methylundecane (200 °C), 1-decanol (233 °C), 1-decanol, 2-octanol (178.5 °C), 2-ethyl-1-hexanol (186 °C), 1-chloronaphthalene (113 °C), tetrachloroethene (TCE, 121 °C), decahydronaphthalene (186 °C) and cyclohexanone (156 °C) were used as received as adsorption promoting solvents. 1,2,4-trichlorobenzene (TCB, 214 °C), and 1,2-dichlorobenzene (ODCB, 180 °C) were distilled prior to use as desorption promoting solvents. The solvents were obtained from Merck, Darmstadt, Germany.

6.4. High Temperature Size Exclusion Chromatography

A high temperature chromatograph PL 220 (Polymer Laboratories, Agilent, Church Stretton, England) was used to determine the MMD. The temperature of the injection sample block and of the column compartment was set at 150 °C. The flow rate of the mobile phase (TCB containing 2,6-di-tert-butyl-4-methylphenol at 2 g/L) was 1 mL/min. The polymers were dissolved for 3 h in TCB (containing 2,6-di-tert-butyl-4-methylphenol) at a concentration of ~1 mg/mL at 150 °C. 200 µL of a polymer solution were injected. Polystyrene standards (Polymer Standards Service, PSS, Mainz, Germany) were used for calibration of a column set (3 x PLgel Olexis). Universal calibration was created for PE using the Mark-Houwink equation. The respective Mark-Houwink coefficients used for PE in TCB are mentioned below. An infrared detector (IR4 from PolymerChar, Valencia) was used for detection.

For polystyrene: $[\eta] = 1.26 \times 10^{-4} M^{0.702}$

For polyethylene: $[\eta] = 3.8 \times 10^{-4} M^{0.73}$

6.5. Analytical SEC (ASEC) – LC-Transform – FTIR Off-line

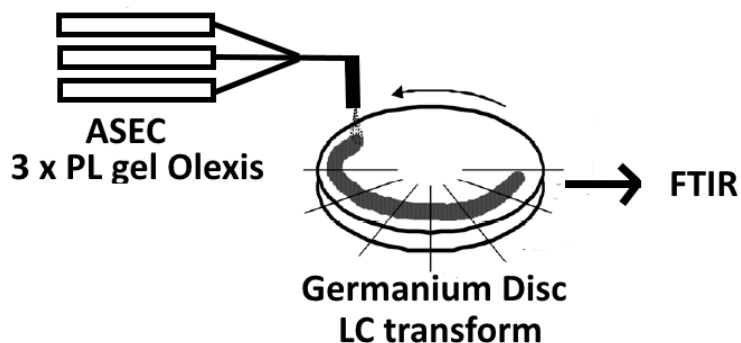


Figure 23 Schematic setup of ASEC – LC-Transform – FTIR

Figure 23 schematically shows the procedure followed: The polymer sample of interest was separated using a PL GPC 120 (Polymer Laboratories, Church Stretton, England). Three PLgel Olexis columns were used with TCB as the mobile phase at a flow rate of 0.5 mL/min. The entire system was thermostated at 150 °C. After HT-SEC fractionation, the analyte was deposited on a rotating germanium disc in the LC-Transform solvent evaporation interface (Series 300, Lab Connections, Marlborough, MA, USA). The rotating speed of the germanium disc was 10 °/min. The deposited trace of the polymer was analyzed off-line by FTIR spectroscopy (Nicolet™ iS™ 10 FTIR spectrometer, Thermo Scientific, Dreieich, Germany)

with a scan rate of 1 %/spectrum. 16 scans were accumulated per spectrum and a baseline was automatically subtracted for each measurement.

Gram-Schmidt plots [193-195] and the profiles of the carbonyl index (CI) were calculated from the obtained data sets. The Gram-Schmidt plot reflects the overall integrated intensity of the IR absorption (2800 – 3000 cm^{-1}) along the chromatographic run. The CI is defined as the ratio of the carbonyl absorption (range 1700-1780 cm^{-1}) to the $-\text{CH}_2-$ and $-\text{CH}_3$ vibration (2800 – 3000 cm^{-1}) of the polymer.

6.6. Steps for Preparative Fractionation of HT-SEC Coupled with ^1H NMR Off-line (Off-flow HT-SEC \rightarrow ^1H NMR)

The following protocol was used for hyphenating HT-SEC and NMR;

- 1) The polymer sample was dissolved in TCB at 160 °C and injected into the HT-SEC column (PLgel Olexis) at a flow rate 1 mL/min.
- 2) The elution time window for each fraction was marked in the HT-SEC chromatogram.
- 3) The ELSD was replaced by the portable automatic fraction collector.
- 4) A table was created (should be saved as .REL format) listing the elution time for each fraction (valve rotation time).
- 5) The created table was loaded in the relay 01 in the WinGPC PSS software and the time at which the valve should return to home position was mentioned in relay 02.
- 6) The relay starts as soon as the sample gets injected in the HT-SEC column and the fractions were collected as per program (table).
- 7) 20 mL vial was used to collect the fractions and a specially designed in-house aluminum holder was utilized to hold the vials.
- 8) After collecting sufficient amount of fractions the TCB was evaporated in vacuo at 100 °C.
- 9) 0.5 mL of deuterated TCE were added to the polymer residue and heated in a rotary heater to ensure dissolution of the sample as confirmed by visual inspection.

6.7. Calculations to Collect Sufficient Amount of Sample for Off-flow HT-SEC \rightarrow ^1H NMR

The number of injections has to be calculated to collect sufficient amounts of sample for each fraction for NMR analysis. Due to the technical limitation of the 1D (HT-HPLC) instrument, the maximum amount of the sample solution which can be injected into the column is 150 μL . From the dissolution study it was observed that only 3 mg/mL of the given BiHDPE sample can be dissolved completely in TCB. Thus, the total amount of material injected into the HT-SEC column per injection is 0.150 mL x 3 mg/mL = 0.45 mg. If the peak is divided into 8 fractions then 0.45 mg/8 fractions equals 0.05 mg/fraction. Thus 20 injections are needed to collect ~1 mg/fraction. Similarly, for 3 and 5 fractions, 7 and 12 injections are needed respectively to obtain ~1 mg/fraction.

6.8. Crystallization Analysis Fractionation (CRYSTAF)

A CRYSTAF [77] apparatus, model 200, manufactured by Polymer Char S.A. (Valencia, Spain) was used. About 20 mg of the sample were dissolved in 30 mL of distilled ODCB at 160 °C. After dissolution, the temperature of the sample solution was decreased at a rate of 0.1

°C/min from 100 °C→30 °C. The polymer concentration in solution was monitored by an IR detector operating at 160 °C and using 3.5 µm as the measuring wavelength.

6.9. Preparative CRYSTAF

A Prep mc² (Polymer Char, Valencia, Spain) was used to collect fractions from CRYSTAF. 1.5 mg/mL of polymer were analyzed in ODCB. The fractionation was performed according to the selected method (Figure 24).

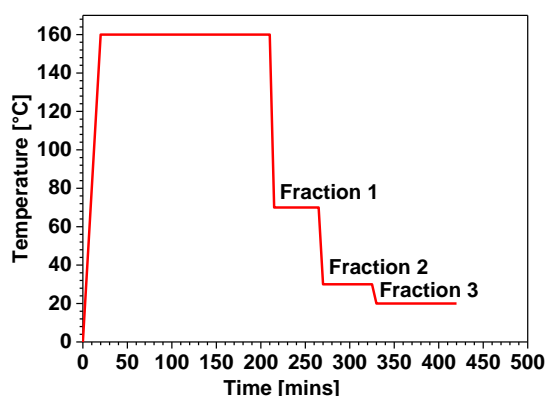


Figure 24 Temperature profile of preparative CRYSTAF

6.10. High Temperature High Performance Liquid Chromatography (HT-HPLC)

All measurements were conducted with a PL GPC 120 high temperature liquid chromatograph (Polymer Laboratories, Church Stretton, England), which included a robotic sample handling system (PL-XTR 220) for injection of sample solutions. A sample loop of 100 µL was used. Binary mobile phases of varying composition were generated by a high pressure gradient pump (Agilent, Waldbronn, Germany) operating at room temperature. They were then heated to 140 °C in the transfer capillary before entering the injector. An evaporative light scattering detector (ELSD), model PL-ELS 1000 (Polymer Laboratories), was used: The nebulizer temperature and the evaporation temperature were set to 160 and 260 °C, respectively and the nitrogen flow rate was 1.5 L/min. The gradient reaches the detector with a delay of 3.7 min, which was determined according to method of Ginzburg et al. [167]. The composition of the mobile phase in the cell of the ELSD corresponding to gradients with different slope (Figure 25) was calculated taking into account the delay volume of 3.7 mL. Data were collected and processed using WinGPC-software from Polymer Standards Services, Mainz, Germany.

For Non-Polar Polyolefins: (e.g., BiHDPE)

A HypercarbTM column was used at a flow rate of 1 mL/min and a constant temperature (160 °C) was maintained for all experiments. A linear gradient from 100 % 1-decanol → 100 % TCB was employed

For Polar Polyolefins: (e.g., PP-g-MA)

A PerfectSil[®] and column filled with Mica was used at a flow rate of 0.8 mL/min and a constant temperature (140 °C) was maintained for all experiments. A linear gradient from 100 % 1-decalin → 100 % cyclohexanone was employed.

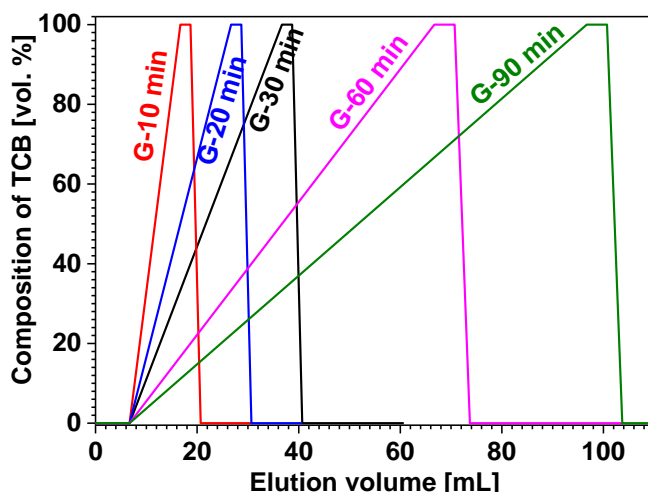


Figure 25 Gradient profiles corresponding to HT-HPLC chromatograms
Notice: The delay volume was added and the gradient started 3 min after injection.

6.11. Preparative HT-HPLC→FTIR

The polymer eluting in the mobile phase before and after starting the gradient was collected 20 times separately in two 20 mL vials (i.e., in total 4.0 mg of a sample were fractionated). The solvent in the bottles was evaporated at 100 °C in vacuum and the obtained polymer was analyzed with FTIR spectroscopy. This was carried out to confirm the HT-HPLC separation of grafted from non-grafted macromolecules.

The infrared spectra of the polymer samples were recorded with a Nicolet 8700 spectrometer (Continuum, Thermo Nicolet, Madison, WI) with a MCT detector with a spectral resolution of 4 cm⁻¹ in ATR mode. Each spectrum of a sample and of background has been averaged over 16 scans. The half peak area of the peaks was used for the determination of crystallinity and carbonyl index.

6.12. High Temperature Two Dimensional Liquid Chromatography (HT 2D-LC)

Chromatographic measurements were carried out using a chromatographic system for high temperature two dimensional liquid chromatography, constructed by PolymerChar (Valencia, Spain), comprising an autosampler, two separate ovens, valves and two pumps equipped with vacuum degassers (Agilent, Waldbronn, Germany). One oven was used for thermostating the HT-HPLC column, while the second one, where the injector and a switching valve were housed, was used to thermostat the HT-SEC column. A scheme of the HT 2D-LC setup is shown in Figure 26. The HT-HPLC and HT-SEC columns were hyphenated by an electronically controlled eight-port valve EC8W (VICI Valco instruments, Houston, Texas, USA) equipped with two loops (with volumes varying between 50 and 200 µL, Table 4). First dimension separations were carried out on a HypercarbTM column for non-polar polyolefins. Similar for analyzing polar polyolefins a PerfectSil[®] column was used. Two column variants were used in the HT-SEC dimension: A PL Rapide H column and PLgel Olexis.

From the moment of injection into the HT-HPLC column (100 µL injection loop) the 8-port valve was periodically switched in order to inject the desired volume of effluent from the HT-

HPLC into the HT-SEC column. The sample solution was filtered through an in-built stainless filter in the HT 2D-LC instrument. This filter was automatically flushed back after each filtration. Moreover, stainless steel frits with a pore size of 2 μm are part of the Hypercarb™ column.

The effluent from the HT-SEC column was monitored by an ELS and IR4 detector (PolymerChar, Valencia, Spain), which were sequentially connected. The concentration of polyolefins in the effluent was monitored by a broadband IR filter centered around a wavelength of 2900 cm^{-1} , which monitors the absorbance due to C-H bonds in macromolecules. Use of the broadband filter reduces the effect of end groups, which gains significant for the IR response in the oligomeric region. The ovens, the autosampler as well as the transfer lines between the autosampler and the columns and the ELSD, were thermostated at $160\text{ }^{\circ}\text{C}$. The HT 2D-LC instrument was handled by software provided by PolymerChar (Valencia, Spain). Software WinGPC 7.0 (Polymer Standards Service, Mainz, Germany) was used for data acquisition and evaluation.

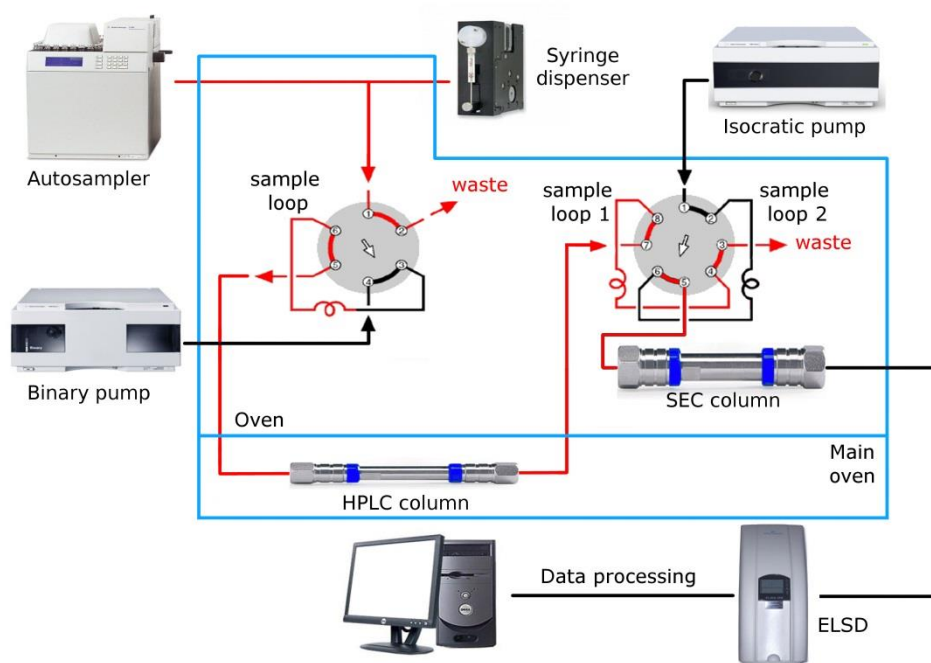


Figure 26 Schematic setup of the instrument for HT 2D-LC→ELSD [62]

Table 4 Experimental parameters used for HT 2D-LC measurements

Experimental parameters	HT 2D-LC method				
	I	II	III	IV	V
Transfer loop volume [μL]	200	100	50	100	100
Flow rate in HT-HPLC column [mL/min]	0.2	0.1	0.05	0.02	0.01
Flow rate in HT-SEC column [mL/min]	2.5	2.5	2.5	1.5	1.5
Length of the HT-SEC column [mm]	150	150	150	300	300
Time between injections into HT-SEC column [min]	1	1	1	5	10
Total number of HT-HPLC fractions [No. of HT-SEC analysis]	100	200	400	200	200
Total volume of the solvent gradient [mL]	10	10	10	10	10
Number of fractions in the gradient	50	100	200	100	100
Time of complete HT 2D-LC analysis [min]	100	200	400	1000	2000

Method I-III varies the transfer loop volume (from HT-HPLC to HT-SEC) with the intention to increase the number of fractions and to improve the HT-HPLC resolution. Method IV and V apply a different HT-SEC column and longer analysis time with the aim to improve the HT-SEC separation and in turn the overall resolution.

As low flow rates in HT-HPLC reduce the efficiency of the HT-HPLC separation [110] a longer HT-HPLC column was chosen for the 2D-LC measurements (250 mm instead 100 mm) and sorbent particles with smaller particle size were used (5 μm average instead of 10 μm diameter), with an intention to increase the efficiency of the HT-HPLC separation. Furthermore, the use of temperatures as high as 160 $^{\circ}\text{C}$ substantially reduces the viscosity and thereby increases the diffusion of analytes, which also effectively influences the efficiency of the HT-HPLC separation.

6.13. Calculation of Resolution and Column Efficiency of HT-SEC

Two HT-SEC column variants, differing in their theoretical plate number (N), were used for HT 2D-LC. N was determined by using two narrow disperse PS standards (M_w 32 and 67 kg/mol, respectively), applying a 20 μL sample loop and was calculated using Eq. 10 [196].

$$N = 5.54(t_r/w_{1/2})^2 \quad (10)$$

Where, N = number of theoretical plates
 t_r = retention time of the analyte,
and $w_{1/2}$ = full width half maxima

The resolution R was calculated by using Eq. 11.

$$R = 2(t_1 - t_2)/(w_1 + w_2) \quad (11)$$

Where, t_1 and t_2 = retention time of two peaks
and w_1 and w_2 = the peak width at the base of each peak

At $R = 1.0$ two peaks overlap by about 4 %. Values < 1.0 indicate peaks that overlap, while at a resolution of 1.5 the peaks are considered fully separated [196].

6.14. Raman Spectroscopy

Two confocal Raman microscopes (WITec GmbH) were used for the investigations: The high temperature (HT) measurements were carried out at IPF, Dresden, Germany (model alpha 300R+) and the room temperature (RT) measurements at Fraunhofer LBF, Darmstadt, Germany (model alpha 500R). Both instruments were equipped with a laser with an excitation wavelength of 532 nm and a beam diameter of about 1 μm . The samples were analyzed by an objective with 20x magnification and an integration time of 0.5 s (2 s for the RT measurements) was used. The laser power was 500 μW (10 mW for the RT measurements), and to improve the signal to noise ratio 200 scans were accumulated. A charged coupled detector was used for detection. All spectra were smoothed by the Savitzky-Golay method (SG) and cosmic rays were removed (CRR). The measurements at high temperature were carried out on a heatable microscope stage. The reproducibility was checked by two independent measurements of the same sample at two different spots.

For the experiments at room temperature (RT) an aluminum block with a square cut in the middle (to accommodate the sample) and a top cover with a glass slide were constructed to avoid interaction of the sample with the outside atmosphere (Figure 27). It was found that stainless steel and Teflon made sample holders can also be used for this purpose. For all experiments the temperature was measured using a thermocouple. For the HT experiments an in-built thermocouple was employed, which was hyphenated to the heatable microscopic stage and controlled by the WiTec project 4+ software.

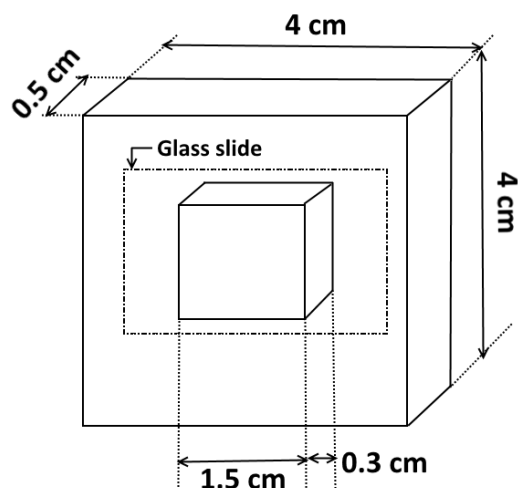


Figure 27 Sample holder with glass slide

6.15. NMR Spectroscopy

The ^1H and ^{13}C NMR measurements were carried out using a Varian (Sao Palo, US) Mercury-VX 400 spectrometer (9.4 T). The ^1H NMR spectra were acquired at a Larmor frequency of 400.11 MHz using a 10° excitation pulse, 32 k data points (corresponding with an acquisition time of 2.3 s at a spectral width of 6.4 kHz), a relaxation delay of 2 s, and a total of 256 scans. Fourier transformation was done after zero filling the data to 32 k time domain points and exponential filtering of 0.3 Hz.

The ^{13}C NMR spectra were recorded at a Larmor frequency of 100.6 MHz using a 90° excitation pulse with 1H decoupling during the acquisition time (inverse-gated decoupling for quantitative evaluation). The acquisition of the spectra was set by 64 k data points (corresponding with an acquisition time of 1.3 s at a spectral width of 25 kHz), a relaxation delay of 15 s, and a total of 1000 – 3000 scans. Fourier transformation was done after zero filling the data to 64 k time domain points and exponential filtering of 1.0 Hz. All ^1H and spectra ^{13}C NMR spectra were calibrated to the resonance lines of benzene [δ (^1H) = 7.16 ppm] and of the $-\text{CH}_2-$ units of PE [δ (^{13}C) = 29.98 ppm], respectively.

7. Results and Discussion

7.1. Development of Separation of Bimodal HDPE using HT 2D-LC→IR

7.1.1. Introduction

In order to gain insight into the bivariate distribution (CCD x MMD) of BiHDPE it is essential to characterize the molecular heterogeneities with regard to molar mass (MM) and chemical composition (CC) and their interrelationship. A particular incentive to determine the bivariate distribution for BiHDPE lies in the fact that the second reactor product is not accessible from the in vivo process. Thus, detailed information on molar mass and compositional distributions can only be evaluated by a rigorous deformation of the final product into its constituents.

Coupling HT-SEC with FTIR spectroscopy enables to visualize the distribution of comonomer in BiHDPE along the molar mass axis [63,104,118,197-200]. This means that an average chemical composition to each hydrodynamic volume may be determined, but not the corresponding CCD, as copolymers with different compositions will co-elute [179-182].

It is well known that co-crystallization may impact the separation in both TREF and CRYSTAF [201]. When a polymer sample consists of macromolecules, which substantially differ in their crystallinity, co-crystallization will be minimal [201,202]. Yet, when the crystallization temperatures of two polymers are close then co-crystallization of components can become significant, and as result components will not be completely separated one from another. Co-crystallization has been studied in detail from the melt [203,204]. Thus, Galante et al. [205] observed co-crystallization after slow cooling or at isothermal conditions for a HDPE/LLDPE blend. Generally, co-crystallization from the melt can be explained on the basis of crystallization kinetics and the resemblance of the crystallization rates of each component [206]. Co-crystallization from solution was observed for BiHDPE by García et al. [207], who showed that the HDPE could not be separated from the LLDPE when using TREF. This has been systematically studied by Anantawaraskul et al. [85,92], who reported that fast cooling rates can promote co-crystallization during the analysis of ethylene/ α -olefin blends when using CRYSTAF or CEF. They also demonstrated that even at slow cooling rates co-crystallization will become significant when two components crystallize within relatively close temperature ranges. The second aspect which limits the applicability of crystallization based technique for BiHDPE is the influence of molar mass on the crystallization. The effect of molar mass on crystallization has been studied for crystallization from the melt [203,204]. For the case of crystallization from solution, namely in CRYSTAF, Nieto et al. [83] observed that up to a M_n of 16 kg/mol the molar mass influences the separation efficiency of ethylene/1-hexene copolymers. Fatou et al. [208,209] reported an influence of molar mass on the crystallization temperature of linear PE in CRYSTAF up to a value of 15 kg/mol. In addition, Anantawaraskul et al. [85,92] reported that CRYSTAF profiles of linear PE broaden with decreasing molar mass. As a consequence low molar mass linear PE fractions can co-crystallize with copolymers containing high comonomer content. For TREF Wild et al. [76] reported a molar mass influence on the crystallization temperature of linear PE up to 30 kg/mol.

Thus HT-HPLC was employed to investigate the CCD of the BiHDPE and HT 2D-LC was chosen to investigate the bivariate distribution (CCD x MMD). Ginzburg et al. [145] were the first to apply HT 2D-LC to BiHDPE and examined the effect of temperature on the separation. In this study we want to show how the experimental parameters of the individual dimensions can be used to maximize the chromatographic information. Particular emphasis will be given to the use of infrared detection and its requirements on the chromatographic side. All three axes

will be calibrated with regard to molar mass, composition, and concentration by IR with the aim to obtain quantitative data from HT 2D-LC→ELSD-IR.

7.1.2. CRYSTAF→IR and HT-SEC→IR of HDPE, LLDPE and BiHDPE

The overlap of the distributions of BiHDPE with regard to MM and CC illustrated by the HT-SEC traces and the CRYSTAF profiles (Figure 28).

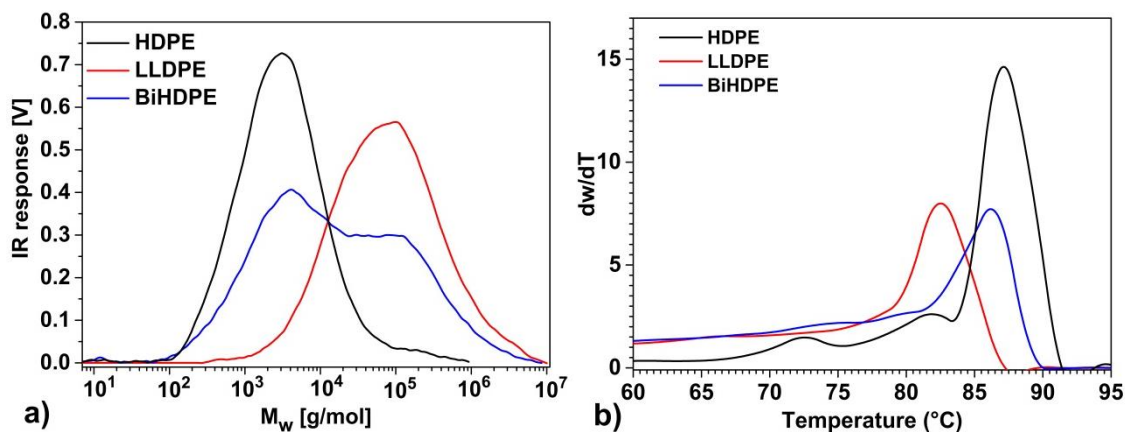


Figure 28 Overlay of the a) molar mass distributions and b) the first derivatives of the polymer concentration in solution, dw/dT , of HDPE, LLDPE, and BiHDPE

Although HDPE and LLDPE differ substantially in their average molar mass (M_w), their MMDs overlap significantly (Figure 28a). Fig. 3a shows that HDPE and BiHDPE contain a significant amount of low molar mass material ($< 10^3$ g/mol), while LLDPE contributes with high molar mass fractions ($> 10^6$ g/mol) to the MMD of BiHDPE.

HDPE crystallizes with a bimodal characteristic, where the part crystallizing at lower temperature may be attributed to the low molar mass components, thus reflecting the impact of molar mass on the crystallization temperature [201]. BiHDPE also crystallizes with a broad peak and two shoulders. It is evident from the CRYSTAF profiles (Figure 28b) that this technique fails to separate BiHDPE, first of all due to the fairly small differences in the composition of its components, and secondly as a result of the influence of molar mass on the crystallization.

7.1.3. HT-HPLC→ELSD of Polyethylene and Ethylene/1-Butene Copolymers

Thus, when developing an HT-HPLC method to deformulate BiHDPE, the challenge is to maximize the compositional separation and at the same time to suppress the impact of molar mass on the elution i.e., to achieve orthogonality of the separation. In order to probe the selectivity of the chromatographic system HypercarbTM/1-decanol→TCB^{G-10 min} for the compositional separation, two series of ethylene/1-butene (EB) copolymers with varying average 1-butene content were analyzed (Figure 29). 1-decanol was chosen as adsorption promoting liquid as the retention of HDPE is larger in comparison to other solvents like 2-octanol and 2-ethyl-1-hexanol and furthermore dissolution was good in 1-decanol and TCB

[141], which is the solvent commonly used in HT-SEC of polyolefins, was applied as desorption promoting liquid.

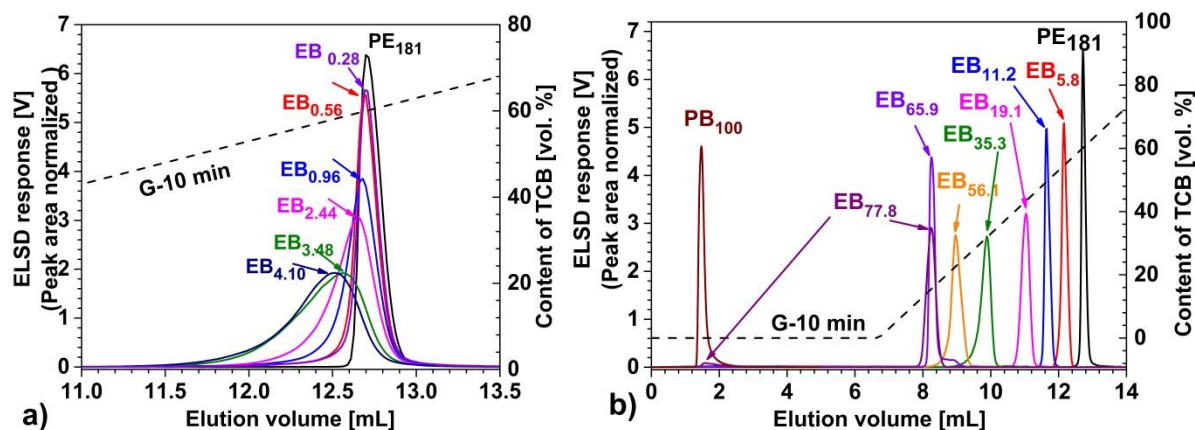


Figure 29 Overlay of chromatograms of EB copolymers synthesized with a) a Z-N and b) a metallocene catalyst at 160 °C

Notice: Composition of the mobile phase in the ELSD is indicated in the figure.

Figure 29 illustrates that the elution volume at peak maximum (E_{pmax}) of the copolymers decreases with the 1-butene content. For the Z-N based series the peaks substantially broaden with increasing incorporation of 1-butene (Figure 29a), while the width of the elugrams of the metallocene made copolymers does not vary substantially with the comonomer content (Fig. 4b). Sarzotti et al. [210] observed broadening of the crystallization profile in CRYSTAF with increasing comonomer incorporation for metallocene synthesized ethylene/1-hexene copolymers. Yet, in HT-HPLC this is not the case for the EB metallocene based series, which underlines that HT-HPLC can determine the CCD in a semi-quantitative manner. This suggests a relatively narrow CCD, which is also expected for metallocene based LLDPE materials. Another interesting observation is that the metallocene made sample with 77.8 mol % of 1-butene eluted in two peaks, namely a small portion of the copolymer was not adsorbed and eluted in 1-decanol i.e., before the gradient and that PB 100 % elutes completely before the gradient. This reveals the limit of this mobile phase for a compositional separation.

Compositional heterogeneity may arise from the instantaneous as well as conversion heterogeneity. The instantaneous heterogeneity was first described by Stockmayer [95], assuming the molar masses of the monomers were equal and later extended by Tacx et al. [211] for the case that monomers do not have the same molar mass. The conversion heterogeneity arises from the feed composition drift and has been described by Tacx [212] for batch copolymerization assuming first order Markov statistics. In the case of EB samples from Sühm a calculation and comparison of the experimental and theoretical CCD is not feasible as the process is not carried out in a batch way. The predicted instantaneous distribution is very narrow. The distribution has a baseline width of approximately 1 % of comonomer. The experimental CCD of all metallocene based LLDPE copolymers is broader. Also the PE standard also has a certain width. This indicates that the separation process adds to the width of the CCD. This is always present in the chromatographic separation. However, also the way the materials were synthesized plays a significant role in additional broadening. Hence it is concluded that the peaks are relatively narrow as a result of the very good separation.

Suhm et al. [192] carried out the experiments using a constant gas composition to synthesize the EB copolymers. The solvent (toluene) was flushed with it at constant pressure using a separate valve and subsequently, the reaction was started. Here, ethylene reacts preferably because $r_1 > 1$ and $r_2 < 1$. However, the composition of the monomers in the solvent is not necessarily the same as in the gas phase. So, if ethylene reacts preferably the feed in the toluene is enriched in butene which in turn leads to a broadening towards polybutene. This is indeed observed from the chromatograms. From these considerations, it is concluded that HT-HPLC can determine the CCD in a semi-quantitative way.

Two linear gradients with different duration were investigated to probe the influence of the gradient slope on the separation. The relationship between E_{pmax} and the 1-butene content is shown in Figure 30.

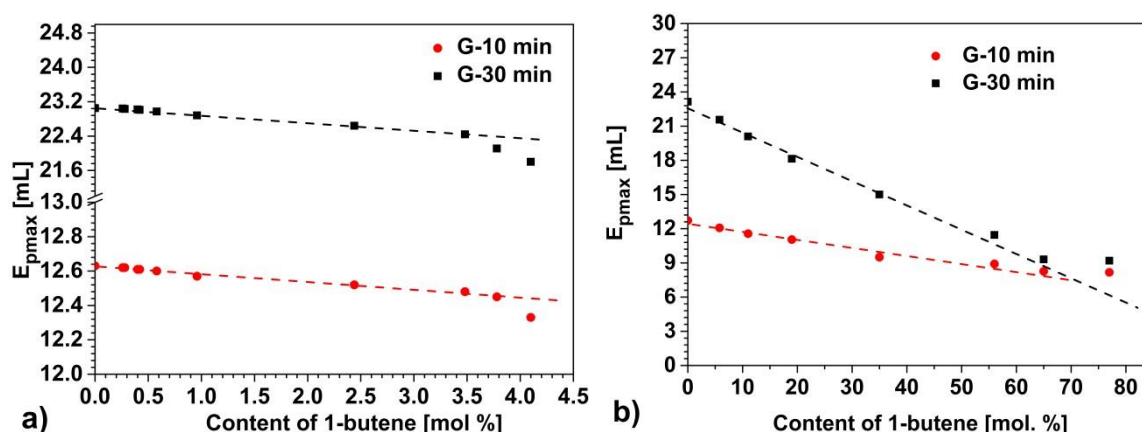


Figure 30 E_{pmax} as a function of the 1-butene content for EB copolymers synthesized with a) Z-N and b) a metallocene catalyst (Hypercarb™/1-decanol→TCB at 160 °C)

E_{pmax} depends linearly on the 1-butene content, and prolonging the gradient increases the distance between the E_{pmax} of the samples. Interestingly, for the Z-N series E_{pmax} deviates from the linearity at higher comonomer content. This is a consequence of the non-symmetric CCD of the samples (for e.g., EB_{3.78} and EB_{4.10} in Figure 30a) i.e., the average chemical composition does not correspond to the peak maximum, which then leads to scattering of the points around the lines in Figure 30.

E_{pmax} was plotted against the respective M_w (Figure 31) to probe the influence of the molar mass on the elution behavior.

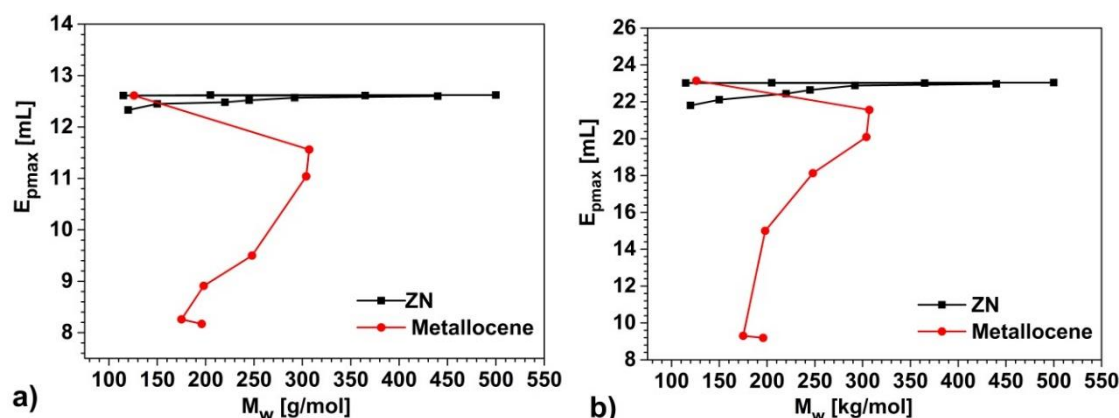


Figure 31 Dependence between E_{pmax} of the EB copolymers and M_w for a) G-10 min b) G-30 min

As a rule, an increase in molar mass of the polymer increases the retention. However, Figure 31 illustrates that the molar mass doesn't show a linear correlation with E_{pmax} . Consequently, the chemical composition and not the molar mass mainly govern the chromatographic separation (synthesized by both Z-N catalyst and metallocene catalyst) for the range considered here in both gradients. Yet it can also be recognized that the molar mass influence on the elution is less for the system HypercarbTM/1-decanol→TCB^{G-10 min}.

Analogously, the influence of the M_w of polyethylene on the elution was investigated using linear PE standards. The elugrams are shown in Figure 32 and Figure 33 correlates M_w with E_{pmax} .

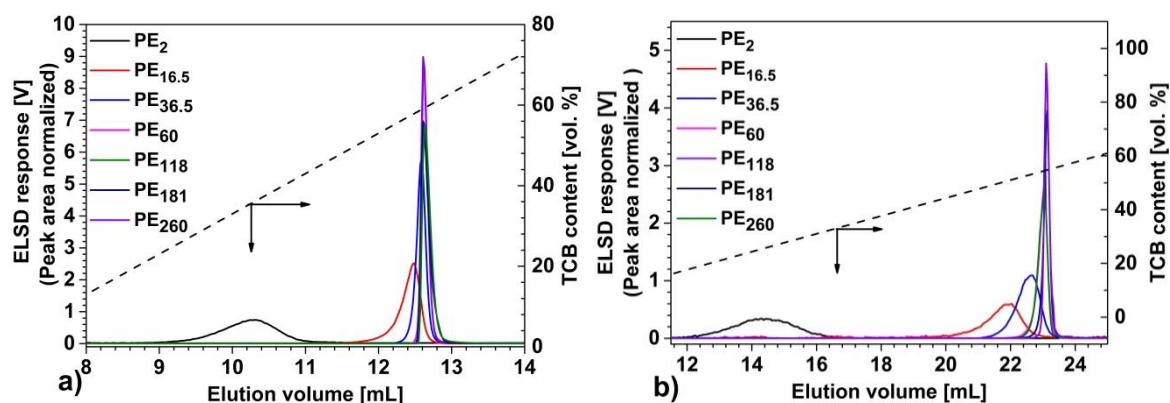


Figure 32 Overlay of chromatograms of PE standards in the system HypercarbTM/1-decanol→TCB with gradient a) G-10 min and b) G-30 min

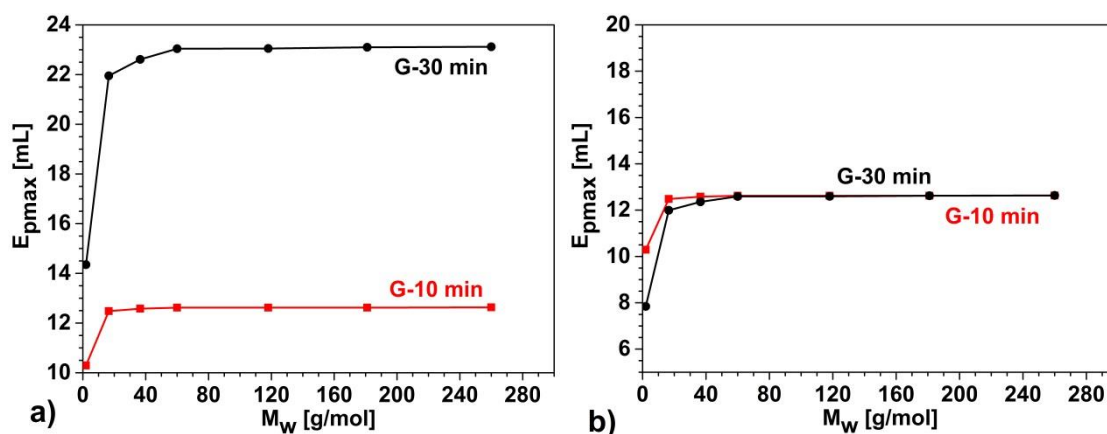


Figure 33 a) Dependence between E_{pmax} and M_w of linear PE standards and b) after applying a correction factor of 1.83

Figure 33 illustrates that the E_{pmax} of PE converges towards a constant value above an M_w of 16.5 kg/mol when applying a 10 min long gradient. Prolonging the gradient duration to 30 min increases the distance between the peaks (which can be noticed from the 3-4 times stretch in y-axis), but at the same time peaks broaden and the molar mass influences E_{pmax} up to a value of 36.5 kg/mol. The molar mass influence at a 30 min gradient is evident even after applying the correction factor (Figure 33b). This can be explained by the fact that when using a longer gradient longitudinal diffusion becomes more significant, resulting in band broadening [213].

7.1.4. HT-HPLC→ELSD of HDPE, LLDPE and BiHDPE

The elugrams of HDPE, LLDPE and BiHDPE in the system Hypercarb™/1-decanol→TCB are illustrated in Figure 34.

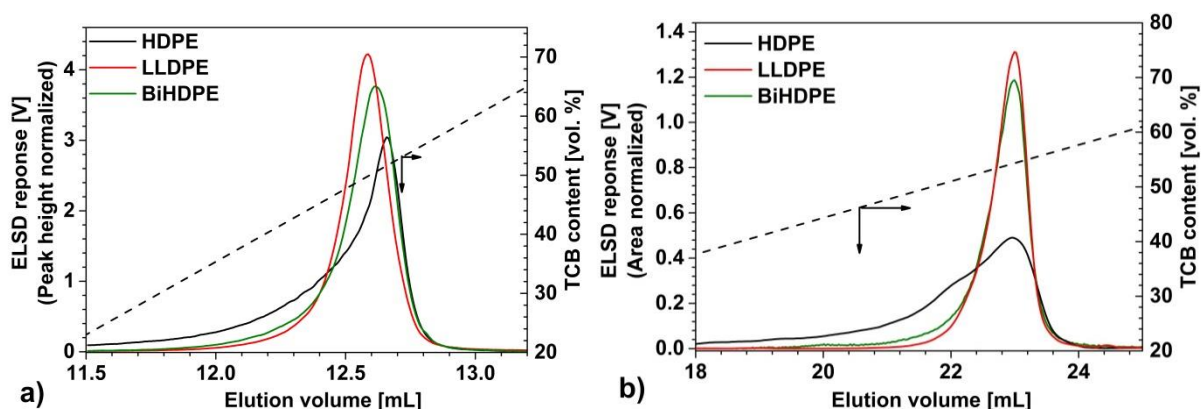


Figure 34 Overlay of chromatograms of HDPE, LLDPE, and BiHDPE in HT-HPLC at 160 °C with a) G-10 min and b) G-30 min

Figure 34 shows that HDPE eluted in the respective HT-HPLC system at the largest elution volume, and LLDPE with the smallest elution volume (considering E_{pmax}). Both peaks are broad and they overlap. BiHDPE, which contains HDPE as well as copolymer with a range of 1-butene content, eluted in a broad peak. However, the E_{pmax} for HDPE (12.61 mL), LLDPE (12.51 mL) and BiHDPE (12.56 mL) differ slightly. Upon prolonging the gradient (Figure 34b)

the HDPE elutes with a shoulder, which can be explained by the molar mass influence on the HT-HPLC separation (Figure 33b).

7.1.5. HT-HPLC→ELSD of Oligomers in HDPE and BiHDPE

The presence of oligomers in HDPE and BiHDPE could be observed in their HT-HPLC elugrams (Figure 28). With the aim to better separate these, different solvent systems were investigated. 1-decanol, n-decane, 2-ethyl-1-hexanol, diisobutylketone, 2-octanol and mesitylene were investigated as adsorption promoting solvent and TCB and ODCB as desorption promoting solvents. These solvents were screened based on their cloud points [214]. Higher and lower cloud points are the indication for relatively good adsorption and desorption promoting solvents respectively.

HypercarbTM/n-decane→ODCB^{G-30 min} and HypercarbTM/diisobutylketone→ODCB^{G-30 min} were the only two system shows the separation of oligomers and the chromatograms are illustrated below Figure 35.

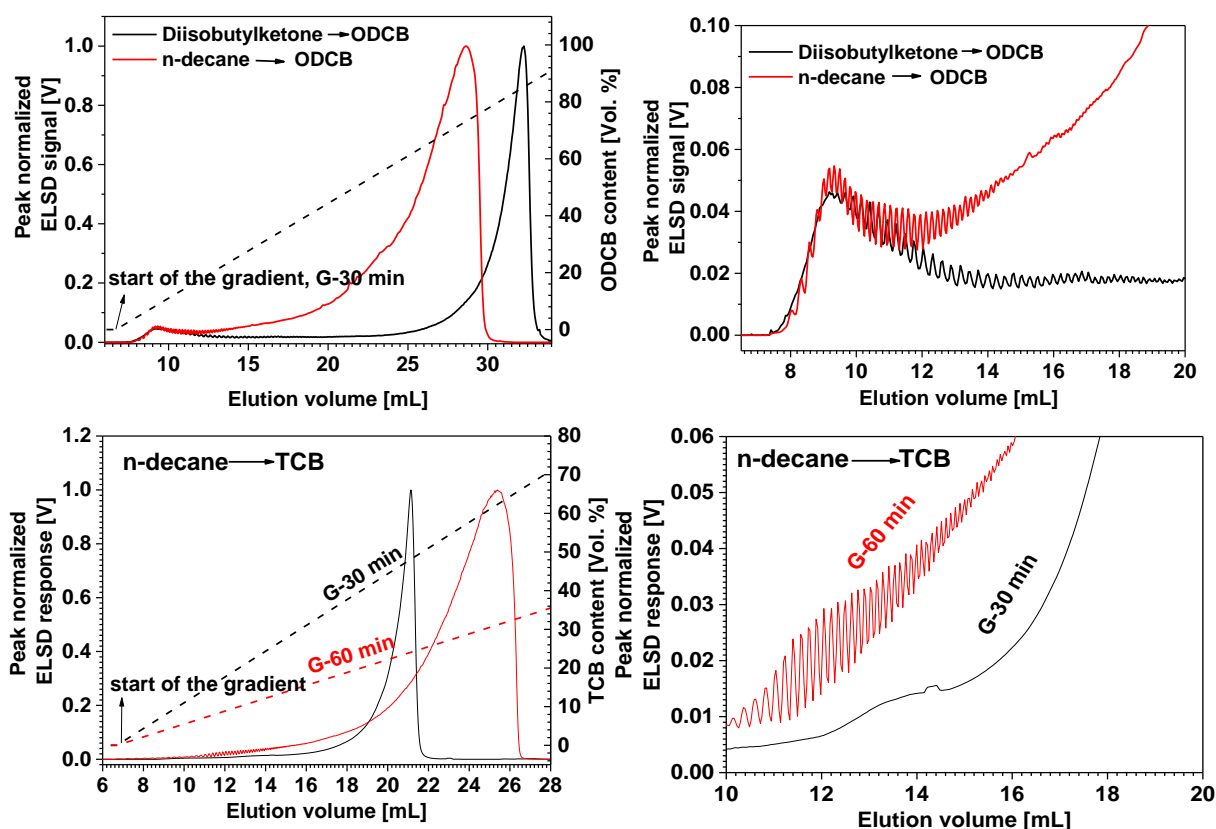


Figure 35 Overlay of HT-HPLC chromatogram of HDPE a) comparison of two system b) magnified version of (a) c) different gradient comparison and d) magnified version of (c)

From Figure 35a and b it is evident that the systems HypercarbTM/n-decane→ODCB^{G-30 min} and HypercarbTM/diisobutylketone→ODCB^{G-30 min} enables separation of oligomers. Mekap et al. [215] also reported separation of oligomers in HDPE, and in PE standards (PE¹) using HypercarbTM/n-decane→TCB^{G-30 min}. Diisobutylketone exhibits stronger retention (Figure 35a) than n-decane. Furthermore, both the system exhibits different profile of oligomers (Figure

35b). These can be explained by the fact that diisobutylketone is relatively polar and it has different selectivity than n-decane. Figure 35c and d show that Hypercarb™/n-decane→TCB^{G-30 min} doesn't show any presence of oligomers. This may be that the resolution is poor. Thus by prolonging the gradient from 30 min to 60 min enables separation of oligomers. N-decane with TCB and ODCB system which can separate oligomers were investigated and compared with 1-decanol→TCB to understand the correlation between the molar mass of the polymer and the elution volume and the results are illustrated in Figure 36.

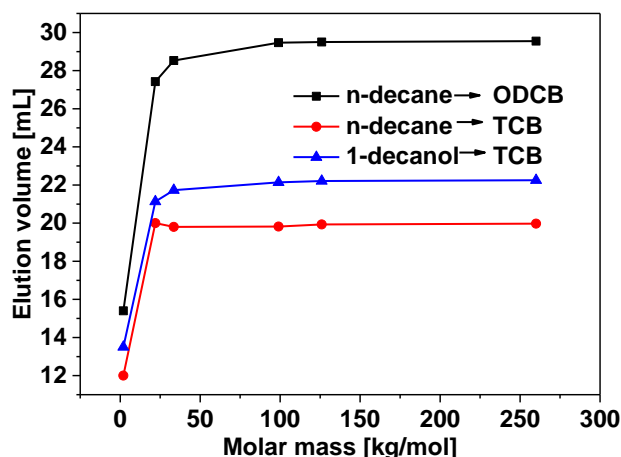


Figure 36 Dependence between the average molar mass and the elution volume of linear PE standards in different mobile phases at 160 °C with G-30 min

Figure 36 shows that in the system 1-decanol→TCB and n-decane→TCB the elution volume converge towards a constant value at a molar mass of 30 kg/mol, while in n-decane→ODCB the elution volume converges to a constant value only at 100 kg/mol. This means that the polymer molar mass influences the HT-HPLC separation in n-decane→ODCB to a larger extent than in the 1-decanol→TCB or n-decane→TCB. As a result of high molar mass influence in n-decane→ODCB it enables better resolution with regard to separation of oligomers of HDPE.

On comparison of the results (Figure 36) it demonstrates that HT-HPLC separation in the system Hypercarb™/1-decanol→TCB is governed mainly by chemical composition and in smaller extent with molar mass of polymers. Thus Hypercarb™/1-decanol→TCB is used for the further investigations.

7.1.6. Effect of Temperature on HT-HPLC Separation

Keeping in mind that the retention in interactive chromatography is based on enthalpic interactions, temperature is a factor to consider. Thus, raising the temperature leads to faster mass transfer due to increased diffusion [213], and at the same time reduces the interactions between the analyte and the sorbent i.e., the elution volume of the analyte should increase. This was observed in HT-HPLC of BiHDPE in the temperature range 140 – 180 °C by Ginzburg et al. [145]. As a consequence of the presence of significant portions of high molar mass material in the LLDPE investigated here (Fig. 3b and Table 3), both LLDPE and BiHDPE were not fully dissolvable at a concentration of about 1 mg/mL below 150 °C in 1-decanol. Hence, the effect of temperature on the HT-HPLC separation was studied in the range 160 – 200 °C, as decreasing the temperature should increase the selectivity of separation between homo and copolymers (Table 5).

Table 5 E_{pmax} of polymers at different temperatures

Temperature [°C]	E_{pmax} of HDPE [mL]	E_{pmax} of LLDPE [mL]	ΔE_{pmax} [mL]
160	12.63	12.53	0.10
180	12.38	12.30	0.08
200	12.09	12.04	0.05

Table 5 shows that the retention volume decreases with increasing temperature. ΔE_{pmax} between HDPE and LLDPE is 0.1 mL at 160 °C, which upon increasing the temperature to 200 °C is reduced to 0.05 mL. As the variation in temperature did not improve the separation of HDPE and LLDPE the following chromatographic measurements were carried out at 160 °C.

7.1.7. HT 2D-LC→ELSD of HDPE, LLDPE and BiHDPE

7.1.7.1. Influence of the Transfer Loop Volume on the HT 2D-LC→ELSD Separation (Method I-III)

The separation in the chromatographic system used here is governed primarily by the comonomer content (Figure 29 and Figure 33) and thus, HDPE elutes after LLDPE. However, portions of HDPE with a molar mass below 16.5 kg/mol may co-elute with the copolymer, LLDPE. Although HDPE and LLDPE elute with different elution volumes, their peaks overlap to a large extent (Figure 34), and as a consequence BiHDPE eluted from the HT-HPLC column in a single broad peak. BiHDPE exhibits a bivariate distribution (CCD x MMD), and it is therefore an interesting question, if the interrelationship between these distributions can be exploited to augment a chromatographic separation. Technically, this has been realized by hyphenating the separation with regard to composition and molar mass in HT 2D-LC (HT-HPLC x HT-SEC). HT 2D-LC does not only hold the potential to improve the separation by adding the second dimension, it also offers the possibility to use additional experimental parameters (Table 4) for this purpose [216,217]. Thus, HT 2D-LC of BiHDPE was carried out to resolve the separation of the constituents in BiHDPE.

The transfer loop between the chromatographic dimensions determines the number of fractions and thereby HT-SEC analysis. The clustered HT-SEC traces obtained from HT 2D-LC of BiHDPE by using transfer loops of different volume are shown in Figure 37 and the color coded contour plot from BiHDPE and its constituents in Figure 38.

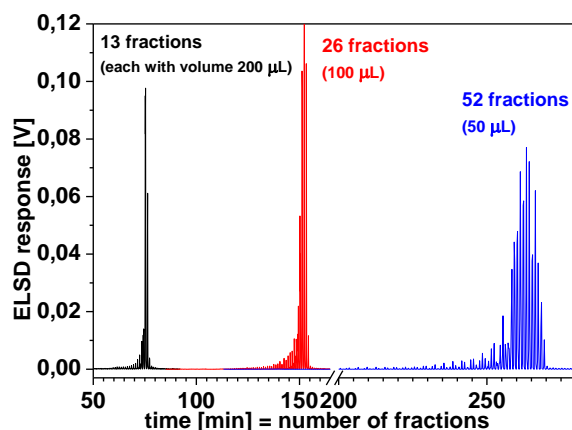


Figure 37 HT-SEC traces from HT 2D-LC of BiHDPE (Method I-III, in Table 4)

Notice: The volume of the transfer loop and the resulting number of fractions per sample are indicated in the figure.

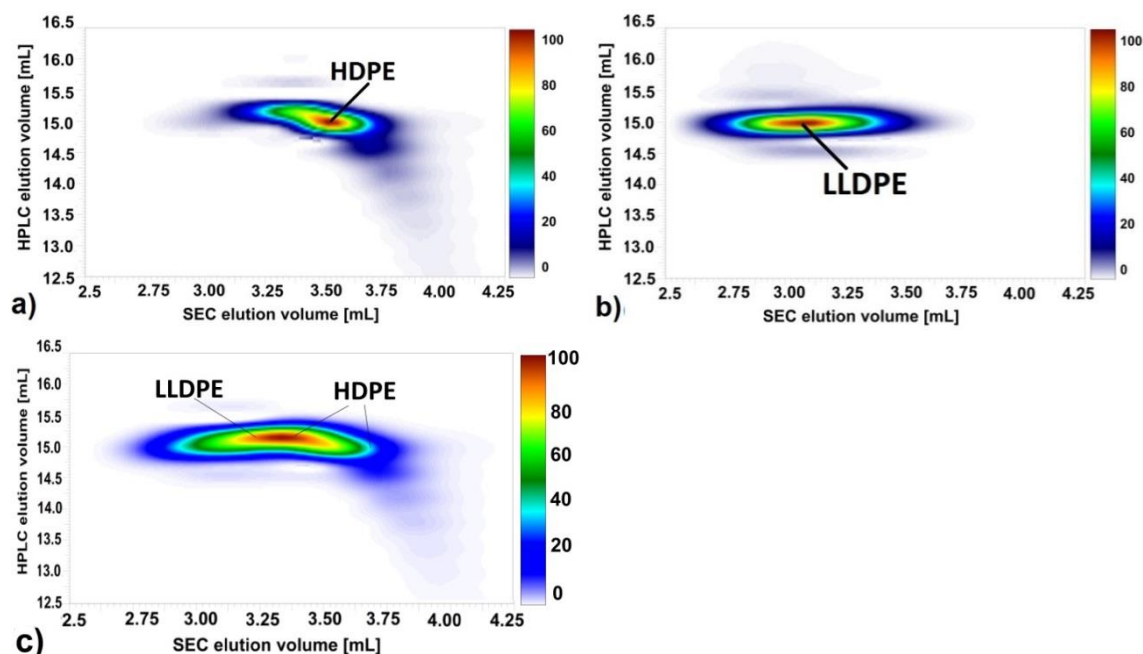


Figure 38 Contour plots obtained from HT 2D-LC for a) HDPE, b) LLDPE and c) BiHDPE (method I in Table 4)

The spot corresponding to HDPE is distorted, showing a diffuse region corresponding to oligomers on the low molar mass side. On the contrary, the spot of LLDPE is symmetric, without an indication of oligomers. The contour plot of BiHDPE shows a banana shape and its constituents, HDPE and LLDPE, cannot be distinguished. Yet, a diffuse region, which corresponds to fractions of low molar mass, can be recognized on the HDPE end. Decreasing the volume of the transfer loop enables to increase the number of the HT-HPLC fractions (Table 4 and Figure 37) and thus, the resolution of the components in the contour plot could potentially be improved. The contour plot of BiHDPE for a 100 µL transfer loop is shown in Figure 39.

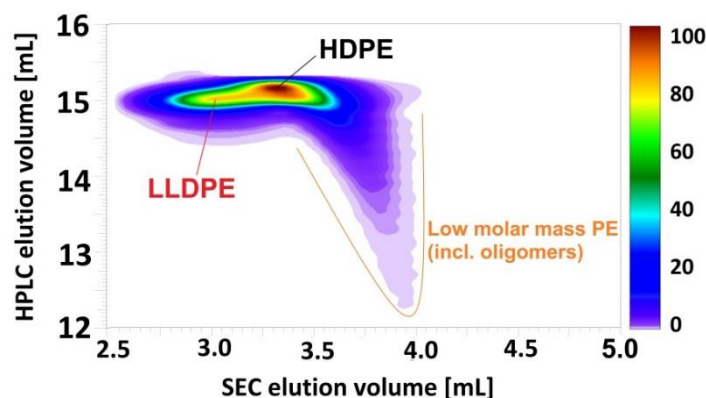


Figure 39 Contour plot of BiHDPE obtained from HT 2D-LC (method II in Table 4)

Figure 39 shows that LLDPE elutes at a lower elution volume (HT-HPLC axis) in a region of high molar mass (HT-SEC axis), while HDPE elutes at a higher elution volume (HT-HPLC axis) in a region of low molar mass (HT-SEC axis). Additionally, the presence of low molar mass fractions is visible as a diffuse region (Figure 38 a, c and Figure 39). To further increase the resolution, the volume of the HT-HPLC fractions was decreased to 50 μL . The respective 3D surface plot is shown in Figure 40.

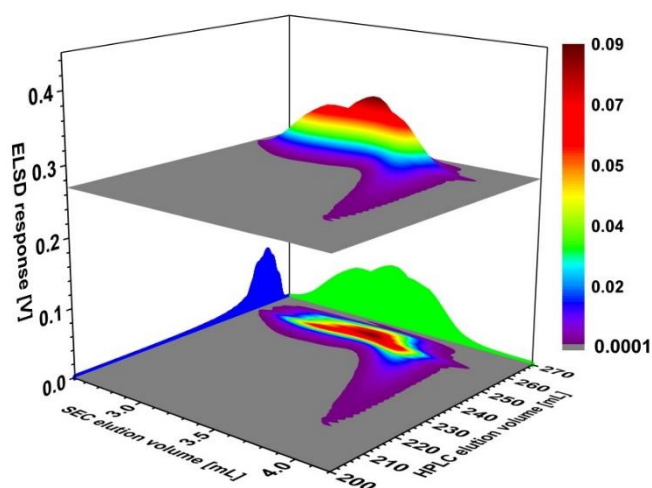


Figure 40 3D surface plot of BiHDPE obtained from HT 2D-LC (method III in Table 4)

The spots of HDPE and LLDPE significantly overlap and long tailing at larger elution volume in the HT-SEC direction is clearly visible in the projections (Figure 40). Comparing the contour plots and the surface plot obtained for different transfer volumes (Figure 40) confirms that increasing the number of HT-HPLC fractions is a suitable strategy to improve the separation resolution of the components. However, when using a transfer volume of 50 μL HDPE elutes with a shoulder at higher elution volume in HT-SEC dimension (lower elution volume in HT-HPLC). As an optimum number of fractions should avoid co-elution of low molar mass components of HDPE with LLDPE (in HT-HPLC direction), a transfer volume of 100 μL was used for the following investigations.

7.1.7.2. Influence of the HT-SEC Separation and Use of IR Detection in 2D-LC (HT 2D-LC→IR)

The resolution of the HT-SEC dimension is a crucial parameter contributing to the overall resolution of the 2D experiment. A short HT-SEC column (150 x 7.5 mm, L. x I.D.) was used in our previous [145] and current HT 2D-LC measurements (Figure 40), which gears at decreasing the time needed for a single HT 2D-LC experiment (method I-III in Table 4). Yet, less time is available for an individual HT-SEC analysis, which may lead to overlap of two fractions [218-221]. The theoretical plate number (N) (column efficiency) and the resolution (R) of this column were determined to be 4500 (N_{4500}) and 0.35, respectively (Eq. 10 and 11). As the constituents of BiHDPE i.e., HDPE and LLDPE, significantly differ in their M_w and \bar{D} (Table 3), using a HT-SEC column with higher N should increase the resolution in the HT-SEC dimension. This in turn can also aid to increase the overall resolution of the contour plot from HT 2D-LC. A HT-SEC column with an N of 11000 (N_{11000}) was used to probe the separation of BiHDPE in HT 2D-LC (Method IV) and the 2D contour plot as well as the 3D surface plot are presented in Figure 41. In order to calibrate the y-axis (which reflects the CCD) and the x-axis (which reflects the MMD), the EB copolymers as well as the PE standards were analyzed with HT 2D-LC under identical conditions as the BiHDPE.

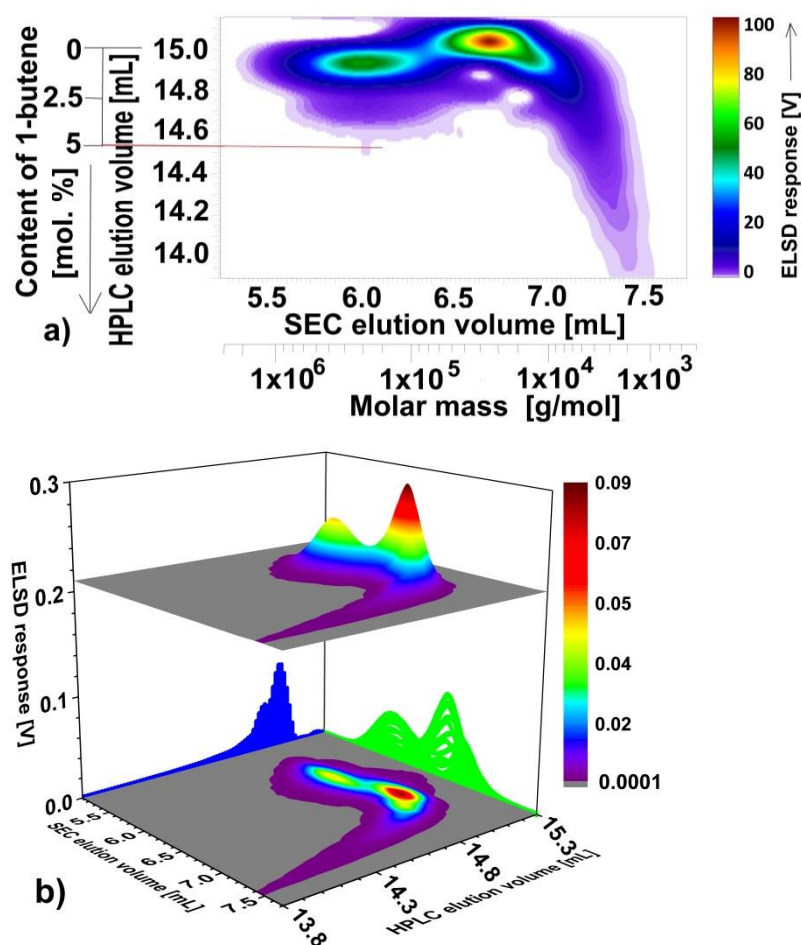


Figure 41 a) 2D contour plot and b) 3D surface plot obtained from HT 2D-LC (method IV in Table 4) of BiHDPE

In difference to the HT 2D-LC results obtained previously (Fig. 11-13), the contour plot of BiHDPE in Figure 41 reveals a pronounced two spot regime with bimodal elution in both the HT-HPLC and HT-SEC dimension. The region assigned to the LLDPE part of BiHDPE also has a diffuse region at lower elution volume, which, applying the calibration of the HT-HPLC axis can be assigned to fractions containing up to ~5 mol % of comonomer.

For a meaningful interpretation of chromatographic results a quantitative detector response is essential. While the ELSD remains the sole option for one dimensional HT-HPLC, its signal is in a complex manner influenced by the solvent gradient as well as the molecular parameters of the eluting polymer [96], which in the case considered here are primarily the molar mass and comonomer content. Although the effect of solvent gradient has been widely eliminated in HT 2D-LC (due to the quasi isocratic conditions in HT-SEC), the parameters of the polymer itself still influence the aerosol formation. Thus, well crystallizable fractions may be over emphasized, while low molar mass components are, due to their volatility, not detectable at all as these rather evaporate in the nebulizer [215,222]. IR detection has been widely used to monitor the concentration of eluting fractions as well as their comonomer content in HT-SEC of ethylene/1-alkene copolymers [79,168,223,224]. Only a few IR transparent solvents (C-H absorbance) exist: TCB, ODCB, TCE and 1-chloronaphthalene. ODCB and 1-chloronaphthalene were observed to be a poor desorption promoting solvents in comparison with TCB. Furthermore, the molar mass influence in the retention of PE is high in 1-decanol→ODCB (up to 60 kg/mol) compared to 1-decanol→TCB (up to 16 kg/mol, Figure 33). TCE is a poor adsorption promoting solvent i.e., PE standards with low molar mass were not adsorbed from TCE. Thus, TCB was chosen as desorption promoting solvent. The response of ELSD and IR with regard to both composition and concentration in HT 2D-LC of HDPE and LLDPE was probed (Figure 42).

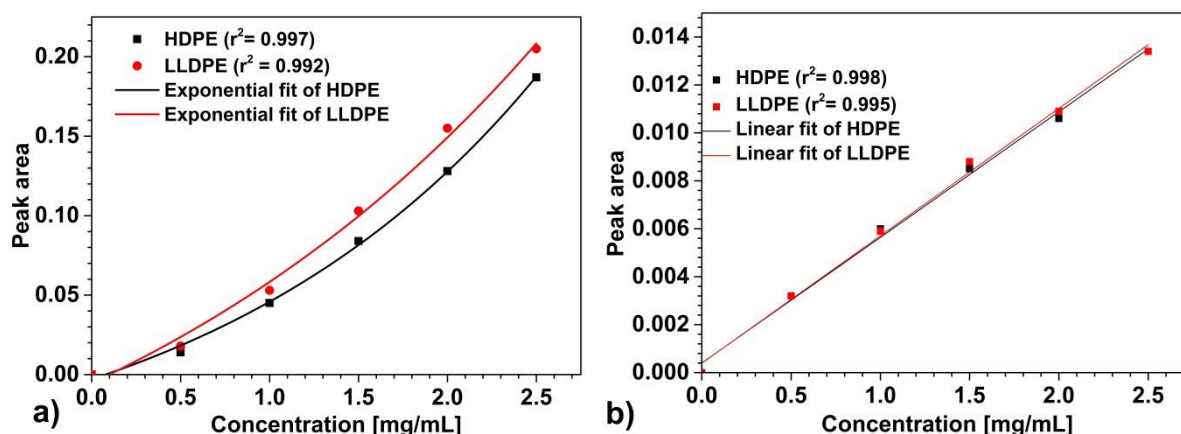


Figure 42 Peak area recorded with a) ELS and b) IR detector as a function of injected polymer concentration

Notice: The IR detector was sequentially connected with the ELSD in HT 2D-LC (HT 2D-LC→ELSD→IR).

Figure 42a shows that the response of the ELSD depends exponentially on the concentration and, additionally, on the content of short chain branching, while in the case of IR detection the response is linear with regard to concentration and not influenced by the composition of the polymer.

As the constituents of BiHDPE differ significantly in their M_w , representatively a low and high molar mass PE standard were investigated to probe the separation between these, as well as between the low molar mass standard and the solvent (Figure 43).

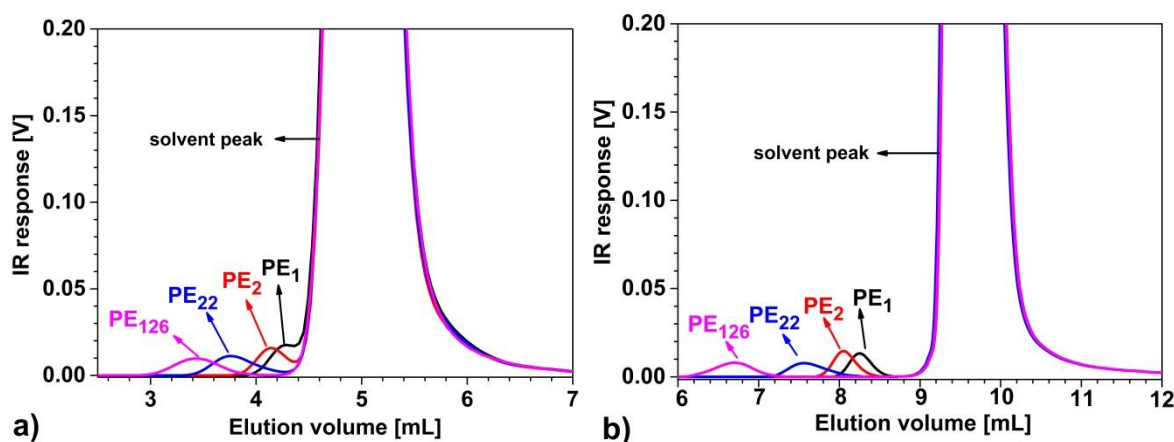
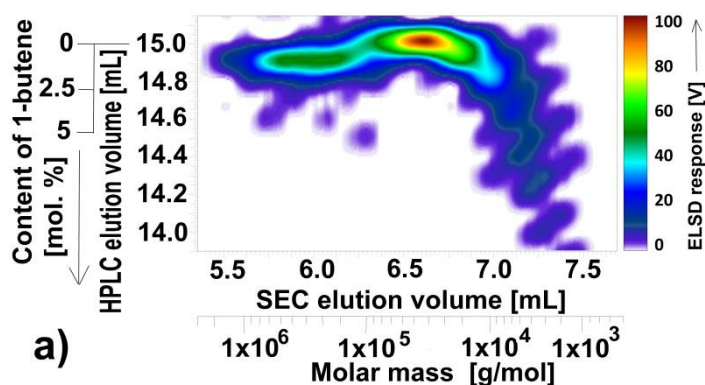


Figure 43 Overlay of HT-SEC traces recorded with IR detection in HT-SEC column: a) PL Rapide H (150 x 7.5 mm, L. x I.D.) (Method III) and b) PLgel Olexis (300 x 7.5 mm, L. x I.D.) (Method: IV), at 160 °C with mobile phase TCB

With each fraction transfer from the HT-HPLC into the HT-SEC dimension, a small amount of 1-decanol (solvent plug) is injected, with the amount depending on the gradient. Since the IR detector used here is tuned to the stretching vibration of the methyl and methylene groups, 1-decanol causes an intense broad peak in the chromatograms (Figure 43), which may significantly overlap with the polymer peak when a column of low plate number is used (Figure 43a). Using a HT-SEC column with N_{11000} , PE₁ as well as PE₂₂ and PE₁₂₆ were baseline separated, and PE₁ was baseline separated from the solvent peak (Figure 43b).

HT 2D-LC→IR separation of BiHDPE was carried out using the above mentioned method. The 2D contour plot and the 3D surface plot with projections are shown in Figure 44a, b. For comparison the 3D surface plot from HT 2D-LC→ELSD is shown in Figure 44c.



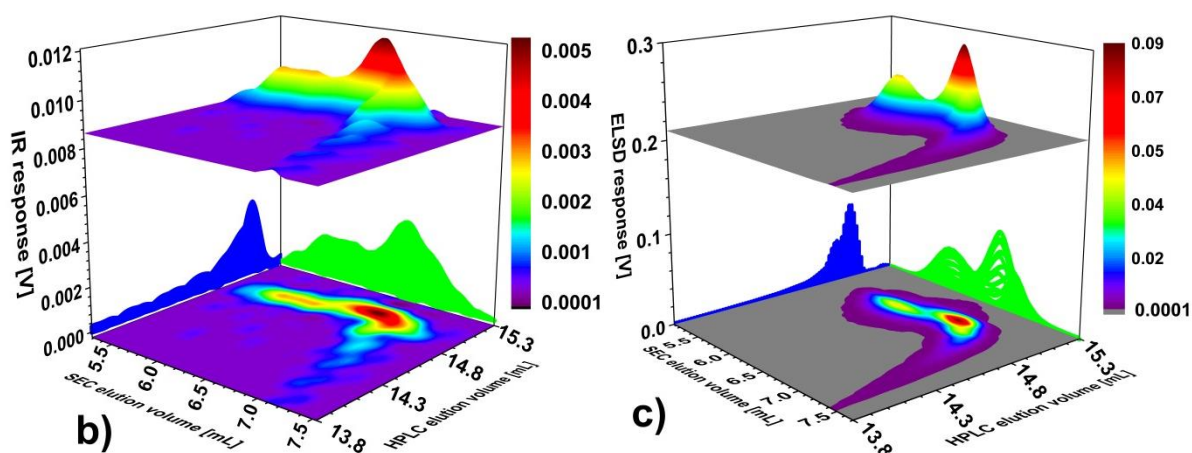


Figure 44 2D contour plot and 3D surface plot of BiHDPE obtained from HT 2D-LC (method IV in Table 4) using a) and b) IR and c) ELSD

Figure 44 shows two spots for BiHDPE sample: According to the calibration of the HT-HPLC separation (y-axis) the spot eluting at larger elution volume corresponds to HDPE and the component with smaller elution volume can be assigned to LLDPE. However, the contour plot obtained from IR (Figure 44b) is less intense than the one recorded with the ELSD due to the lower sensitivity of the IR detection in comparison to the ELSD (Figure 44c). Transforming the 2D contour plot (Figure 44a) to a 3D surface plot with projections (Figure 44b and c) illustrates that IR delivers more information with regard to oligomers in comparison to ELSD, which can be explained by the fact that the low molar mass PE vaporizes in the ELSD [215]. The projection on both axes in the 3D surface plot clearly indicates bimodality with regard to CCD and MMD.

Comparing Figure 41a and Figure 44a it becomes evident that Figure 41a shows fractions with comonomer content up to ~5 mol %, while in Figure 44a this only reaches a value of ~3.5 mol %. To investigate the reason for this difference, a comparison of the response of the polymer and the solvent peak from ELSD and IR is illustrated in Figure 45.

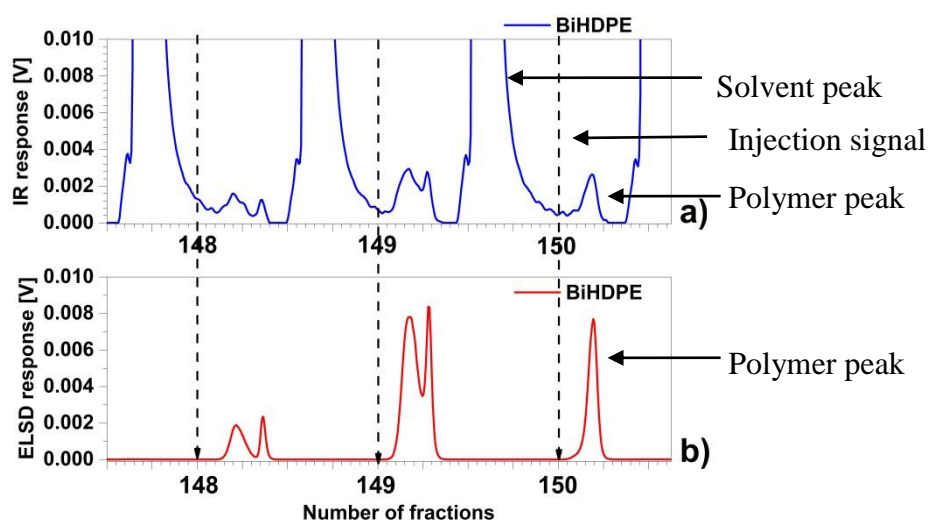


Figure 45 Comparison of HT-SEC traces of BiHDPE obtained from HT 2D-LC (method IV in Table 4) recorded with: a) IR and b) ELSD

Figure 45 shows that the peaks corresponding to the polymer and the solvent were baseline separated only in the low molar mass range in this particular system, while in the high molar mass region they partly overlap.

An explanation can be found in the residence time of the polymer and the solvent plug in the column: Figure 43b shows that for complete elution of the polymer (PE_1) and the solvent a minimum of 9 and 12 mL is needed, respectively. Yet, with the parameters used for the HT 2D-LC the volume of eluent per HT-SEC trace is 7.5 mL. As a result, low molar mass fractions from a HT-SEC analysis will still be present in the column when the high molar mass fractions of the next inject elute and then co-elute with these. To prevent this switching frequency was reduced and the volume of solvent per HT-SEC analysis was raised to 12.5 mL ($10 \text{ min} \times 1.5 \text{ mL/min} = 12.5 \text{ mL}$, Method V in Table 4). Representative HT-SEC traces are shown in Figure 46.

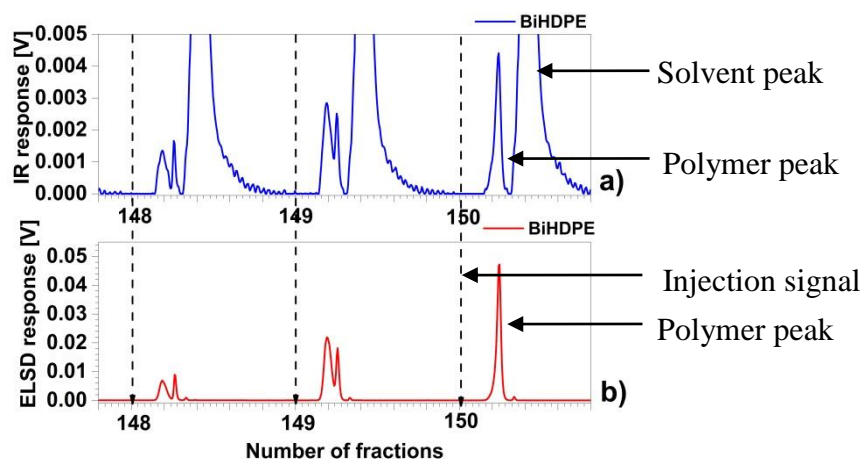


Figure 46 Comparison of HT-SEC traces of BiHDPE obtained from HT 2D-LC (method V in Table 4) recorded with: a) IR and b) ELSD

Figure 46 shows that the polymer peak and the solvent peak are now well separated from each other in both the high and low molar mass region. HT 2D-LC of BiHDPE was carried out at these conditions (Method V in Table 4) and the results are illustrated in Figure 47a and b. The corresponding 3D surface plots are shown in Figure 47c and d. From the 3D surface plot the projections onto the respective axes were overlaid to compare the response of ELSD and IR (Figure 48).

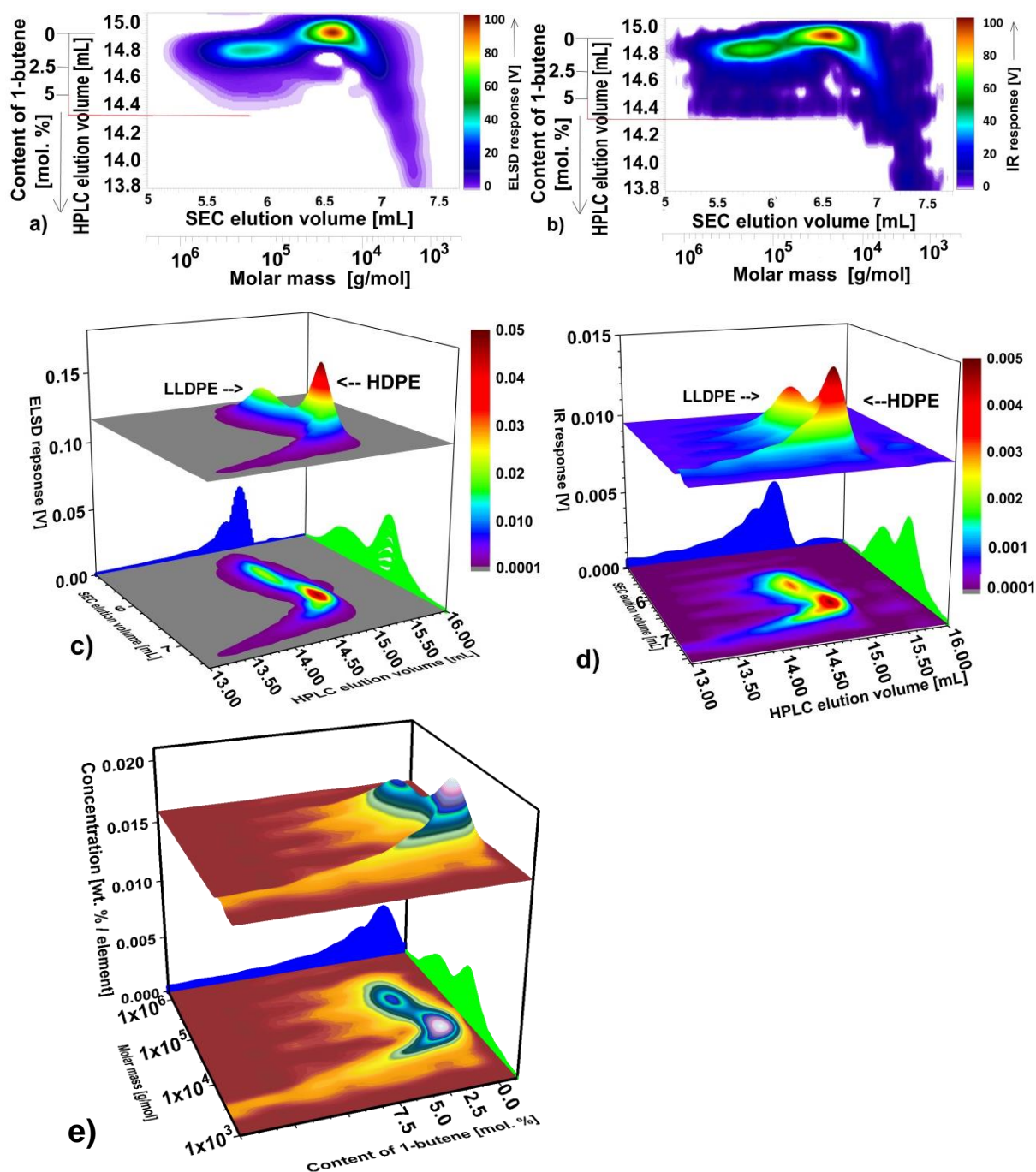


Figure 47 2D contour plot and 3D surface plot of BiHDPE obtained from HT 2D-LC (method V in Table 4) using a) and c) ELSD and b) and d) IR e) with MM, CC and concentration calibration (using IR detection)

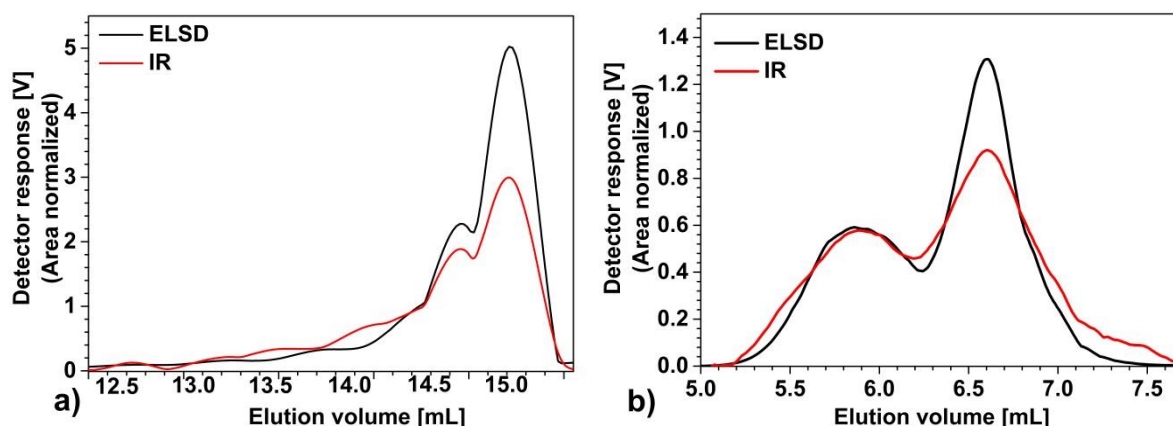


Figure 48 Overlay of chromatograms obtained from HT 2D-LC via projecting on the a) HT-HPLC and b) HT-SEC axis

From the 3D surface plot (Figure 47c, d and e) a bimodal elution in both dimensions is evident from the projections onto the respective axes (also shown in Figure 48). On comparing the ELSD and IR response in Figure 47a and b it can be recognized that both ELSD and IR can also detect fractions with comonomer content up to ~6.5 mol %. To better visualize this HT-HPLC and HT-SEC traces from the 2D contour plot were overlaid (Figure 48). The 3D surface plot by using HT 2D-LC→IR (Figure 48e) with MM, CC and concentration calibration also shows that BiHDPE contains comonomer content up to ~6.5 mol % and oligomers (down to 500 g/mol). The ratio of the constituents (HDPE/LLDPE) of BiHDPE obtained from ELSD and IR was calculated from the distributions (area normalized) after deconvoluting the BiHDPE peak and considering the parental peaks as Gaussian distributions to be 2.5 and 1.3, respectively (Figure 48a). It can be assumed that the reasons behind this difference are a) the exponential response of ELSD with regard to concentration of the polymer (Figure 42) and b) the better aerosol formation of comonomer poor fractions i.e., HDPE, in the nebulization step, which will lead to a more intense signal in the ELSD. Furthermore, Figure 48b indicates that IR detection gives more information on the flanks of low and high molar mass, as there are no volatility issues and no exponential dependency of the detector response as is the case when using ELSD [149,215].

7.1.8. Conclusion

HT-HPLC and HT-HPLC hyphenated with HT-SEC (i.e., HT 2D-LC) were employed to characterize bimodal high density polyethylene (BiHDPE) and its underlying constituents, namely HDPE and LLDPE. It was shown that the chromatographic system Hypercarb™/1-decanol→TCB^{G-10 min} separates LLDPE according to its 1-butene content. HDPE standards varying with different molar mass were investigated and it was found that HDPE fractions with a molar mass < 16.5 kg/mol may co-elute with LLDPE. Starting from there the HT-HPLC was hyphenated with HT-SEC and the effect of column temperature, volume of HT-HPLC fractions injected into HT-SEC and separation efficiency of the HT-SEC was investigated. By using a low transfer volume of 100 µL, a HT-SEC column with high theoretical plate number (N_{11000}) and by providing sufficient time for one HT-SEC analysis, bimodality was observed for the first time in both HT-HPLC and HT-SEC dimension for BiHDPE in HT 2D-LC. However, a partial overlap due to broad MMD and/or CCD of both basic components of BiHDPE was noticed.

To achieve quantitative information the ELSD was replaced by an IR detector and BiHDPE was analyzed by HT 2D-LC. Yet, to fully use the potential of IR detection for HT 2D-LC in the case of BiHDPE the chromatographic parameters have to be carefully optimized. Thus, to separate the solvent peak from the polymer fractions over the entire range of molar mass a HT-SEC column of high theoretical plate number, (N_{11000}) was required. Also, an optimum transfer volume between HT-HPLC and HT-SEC dimension and volume for an individual HT-SEC analysis was identified. By employing these conditions the solvent peak and the polymer peak were baseline separated in all HT-SEC traces of BiHDPE. As a result the contour plot from HT 2D-LC exhibited a two spot regime, reflecting the HDPE and LLDPE component of BiHDPE. A comprehensive calibration with regard to molar mass, composition, and concentration of the HT 2D-LC system was carried out, which revealed the presence of oligomers (down to 500 g/mol) originating from HDPE and the presence of polymer fractions ranging over a 1-butene content from 0 to 6.5 mol %.

7.2. Preparative Fractionation of Bimodal HDPE using Off-flow HT-SEC→NMR

7.2.1. Introduction

Fractionation is required to analyze the molecular distributions in polymers, which for complex polymers means that in addition to a MM fractionation, a fractionation according to composition, topology, or microstructure may be required. The hyphenation of liquid chromatography with NMR spectroscopy is one of the most powerful methods to elucidate structural heterogeneities present in complex polymers. Technically, this can be realized either in on-line (on-flow) or off-line (off-flow) mode. Watanabe and Niki (1978) were the first to on-line hyphenate HPLC with ^1H NMR spectroscopy (on-flow HPLC→ ^1H NMR) [225]. More than a decade later Hatada et al. (1988) on-line hyphenated SEC with ^1H NMR (on-flow SEC→ ^1H NMR) [226]. The hyphenation of liquid chromatography and NMR-spectroscopy has later been extended to on-flow 2D-LC→ ^1H NMR [227,228]. So far the vast majority of LC→ ^1H NMR investigations has been reported for ambient temperature. An overview on the LC→NMR hyphenation has been given by Albert et al. [229]. Hiller et al. [230] were the first to apply on-flow HT-SEC→ ^1H NMR at high temperatures (130 °C). They analyzed polyethylene, poly (methyl methacrylate), and ethylene-methyl methacrylate copolymers. By utilizing HT-SEC→ ^1H NMR blends of these copolymers were separated according to the molar masses of the components and the distribution of the composition along the molar mass axis was studied. The recent developments in LC→NMR of polymers have been reviewed by Hiller et al. [231].

Generally, major constraints in LC→NMR are the limited choice of compatible chromatographic solvents and the notoriously low sensitivity of NMR spectroscopy. So far, all reported studies used on-flow LC→ ^1H NMR. Yet, microstructural information can in the case of polymers only be obtained from ^{13}C NMR spectroscopy, which in turn requires sufficient amounts of sample. ^{13}C NMR lacks in sensitivity and therefore on-flow HT-HPLC/HT-SEC/HT2D-LC→ ^{13}C NMR have not been reported. Recently, off-flow HT-HPLC→ ^{13}C NMR using cryoprobe technology was reported by Zhou et al. [232] who utilized a commercially available fraction collector to analyze ethylene-octene block copolymers. Cryoprobe technology requires significantly less amounts of material for investigation (5 – 10 mg/mL to ~a few mg/mL) [233]. The availability of sufficient material in the chromatographic fractions to be analyzed is a crucial requirement for LC→NMR. For the case of HT-SEC this may be realized by carrying out the separation either in a preparative (prep.) scale or on an analytical scale by using a fraction collector. Peyrouset et al. [234,235] were the first to carry out prep. HT-SEC for PE in 1972. A challenge when using prep. HT-SEC is a loss in separation efficiency at higher column diameters [234]. The experimental setup and the requirement of large volumes of solvents make this process difficult and complicated. Nevertheless, narrowly distributed PE fractions can be obtained on a gram-scale, which can then be further investigated using other chromatographic or spectroscopic techniques. This work was realized before 40 years and since then to our knowledge no work has been carried out on prep. HT-SEC of polyolefins.

For the case of BiHDPE, the comonomer content is very low, which makes the interpretation of on-flow HT-LC→ ^{13}C NMR complicated due to solvent suppression, and consequently working in off-flow mode is the approach of choice here. Thus, a simple and inexpensive fractionation technique which can operate over a wide temperature range is an ideal starting point to explore structural heterogeneities in polyolefins by off-flow HT-HPLC→ ^{13}C NMR.

7.2.2. Manual Fraction Collection from HT-SEC

In the first step a manual approach of collecting fractions from HT-SEC was chosen, using a single column (PLgel Olexis) to speed up the process. Five fractions were collected for the BiHDPE sample according to the protocol as given in section 6.6, each of approximately 1 – 1.5 mg/mL (20 injections). After workup the collected fractions were injected back into the HT-SEC column and the chromatograms are shown Figure 49.

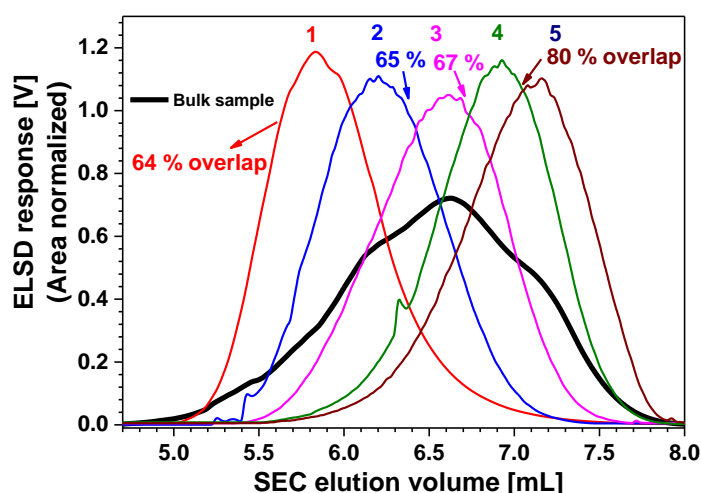


Figure 49 Overlay of chromatograms of the bulk sample and the five HT-SEC fractions of BiHDPE

Overlaps with area percentages ranging from 65 – 80 % between the fractions were observed (Figure 49). It may be assumed that manual errors when changing the vial were the main source for these overlaps, which accumulate with both the number of fractions taken per sample and the number of fractionation cycles. This “handling error” can be avoided by automating the process, which at the same time reduces the manual labour involved. For this purpose a portable automatic fraction collector (PAFC) was designed, which can be plugged in at a series of HPLC instruments.

7.2.3. Portable Automatic Fraction Collector (PAFC)

The PAFC consists of a multi-position actuator, a valve and sensors as shown in Figure 50.

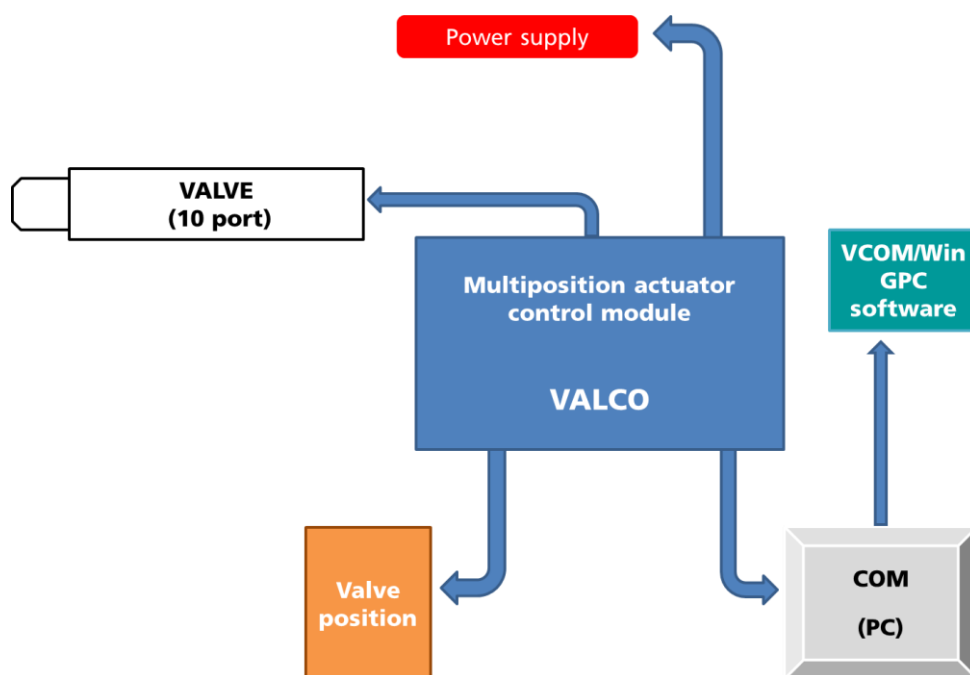


Figure 50 Schematic setup of fraction collector

A multi-position actuator control valve controls the 10 port valve (Figure 50), which was connected to a sensor in order to relay the current valve position. The relay option in the WinGPC software was utilized to control the switching of the valve. These mentioned units were packed close, however, care was taken to separate the electronic and the solvent unit (Figure 51). Figure 51c shows the compact construction of the PAFC with all capillaries thermostated (160 °C) (Figure 51b). Figure 51a and c show the temperature controller and the display of temperature and valve position, respectively. To ensure temperature stability and avoid cold spots high temperature stable polymer foams and glass wool were used for isolation and covered with aluminum sheets.

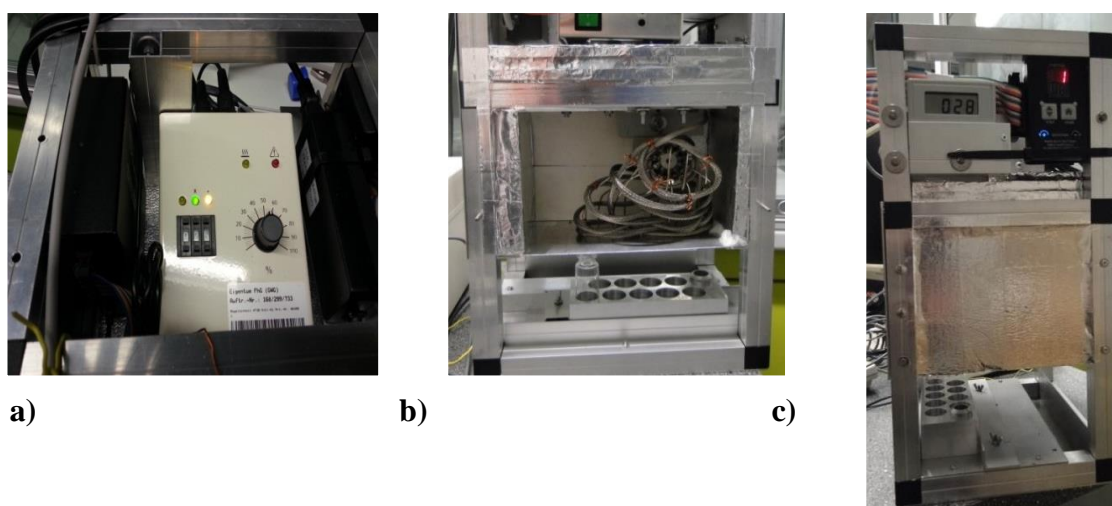


Figure 51 Portable automatic fraction collector a) top view, b) core view and c) side view
The compartment, where the temperature control is placed, has a working temperature ranging from 20 – 220 °C (Figure 51a). A capillary of 0.5 mm diameter was used to prevent shear

degradation of the polymer and minimize the risk of blockages. All capillaries were thermostated at high temperature (160 °C) to avoid precipitation of polymer and consequent blockages (Figure 51b). The PAFC (Figure 51) can be customized for a wide range of operating conditions with regard to temperature and number of fractions. Additionally, the customizable units (temperature controller, valve and vials) are commercially easy accessible.

7.2.3.1. Calculation of delay

After replacing the ELSD by the PAFC a total delay (TD) has to be calculated in order to collect fractions over desired windows of elution volume (molar mass) using Eq. 12.

$$\text{TD} = \text{Delay in the PAFC (D}_{\text{PAFC}}) - \text{Delay in the ELSD (D}_{\text{ELSD}}) \quad (12)$$

The measurement of the D_{PAFC} is pictorially represented in Figure 52.

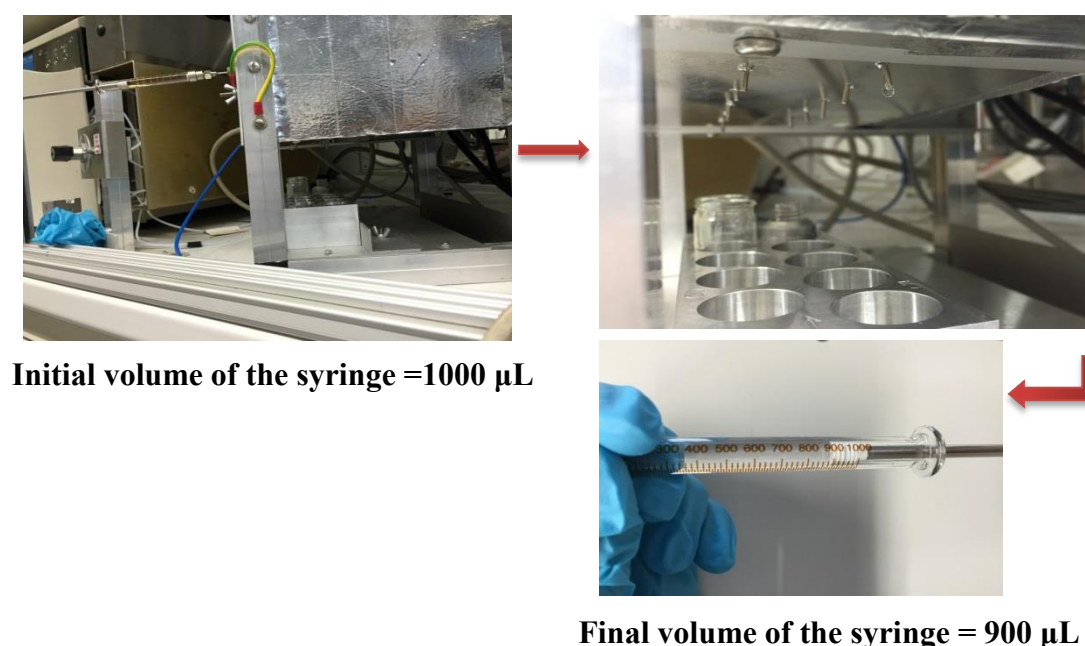


Figure 52 Delay calculations in the PAFC

D_{PAFC} was calculated by injecting a known amount of TCB (1000 µL) through a syringe into the PAFC (Figure 52). The volume of solvent required until the first drop appears at the end of the capillary is the delay volume.

This was determined at 100 µL (initial volume, 1000 µL – final volume, 900 µL (Figure 52). Inside the ELSD a small capillary is placed, and the delay caused by this can be calculated by injecting a PS standard into the ELSD. The time required for the chromatogram to appear is the D_{ELSD} and it was observed to be 65 µL.

Thus TD after replacing the ELSD by the PAFC (by using Eq. 12) is

$$\text{TD} = 100 - 65 \mu\text{L} = 35 \mu\text{L}$$

7.2.4. Steps for Preparative Fractionation of Off-flow HT-SEC→NMR

The flow scheme of HT-SEC using the PAFC followed by NMR analysis is shown in Figure 53 and the individual have been detailed in the experimental part (Section 6.6).

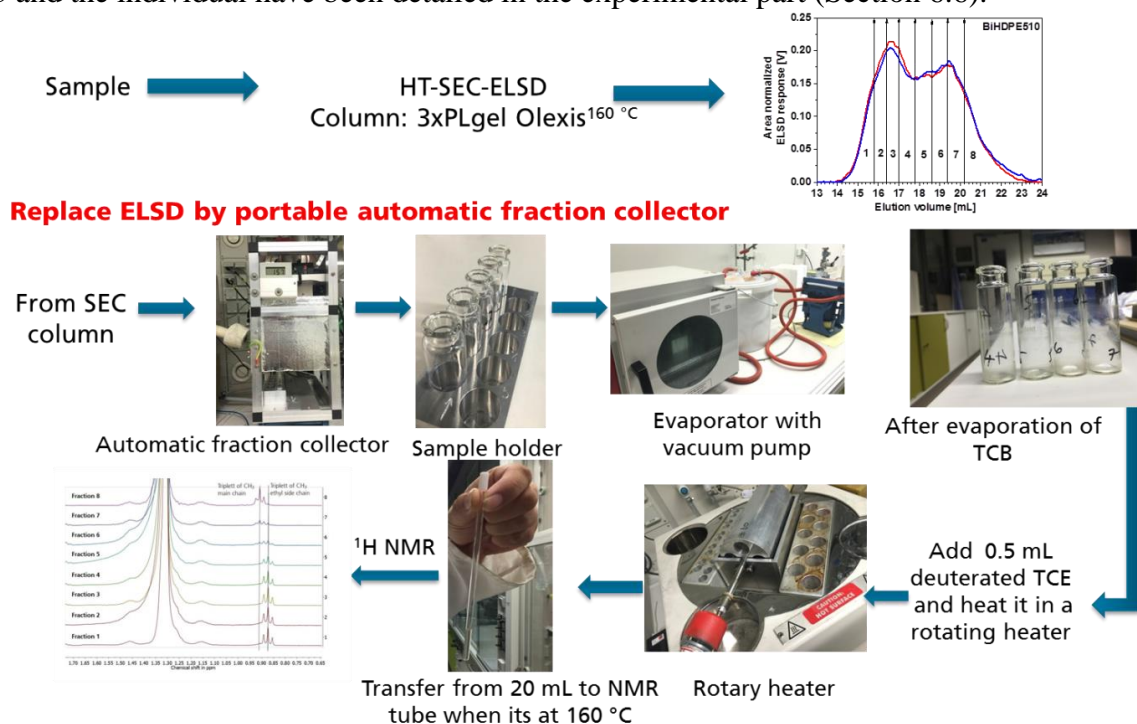


Figure 53 Steps followed in Off-flow HT-SEC→NMR

7.2.5. Preparative Fractionation of BiHDPE using Off-flow HT-SEC→NMR

The MMD of BiHDPE as determined by HT-SEC is shown in Figure 54.

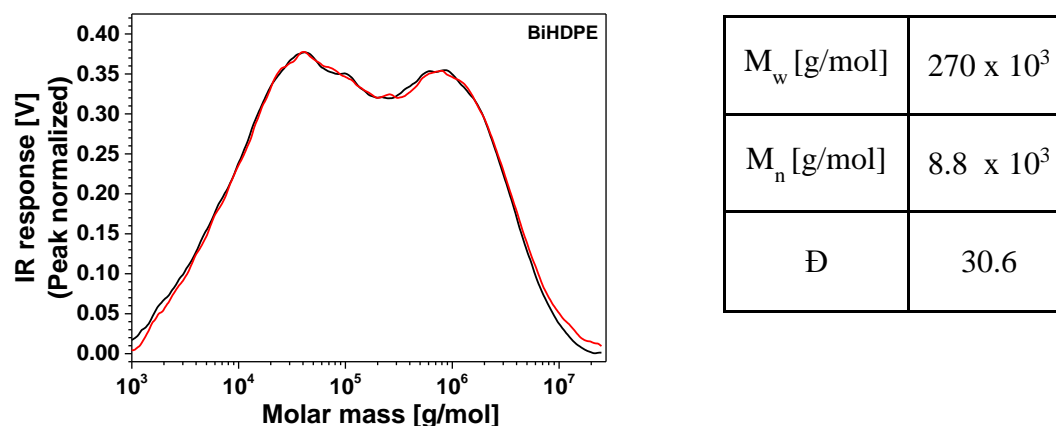


Figure 54 MMD of BiHDPE

It can be recognized that BiHDPE exhibits a broad bimodal MMD ($10^3 - 10^7$ g/mol). In the obtained HT-SEC chromatogram the desired elution volume windows for each fraction were marked as in Figure 55.

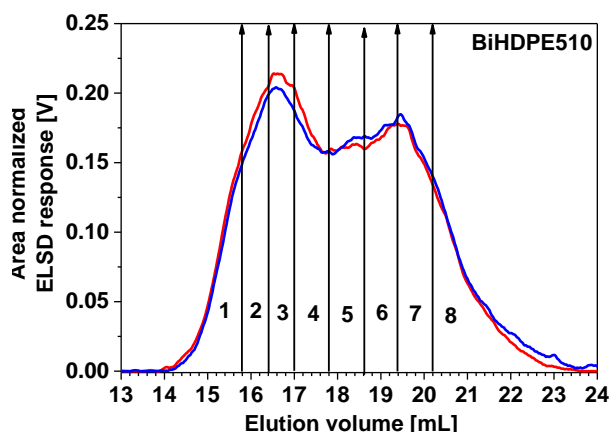


Figure 55 Eight fractions marked in the chromatogram obtained from HT-SEC of BiHDPE

At first 3 fractions (Analysis-I^{7 injections}) of BiHDPE were collected using the PAFC, then the number of fractions was successively raised to 5 (Analysis-II^{12 injections}) and 8 fractions (Analysis-III^{20 injections}). The number of injections for each analysis was calculated as explained in the experimental part (Section 6.7). The collected fractions in each analysis (I-III) were then injected back into the HT-SEC column to evaluate the separation resolution. Stepwise the number of fractions in each analysis (I-III) was increased to determine the overlap percentage between each fraction.

Figure 56 a, b and c show the elugrams of representative fractions with their overlaps and Figure 56d lists the values of \bar{D} for each fraction.

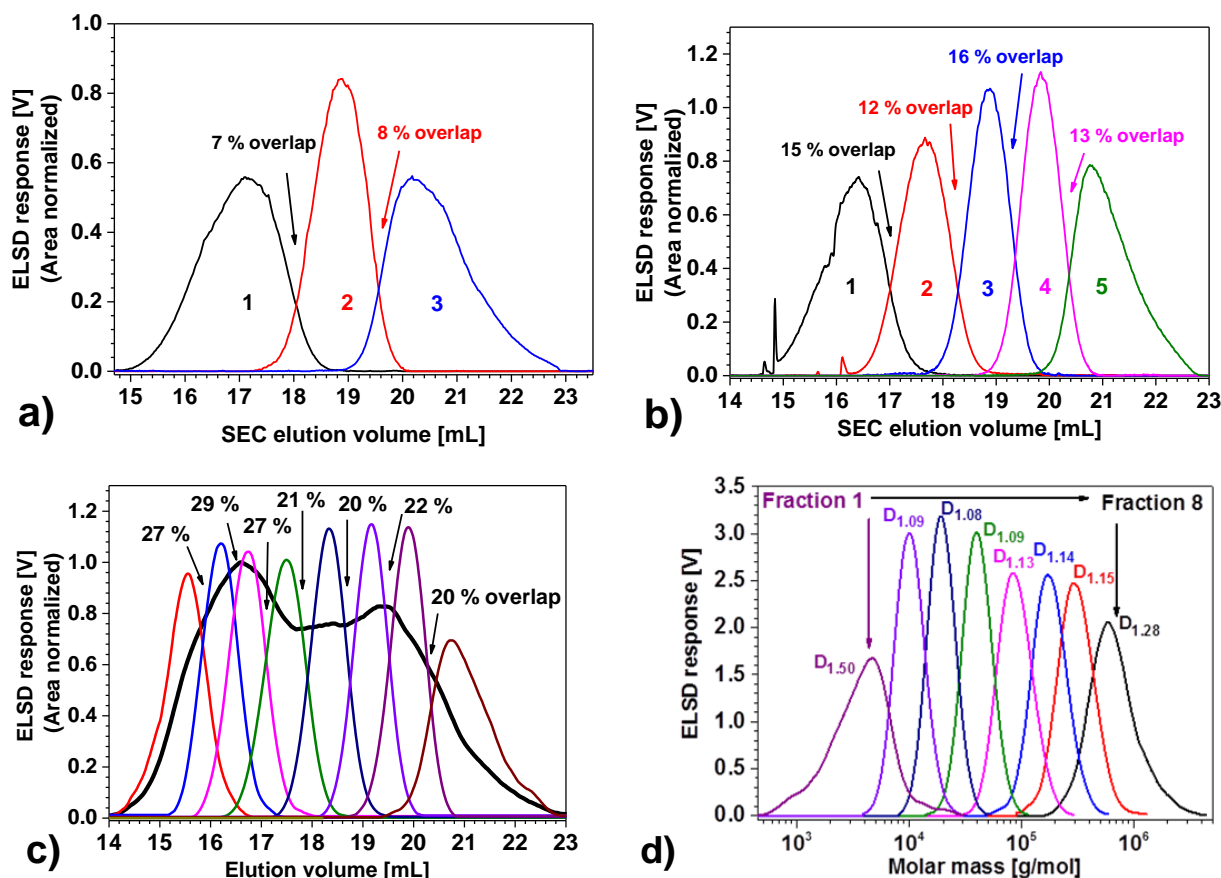


Figure 56 Fractions obtained for BiHDPE with HT-SEC and their overlap for a) Analysis-I⁷ injections b) Analysis-II¹² injections c) Analysis-III²⁰ injections and d) Analysis-III²⁰ injections with MM calibration (PS calibration)

An increase in the number of fractions leads to a larger overlap (Figure 56a, b and c). However, the results are not truly comparable as the number of injections plays a significant role in the overlap % of fractions. With the help of the PAFC the overlap of fractions of BiHDPE could be reduced from about 80 % (Figure 49) by the manual approach to a maximum value of 30 % (Figure 56c). With molar mass calibration it is noticeable that the fractions were separated with a \bar{D} of 1 – 1.50 (Figure 56d). Thus, narrowly molar mass distributed fractions of PE were collected with the PAFC.

7.2.6. ¹H NMR Analysis on all Fractions

After collecting sufficient amounts of material (as mentioned in the steps for prep. fractions step 8 and 9) the fractions were investigated using ¹H NMR (Figure 57). The ¹H NMR spectra of the fractions are shown in Figure 57 and the average contents of 1-butene calculated are listed in Table 6.

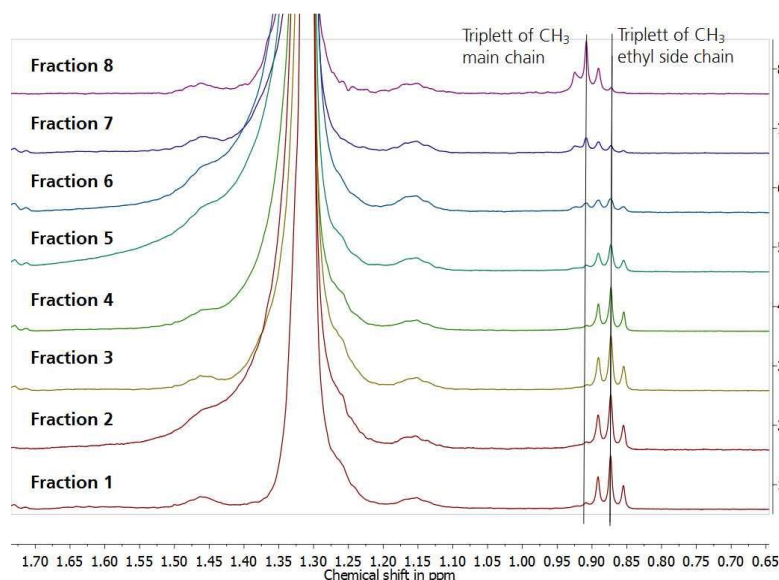


Figure 57 ¹H NMR for all 8 fractions of BiHDPE from HT-SEC

Table 6 Average content of 1-butene (C₄) for 8 fractions calculated using ¹H NMR

Fraction	Content of C ₄ in mol/mol %	Content of methyl end group in mol/mol %
1	1.3	< *LOQ
2	1.1	< LOQ
3	1.2	< LOQ
4	0.6	0.01

5	0.5	0.02
6	0.3	0.08
7	0.2	0.12
8	0.1	0.37

*LOQ - Limit of quantification.

From the spectra (Figure 57) and Table 9 it is evident that the content of methyl end groups increases with the higher fraction number, while concomitant with that the side chain content decreases.

Thus to conclude, the hyphenation of HT-SEC with the PAFC aids in collecting molar mass wise narrowly distributed BiHDPE fractions (\bar{M}_n of 1 – 1.50). ^1H NMR on these determines the correlation between the molar mass and the 1-butene content. The long term perspective would be to use the designed PAFC (working temperature 20 – 220 °C) to a wider range of off-low LC techniques (SGIC, TGIC, 2D-LC)→ ^{13}C NMR to investigate the heterogeneities with regard to microstructure.

7.2.7. Conclusion

In this study for the first time a portable automatic fraction collector (PAFC) was designed which enables rapid plugin at a range of HPLC instruments and have a wide working temperature 20 – 220 °C. In this work, BiHDPE was fractionated by using the PAFC hyphenated to HT-SEC. The collected fractions from HT-SEC were analyzed by NMR (off-line). NMR on HT-SEC fractions of BiHDPE showed that the medium and high molar mass fractions contain a higher comonomer content compared to those of low molar mass. This method has potential to be extended to most of the polymers as the PAFC has a wide working temperature range.

7.3. Development of Separation of Functionalized Polyolefins using HT 2D-LC→IR

7.3.1. Introduction

The application properties of the products of a functionalization of polyolefins by grafting are, for a given overall composition, determined by their heterogeneities with regard to molar mass and chemical composition. MMD and the corresponding average values can be determined by HT-SEC. The average chemical composition of such reaction products can be analyzed by spectroscopic techniques, and FTIR spectroscopy [236-251] has, due to its sensitivity and ease of measurement, been widely used for this purpose. The strengths of nuclear magnetic resonance are structure elucidation and the ability to deliver compositional information without prior calibration.[241,249,251,252] Titration techniques [237,240,253-256] are state of the art to determine the average content of polar groups bound on polyolefins.

However, all these techniques deliver average values for the degree of functionalization, and no information about the molecular heterogeneities i.e., the way the comonomer is distributed along and across the molar mass axis is obtained. For the case of PP-g-MA extraction methods have been investigated to separate the grafted product from unreacted PP [240,257]. However, such techniques are not very selective, and serious drawbacks from an industrial standpoint are low sample throughput and poor reproducibility.

This creates the need for an analytical technique which can separate functionalized polyolefins according to their degree of functionalization. For deformation of olefin copolymers approaches based on crystallization, TREF [76], CRYSTAF or CEF [77-79] have been widely applied. A fundamental problem when applying these techniques to grafted samples is the fact that the graft content is typically very low (< 5 mol %), and that the crystallization temperature, which is the variant for the separation, depends also on the microstructure (with regard to stereo- and regio-chemistry) of the grafted units on the backbone. An additional factor complicating the interpretation of results from crystallization based techniques for PP-g-MA is the fact that the average molar mass is typically fairly low. As a result its influence on the crystallization temperature may become significant [201,202,258].

Liquid chromatographic techniques have shown potential to separate polymers bearing polar groups [259,260]. A particular advantage of HT 2D-LC is that the interrelationship between CCD and MMD can be obtained. This is a particularly interesting incentive to explore this possibility, as from a property point of view a high degree of grafting, concomitant with a high average molar mass is targeted.

Interestingly, none of these modern analytical techniques has yet been applied to post synthesis functionalized polyolefins. In this study we want to show the potential of HT-HPLC to determine the bivariate distribution of PP-g-MA. In detail, we want to investigate the compositional heterogeneity such materials using HT-HPLC, and then hyphenate the compositional separation according to molar mass, to fully reveal the heterogeneity of PP-g-MA.

7.3.2. Determination of Grafting Content across the MMD using HT-SEC→IR

Two samples which differ in their average content of MA were chosen and analyzed by HT-SEC→IR using the LC-Transform approach [182,260-262] (Figure 58).

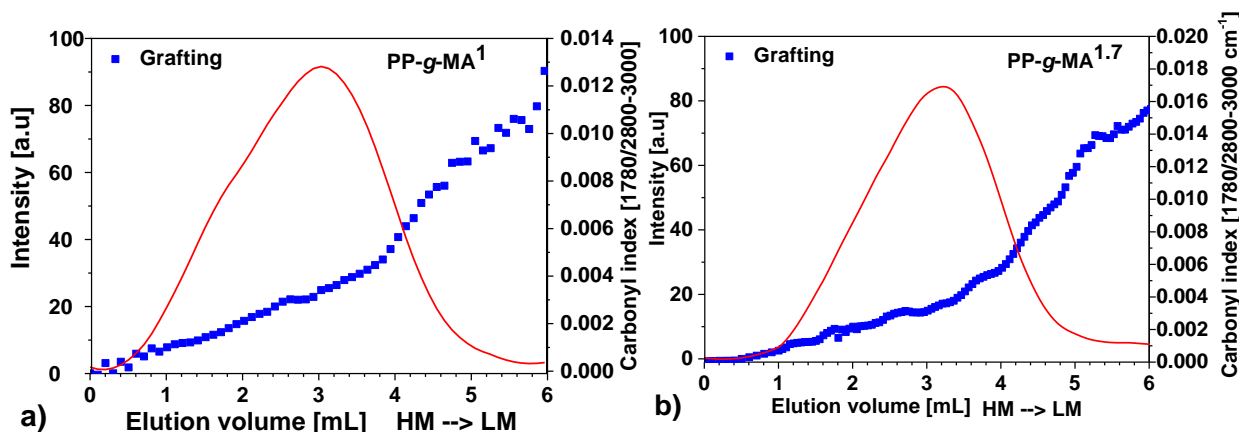


Figure 58 Gram-Schmidt plot (corresponds to the MMD) for a) PP-g-MA¹ and b) PP-g-MA^{1.7}

It can be observed that for both samples the grafting occurred preferentially in the low molecular region, leading to gradients of functionalization along the MMD (Figure 58). From these results the average degree of functionalization along the MM axis can be extracted, while fractions of same molar mass but differing in their degree of functionalization will co-elute, which then necessitates a deformation with regard to CC.

7.3.3. Determination of Compositional Heterogeneity using CRYSTAF→FTIR

To study the compositional distribution perpendicular to the MM axis (CCD) CRYSTAF was utilized. Samples were analyzed by CRYSTAF→FTIR, together with an *i*-PP-H sample as reference (Figure 59). From CRYSTAF a profile of the polymer concentration versus temperature is obtained, and its first derivative (dW/dT) gives information about the CCD. The area under the cumulative curve, which denotes the fraction crystallizing in a respective temperature range, is listed in Table 7.

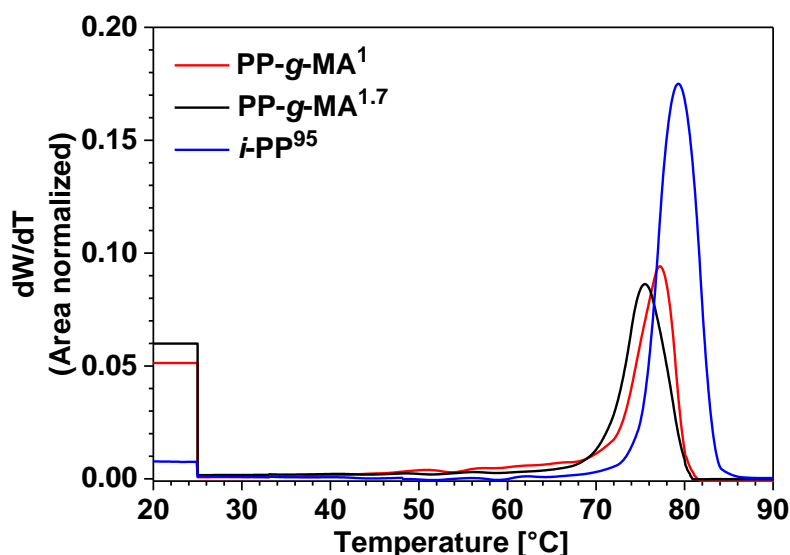


Figure 59 Overlay of the first derivatives of the polymer concentration in solution, dW/dT , of *i*-PP and PP-*g*-MA samples

Table 7 Area percentage and peak crystallization temperature, T_c , for the fractions

Sample	T_c [° C]	Area between two temperatures [%]		
		Fraction 1 (85 – 70 °C)	Fraction 2 (70 – 30 °C)	Fraction 3 (< 30 °C)
<i>i</i> -PP ⁹⁵	79	94	3	3
PP- <i>g</i> -MA ¹	77	54	20	26
PP- <i>g</i> -MA ^{1.7}	75	56	15	29

Figure 59 shows that all samples crystallize with a sharp peak between 85 and 70 °C and a T_c of about 79 °C, 77 °C and 75 °C for *i*-PP⁹⁵, PP-*g*-MA¹, PP-*g*-MA^{1.7} respectively. Both PP-*g*-MA samples exhibit a tailing from 70 to 45 °C, which can be seen to be more pronounced for PP-*g*-MA¹. A significant amount of amorphous fraction, which does not crystallize at 30 °C, is observed for both samples (Figure 59 and Table 7). It may be assumed that this loss of crystallinity is the result of the grafting. Taking into account that the crystallization temperature is related to the degree of functionalization [182] it may be derived that both PP-*g*-MA samples display considerable heterogeneity with regard to their functionalization (Fraction 2 in Table 7).

To further substantiate this, fractions were collected in the temperature range as specified in Table 7 and analyzed by FTIR spectroscopy. The results are presented in Figure 60 and the calculated degree of crystallinity and the CI are compiled in Table 8.

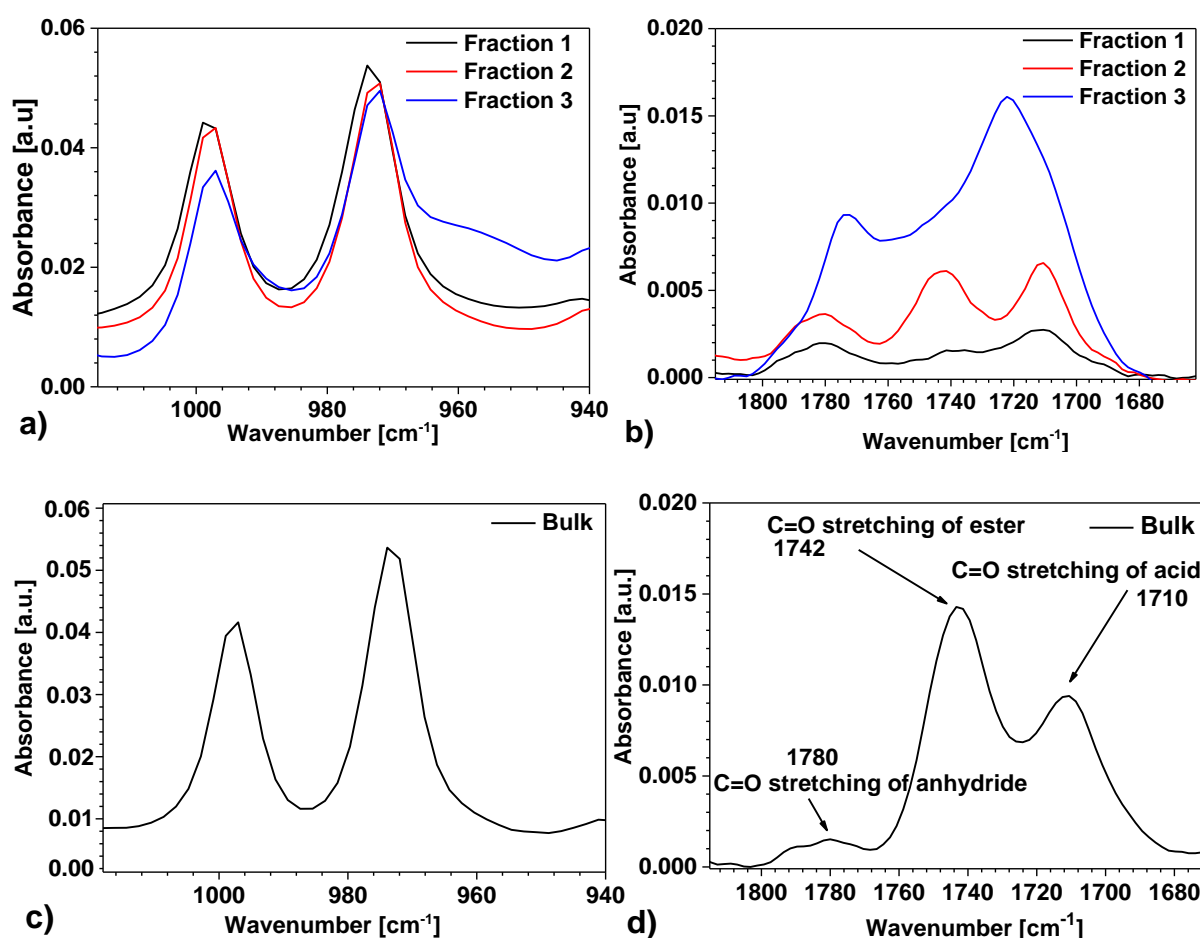


Figure 60 Overlay of the IR spectra of PP-g-MA¹ in the wavenumber range a) 940-1020 cm⁻¹ and b) 1660-1820 cm⁻¹ and bulk sample (PP-g-MA¹) in the region c) 940-1020 cm⁻¹ and d) 1660-1820 cm⁻¹

Table 8 Band area (A) ratio corresponding crystallinity and CI of all three fractions

Fractions	A^{973}/A^{998} (Crystallinity)	CI (A of MA bands/ A^{973})		
		A^{1710}/A^{973}	A^{1740}/A^{973}	A^{1780}/A^{973}
1	0.74	0.06	0.01	0.07
2	0.73	0.15	0.17	0.09
3	0.70	n.f.	n.f.	0.16

*n.f. - not feasible as the peaks merged with other characteristic peak

The three fractions as well as the bulk sample show absorptions characteristic for *i*-PP [263] at 973 cm⁻¹ (representing the amorphous/crystalline phase) and at 998 cm⁻¹ (representing the crystalline phase) (Figure 60a and c), and their area ratio (A^{973}/A^{998}) denotes the degree of crystallinity [264]. All three fractions vary in their degree of crystallinity (Table 8) and, as can be expected from the sequence of crystallization, fraction 3 is less crystalline compared to the other ones.

The bulk sample and all three fractions show absorptions in the carbonyl region (Figure 60b and d). Three bands (1710, 1740 and 1780 cm⁻¹) were observed in the carbonyl region of the

bulk sample (PP-g-MA¹) (Figure 60b): The bands at 1710 and 1742 cm⁻¹ signify the carbonyl vibration of carboxylic acid and ester respectively [239,265] and the band at 1780 cm⁻¹ can be attributed to the symmetric stretching of the carbonyl groups in the MA-ring [237,255,256]. The finding of the acid and the ester group in the bulk sample may be the result of the presence of a different type of grafting [255] or the open chain acid anhydride [266]. It can be noticed that the absorbance at 1780 cm⁻¹ is in all three fractions more intense compared to the bulk sample, while that at 1740 cm⁻¹ is lower (Figure 60b and d). A plausible explanation would be that the acid group reverts back to anhydride during the experimentation. Fraction 1 and 2 (Figure 60b) show similar characteristic bands as the bulk (Figure 60c). Thus it can be concluded that the first fraction has a lower MA content compared to the second one (Table 8 and Figure 60b).

Thus CRYSTAF enables to separate PP-g-MA according to the degree of functionalization, but the resolution is not sufficient to achieve a full deformation into a grafted and non-grafted fraction.

7.3.4. HT-HPLC and HT-HPLC→FTIR on PP-g-MA

Having appropriate chromatographic systems is the main requisite for the realization of HT-HPLC separation of PP-g-MA. Albrecht et al. [182,260,261] investigated polar sorbents and a mobile phases for separating the statistical copolymers of ethylene with various polar monomers [167,182,260,261,267]. Graft copolymers contain polar groups on a non-polar backbone and it can, therefore, be assumed that the polar groups will selectively interact with a polar sorbent and will be retained in the column, while non-polar units will not contribute to the retention. Accordingly, column filled with Mica and silica gel (PerfectSil[®]) was selected as sorbents. PerfectSil[®] has been applied previously for the analysis of random copolymer of ethylene with polar comonomers [182,259], while to the best of our knowledge no applications of Mica for the chromatography of polymers. Mica is a layered silicate with hexagonal morphology, and this arrangement leads to its thermal stability of up to 500 °C. Decalin and cyclohexanone were found to be an adequate adsorption and desorption promoting solvent, respectively [182].

The elugrams of both PP-g-MA samples using the chromatographic system PerfectSil[®]/decalin→cyclohexanone are shown in Figure 61.

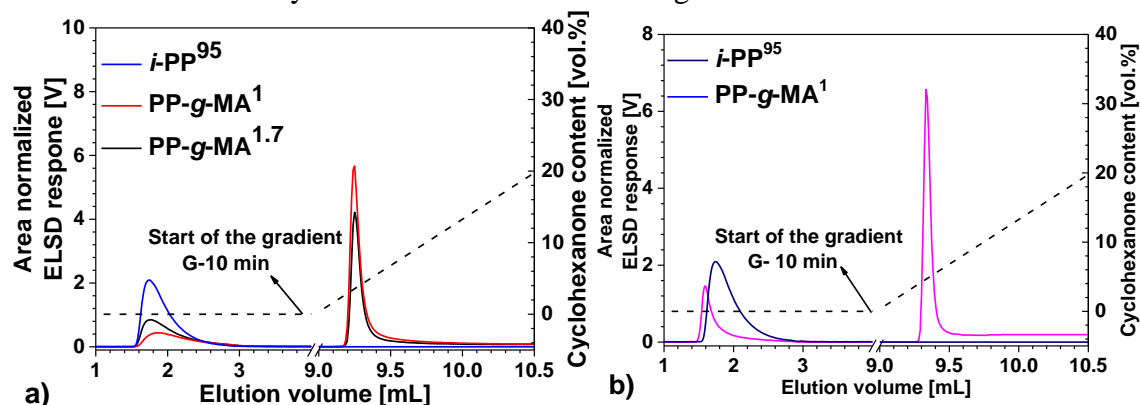


Figure 61 Overlay of chromatograms of *i*-PP⁹⁵ and PP-g-MA samples using a) PerfectSil[®] and b) Mica at 140 °C

Notice: Composition of the mobile phase in the ELSD is indicated in the figures.

Both functionalized samples eluted in two peaks in both sorbents (Figure 61): The first one, eluting before the gradient, represents a portion of the sample which was not adsorbed in the column, while the second one is adsorbed on the sorbent and later desorbed after addition of cyclohexanone to the mobile phase. As a rule the retention of a polar analyte increases with its polarity, and consequently it may be assumed that the latter eluting fraction can be assigned to PP grafted with MA.

To verify this hypothesis, the effluent of PP-g-MA¹ corresponding to both peaks was collected for the system PerfectSil®/decalin→cyclohexanone and analyzed by FTIR spectroscopy (Figure 62).

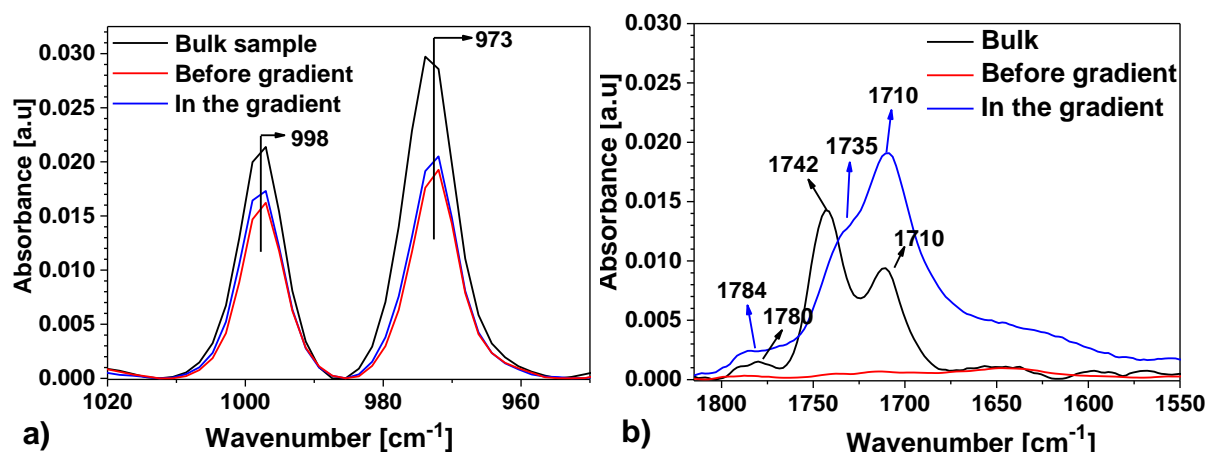


Figure 62 a) Overlay of the IR spectra in wavenumber range 950-1020 cm⁻¹ and b) Overlay of the IR spectra in the wavenumber range 1550-1850 cm⁻¹ corresponding to original PP-g-MA¹ and to the fractions eluted in the gradient and before the gradient

It can be recognized that the polymer eluting before as well as in the gradient shows vibrations at 998 and 972 cm⁻¹, which are indicative for *i*-PP (Figure 62a). The polymer eluting in the gradient shows carbonyl vibrations similar to that of the bulk, which are not present in the fraction eluting before the gradient (Figure 62b). This confirms that HT-HPLC separates the reaction product into a grafted a non-grafted fraction (*i*-PP).

Albrecht et al. [182,260,261] demonstrated that the elution volume of statistical EVA copolymers from silica increases with the increase in the average VA-content. A similar behavior was observed for the PP-g-MA samples. Thus the second peak position in Figure 61 can be correlated with the average content of MA in the samples. Yet, the samples are chemically heterogeneous i.e., only a portion of PP is grafted, and as a result the average MA content does not represent the average composition of the PP-g-MA fraction.

7.3.5. HT 2D-LC→ELSD-IR of PP-g-MA

For a meaningful interpretation of chromatographic data a quantitative detector response is essential. While, the ELSD remains the sole option for one dimensional HT-HPLC, its response is exponential with regard to concentration and depends on the composition of the eluting polymer [268]. Moreover, to derive structure↔property relationships from analytical results knowledge about the bivariate distribution with regard to composition and molar mass is

essential. Two dimensional liquid chromatography (HT-HPLC x HT-SEC) which hyphenates the compositional separation with one according to molar mass has proven the appropriate method for this purpose. [167,168,269]. An additional advantage of adding the HT-SEC dimension is the fact that in the last dimension the elution occurs quasi isocratic, which in turn enables to employ IR spectroscopy for detection as it is state of the art in HT-SEC and CRYSTAF [104,270].

Yet, the challenge in HT 2D-LC→IR is that the sample and the solvent peak have to be separated. This is not an issue with ELSD as the solvent gets completely evaporated. The latter issue with IR was resolved by a column with high theoretical plate number (N_{11000}) for HT-SEC to have a better efficiency of separation between the solvent and the sample peak and between the low and high molar mass sample peak and sufficient time is provided for one HT-SEC analysis. The optimized experimental conditions were applied on PP-g-MA samples and the well separated sample and the solvent peak for both homopolymer and the graft copolymer is presented in the chromatogram below in Figure 63.

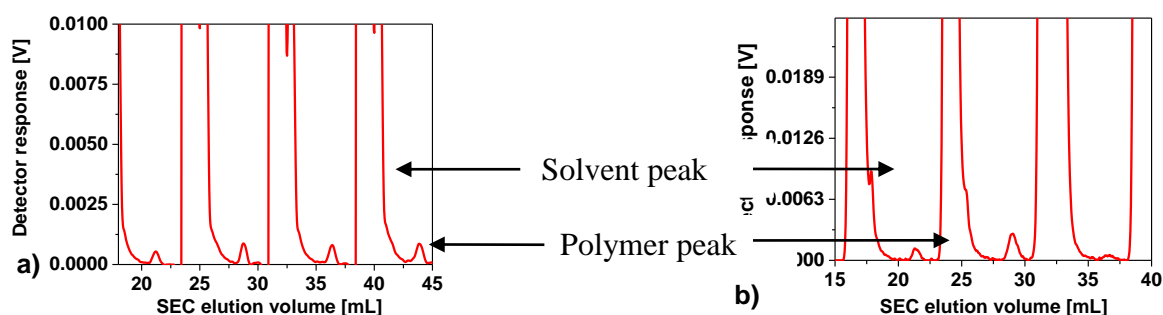


Figure 63 Overlay of HT-SEC traces recorded with IR detection a) before the gradient (*i*-PP) and b) in the gradient (PP-g-MA)

With each fraction transfer from the HT-HPLC into the HT-SEC dimension, a small amount of 1-decalin (solvent plug) is injected, with the amount depending on the gradient. Since the IR detector used here is tuned to the stretching vibration of the methyl- and methylene-groups, 1-decalin causes an intense broad peak in the chromatograms (Figure 63). Yet, by high theoretical plate numbered HT-SEC column and with an optimization of the HT-HPLC (0.02 mL/min) and HT-SEC flow rate (1.5 mL/min) and a transfer loop (100 μ L) a baseline separated solvent and sample peak was observed (Figure 63).

To establish a relationship between IR response and the concentration *i*-PP⁹⁵ was injected at different concentration into the HT 2D-LC→IR and the detector signal is plotted as a function of the injected concentration in Figure 64.

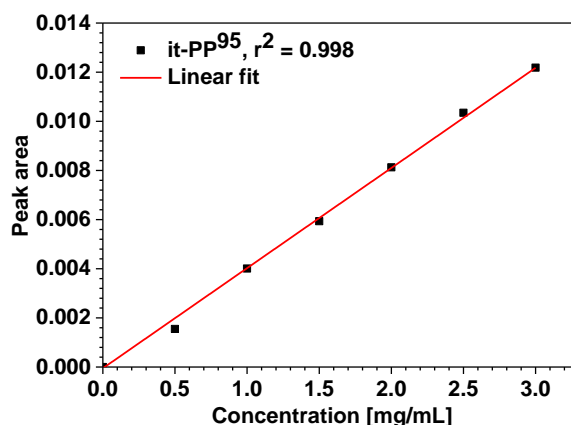


Figure 64 Response of IR detector with respect to concentration of polymers

Figure 64 shows that the IR response of *i*-PP⁹⁵ depends linearly on the concentration of the polymers. PP-*g*-MA samples were analyzed by HT 2D-LC→IR in the above discussed optimized experimental conditions. The results from HT 2D-LC are presented in two dimensional contour plots (Figure 65).

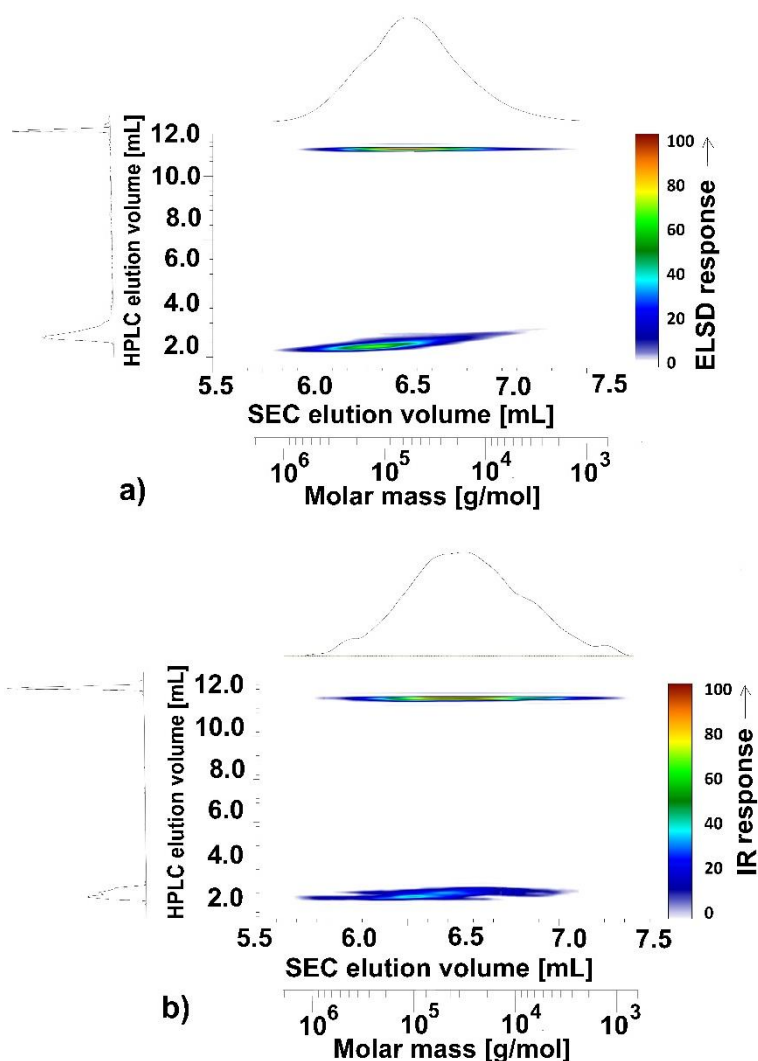
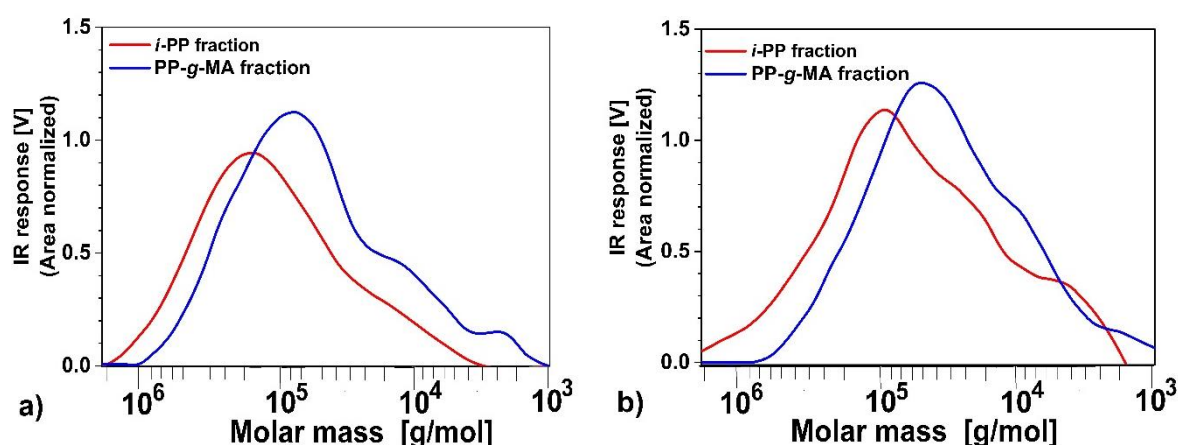


Figure 65 2D contour plot a) PP-g-MA¹ b) PP-g-MA^{1.7}

Notice: The HT-SEC axis was calibrated with regard to MM by PS standards and then converted to *i*-PP by using the Mark-Houwink equation [188].

The contour plot of both samples reveals two spots: The one which elutes before the gradient can be assigned to the homopolymer, *i*-PP, and the other, which elutes in the gradient, to PP-g-MA. The broadness of the first peak on the HT-HPLC axis (i.e., polymer eluting in decalin) reflects the MMD of *i*-PP, while the broadness of the second peak on the same axis reflects the CCD of the PP-g-MA. Differences in the HT-HPLC elution volume (in 1D and 2D) may be the result of different parameters used. To determine the MM and MMD of both constituents the contour plots were projected into the HT-SEC plane (Figure 66).

**Figure 66** Overlay of HT-SEC projections from HT 2D-LC→IR a) PP-g-MA¹ and b) PP-g-MA^{1.7}

Notice: The HT-SEC chromatogram from the HT 2D-LC→IR for PP-g-MA¹ (Figure 66) cannot be compared with the Gram-Schmidt plot along the HT-SEC elution volume (Figure 58) as the origin of the data and the experimental procedures are different.

Using the calibration (Figure 64), the portion of *i*-PP present in the analyzed samples (PP-g-MA¹) may be calculated from the peak areas of *i*-PP eluting before the gradient (Figure 65a). By subtracting the amount of *i*-PP (eluting before the gradient) from the total amount of the injected polymer, the amount of PP-g-MA (eluting in the gradient) was obtained. The results are summarized in Table 9.

Table 9 Composition of the analyzed samples as calculated from the peak areas in chromatograms

Sample	<i>i</i> -PP [wt. %]	M _w of <i>i</i> -PP [g/mol]	PP-g-MA [wt. %] (calculated from wt. % of <i>i</i> -PP)	M _w of PP-g-MA [g/mol]
PP-g-MA ¹	20	2 x 10 ⁵	80	1x10 ⁵
PP-g-MA ^{1.7}	18	8 x 10 ⁴	82	4 x 10 ⁴

It is evident from Figure 66 that both samples exhibit a broad MMD (1×10^3 to 1×10^6 g/mol) and contain significant amounts of low molar mass material in the PP-g-MA part (1×10^3 to 1×10^4 g/mol). Table 9 reveals that the M_w for the homopolymer (*i*-PP) is higher than that of the graft copolymer (PP-g-MA). Furthermore both samples contain around ~20 % of *i*-PP homopolymer and their portion of grafted polymer is similar (Table 9).

7.3.6. Conclusion

Despite the fact that various analytical techniques have been applied in the past to characterize functionalized polyolefins, the challenge of determining the bivariate distribution (MMD and CCD) of such reaction products generated from polypropylene and maleic anhydride remained unsolved. By using HT-SEC→FTIR via the LC-Transform interface we could show that the grafting occurred primarily in the low molar mass part. Although a compositional separation could be achieved via CRYSTAF, the selectivity of such a crystallization based approach is not sufficient for PP-g-MA. Yet, using HT-HPLC with silica gel (PerfectSil®) and column filled with Mica as sorbent and a solvent gradient decalin→cyclohexanone^{G-10 min} at 140 °C two samples of PP-g-MA were baseline separated into a functionalized and a non-functionalized portion. The separation achieved was confirmed by analyzing the HT-HPLC fractions (obtained with PerfectSil® as a sorbent) with FTIR spectroscopy.

This separation according to the chemical composition was hyphenated with a separation according to the molar mass, which enabled for the first time to determine the bivariate distribution of PP-g-MA samples. As a result the contour plot from HT 2D-LC→IR exhibited a two spot regime, reflecting the grafted and non-grafted component. From the contour plots it could be shown that the two samples, which differ in their nominal content of maleic anhydride, are comparable with regard to their portion of the grafted material. Yet, a higher degree of grafting is accompanied by a lower molar mass of the grafted portion. Contrary to that, the MMD of the polypropylene portion of both samples is similar i.e., hardly affected by the graft reaction.

The developed analytical methodology may be highly useful for developing more efficient processes of functionalization, and the analytical information can be applied to derive structure↔property relationships for functionalized polyolefins.

7.4. Investigating Interactions of Polyethylene with Graphite in the Presence of Solvent

7.4.1. Introduction

In interaction based chromatographic techniques the interactions between the stationary phase and the macromolecules are the driving force for separating the polymer chains based on their chemical composition. Porous Graphitic Carbon (PGC) because of its rigid planar graphite surface results in a strong retention of planar molecules [271-274] and a reduced retention of branched ones, for which steric hindrance limits the degree of contact between the analyte and the PGC surface [275]. PGC displays particular strength for the separation of structurally similar compounds such as geometric isomers (e.g. cis, trans, or topic isomers of aromatic) and diastereomers of polar and non-polar character [275-279]. PGC has also been exploited for a liquid chromatographic approach to separate polyolefins (POs) according to the content of alkyl short chain branching or microstructure i.e., the way monomers are linked with regard to their stereo- and regio-chemistry.

The immense interest in HT-HPLC of polyolefins, using PGC as stationary phase, renders pivotal importance to the nature of the interactions between the sorbent and polyolefin macromolecules at the conditions of HT-HPLC i.e., at temperatures significantly above 100 °C and in dilute solution [108,141,146,167,168,280]. Such information is essential to optimize the chromatographic protocols, for examples with regard to the aspects of resolution and selectivity. The interaction between a molecule and graphite is typically characterized as either physisorption or chemisorption, depending on the strength of the interaction. Physisorption generally refers to van der Waals interaction [177,281] and chemisorption implies strong interaction due to a significant charge rearrangement in the adsorbed molecule to facilitate the formation of a covalent or ionic bond with the surface. Several studies were carried out with Scanning Tunnelling Microscopy (STM) [177-179,281-284] to understand the physisorption of alkanes on graphite. Theoretical and experimental studies using STM have shown that self-assembly occurred when a melt of linear alkanes or a solution containing these were brought in contact with the graphite [142,285-287]. STM experiments have been carried out at the interface between long chain alkanes ($n \geq 36$) [177-179,281-284] as well as on alkyl derivatives, including alkanols, [177-179,282,283] and graphite. From these it could be concluded that the sample adsorbs as a densely packed multi-layer on the basal plane of graphite. It has also been shown that long chain cyclic ($n \geq 50$) and linear alkanes ($n \geq 36$) adsorb from non-polar solvents (n-decane) on the graphite surface [177,288-293]. By corroborating the results from STM with those from molecular dynamics simulations [177-179,281-284] it was concluded that the orientation of the alkane molecules on the graphite surface is governed by weak van der Waals interactions between the alkane and graphite. Yet, none of the above techniques delivers direct analytical evidence about the interaction between graphite and alkanes in solution.

Potentially, various spectroscopic techniques could be used to study the interaction between graphite and the analyte in situ: Nuclear magnetic resonance (NMR) excels by high resolution, but suffers from low sensitivity, and the presence of graphite may lead to problems with the homogeneity of the magnetic field. Recently, Mekap et al. [294] studied the interaction of PE with nanographite in the presence of ODCB using high temperature thermal gradient NMR and solution DSC. From the reversibility of the interaction with graphite and the absence of a hysteresis, as determined by NMR, they concluded that crystallization does not play a role. Infrared spectroscopy has very high sensitivity, but the strong absorptions of both, the graphite and solvent, almost exclude the utilization of this technique for studying such interaction.

Several researchers utilized Raman spectroscopy to characterize different carbon materials and focused on the origin of the D and G band [34-39]. The Raman spectrum of graphite exhibits three prominent bands, namely the G-, D-, and the 2D band [169-172,174]. In case of interactions between an analyte and graphite in a solution this G-band can shift [169-172,174-176,178,179]. Numerous researchers employed Raman spectroscopy to study the interaction between ionic liquids and different varieties of carbon, like single walled carbon nanotubes and graphite [175,176,178,179]. They observed a shift in the G-band to higher wavenumber as a result of the interaction between the ionic liquids and the delocalized electrons in the graphite. The latter aids the dispersion of the mentioned carbon materials, and it was speculated that the interactions arise from cation- π/π - π interaction (i.e., dipole-dipole interaction), which is a type of van der Waals interaction. In this study, Raman spectroscopy was utilized to gain more insight into the interaction between graphite (HypercarbTM) and polyethylene (PE) in an organic solution (n-decane) at temperatures above the crystallization temperature of PE.

7.4.2. Interaction Study between Graphite and Alkanes

Confocal Raman microscopy combines a confocal microscope with a spectroscopy system for an improved chemical sensitivity. This method requires only minimal sample preparation, and the data accumulation to obtain a spectrum takes in the order of few seconds. The Raman spectrum of neat HypercarbTM was recorded at room temperature (RT – 20 °C) to determine the characteristic bands of graphite (Figure 67).

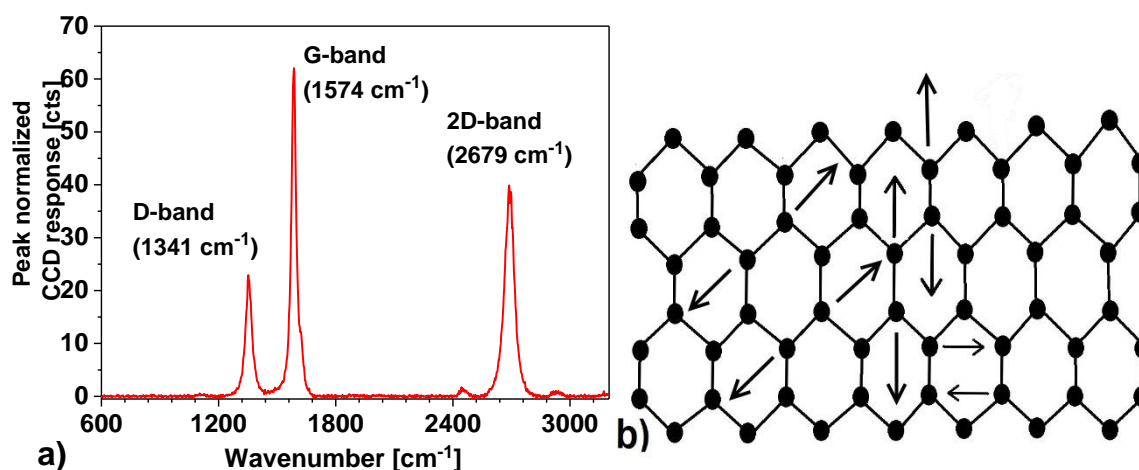


Figure 67 Raman spectrum of HypercarbTM b) C-C vibrations in graphitic material [295] at 20 °C

The Raman spectrum of HypercarbTM [169-172,174] exhibits three prominent bands (Figure 67), namely the G-band (1574 cm^{-1}) - arising from the C-C vibrations in the graphitic material (Figure 67b), the D-band (1351 cm^{-1}) and the 2D band (2689 cm^{-1}).

The homopolymer PE exhibits substantial heterogeneities with regard to chain length, branching, and architecture, which may complicate the interpretation of data. Additionally, high temperatures are required for dissolution, which poses an experimental challenge. Therefore, alkanes were selected as well-defined model samples (n-decane, n-dodecane and 2-methylundecane). Representative widely used solvents in HT-HPLC of PE, like the adsorption promoting (adsorli) n-decane and 1-decanol and the desorption promoting (desorli) TCB and

ODCB, were investigated [141,269,296]. However, as these show a band in the G-band region, complications in determining the G-band shift (δ) of graphite have to be expected. The spectra are shown in Figure 68.

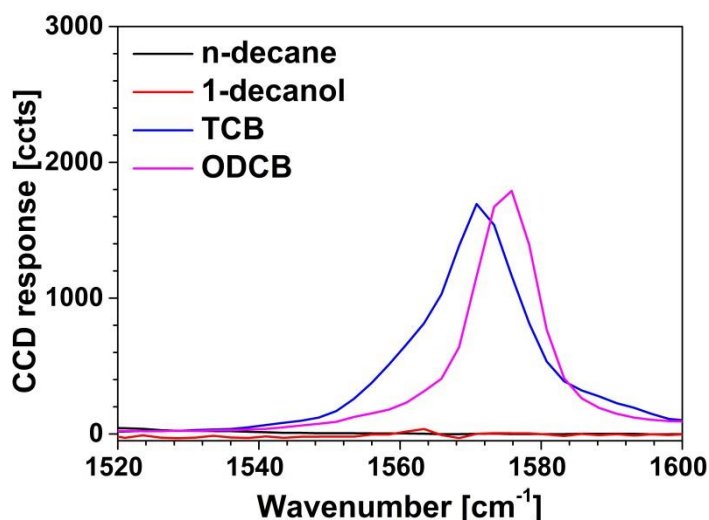


Figure 68 Raman spectra of adsorli and desorli at 20 °C

Figure 68 shows that both TCB and ODCB exhibit an intense band in the G-band region (1560 – 1580 cm^{-1}). Thus, further investigations were carried out with n-decane. N-decane also exhibits a sufficiently high boiling point (solvent) which minimizes evaporation during measurements.

Alkanes are low molecular homologues of polyethylene (PE). n-decane, n-dodecane and 2-methylundecane were chosen as model compounds as these are liquid at room temperature, which simplifies the experimental setup considerably. In the first step an optimization of the ratio HypercarbTM/n-decane is needed, as a surplus of HypercarbTM may lead to dominant graphite spectra, while on the other side an excess of n-decane can lead to dominant n-decane spectra. An optimum concentration was identified at a ratio HypercarbTM/n-decane of 0.5 mg/1 mL at which spectra of all compounds can be recorded with quality sufficient for interpretation. The results for the individual analytes as well as the system using optimum conditions are shown in Figure 69a. The G and 2D band are shown in Figure 69b and c.

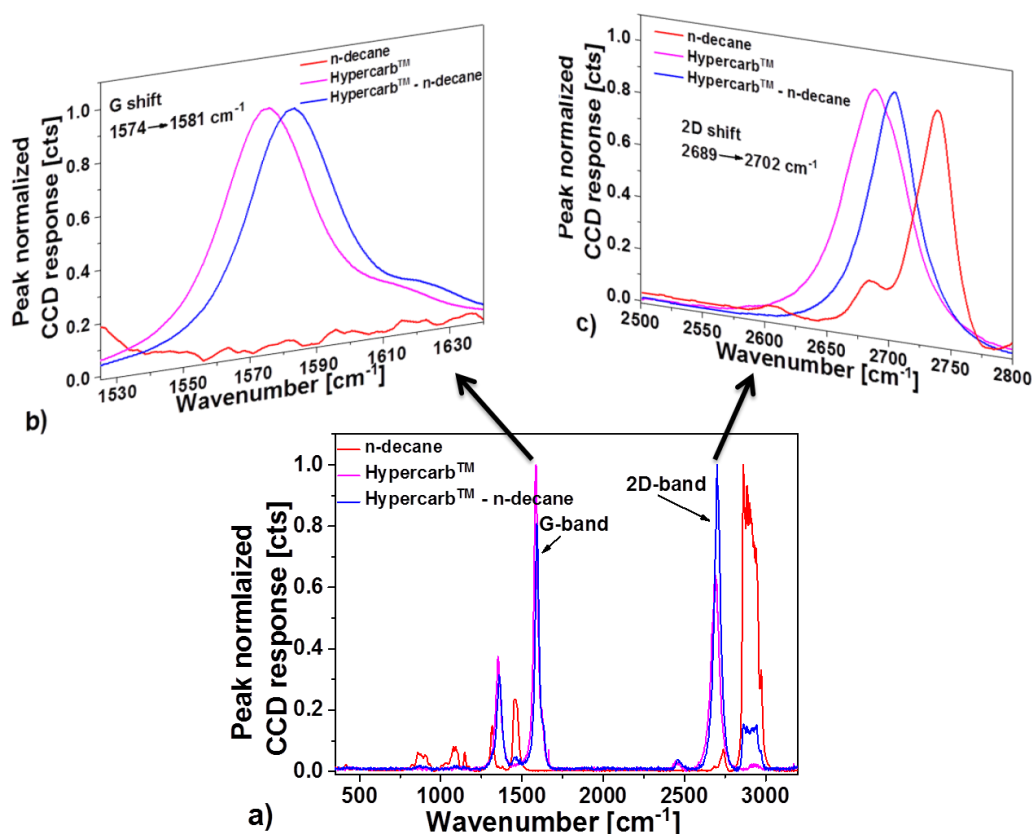


Figure 69 Raman spectra of the individual constituents and the system HypercarbTM/n-decane a) G-band and b) 2D band at 20 °C

Figure 69a and b show a significant shift in position of the G-band (δ) by 7 cm^{-1} and 13 cm^{-1} for the 2D-band. Thus it can be speculated that the interaction between HypercarbTM and n-decane at RT is of van der Waals type [172,175]. The D-band and 2D-band were not given consideration as n-decane also exhibits a band in the region of both these bands of HypercarbTM (Figure 69c).

7.4.3. Effect of Chain Length and Branching in the Interaction with Graphite

It has been shown that an increase in chain length (especially in case of PE) leads to longer retention of the analyte on the stationary phase in both SGIC [145,297] and TGIC [79,280,298]. Yet, an interesting question is if this will be reflected in the Raman spectrum. To probe this, measurements were carried out with n-decane and n-dodecane and the spectra are shown in Figure 70.

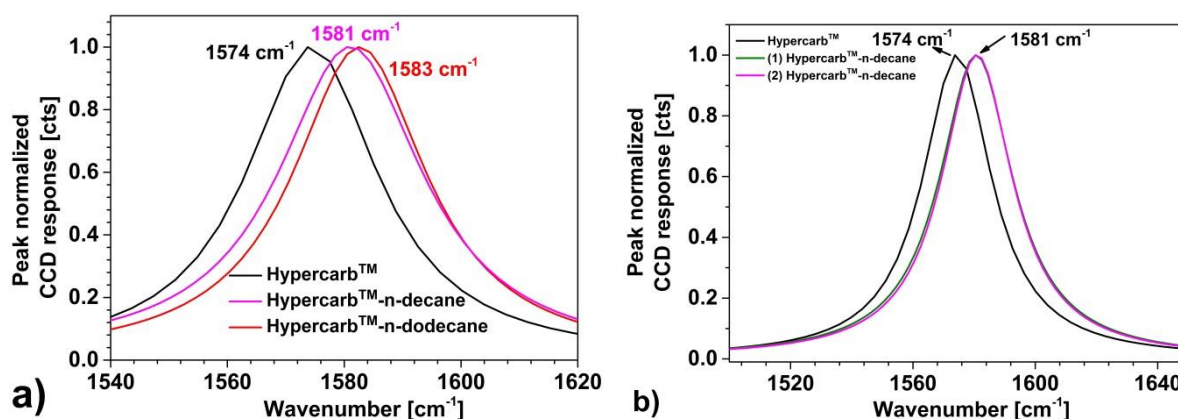


Figure 70 a) G-band of Hypercarb™ and Hypercarb™ with n-decane and n-dodecane; b) results of two independent measurements at 20 °C

From Figure 70a it can be noticed that an increase in chain length leads to a higher value for δ , namely a 2 cm^{-1} wavenumber difference in band position is observed between n-decane/Hypercarb™ and n-dodecane/Hypercarb™. These shifts in the G-band position for both the above mentioned systems were reproducible (Figure 70b), and their magnitude is in agreement with values reported by Subramaniam et al. [176] and Hermann et al. [175] for the system ionic liquid/carbon materials. The δ between Hypercarb™ and Hypercarb™/n-dodecane is 12 cm^{-1} which may in same sense be attributed to weak van der Waals interaction [172,175,176,299-301].

The second molecular parameter determining the retention in HT-HPLC of polymers is the presence of branching: For alkyl short chain branches in polyolefins it has been shown that increasing their content decreases the chromatographic retention [287,302]. Linear and branched dodecane (2-methylundecane) were selected as well-defined model samples and the spectra of the system Hypercarb™/n-dodecane are presented in Figure 71.

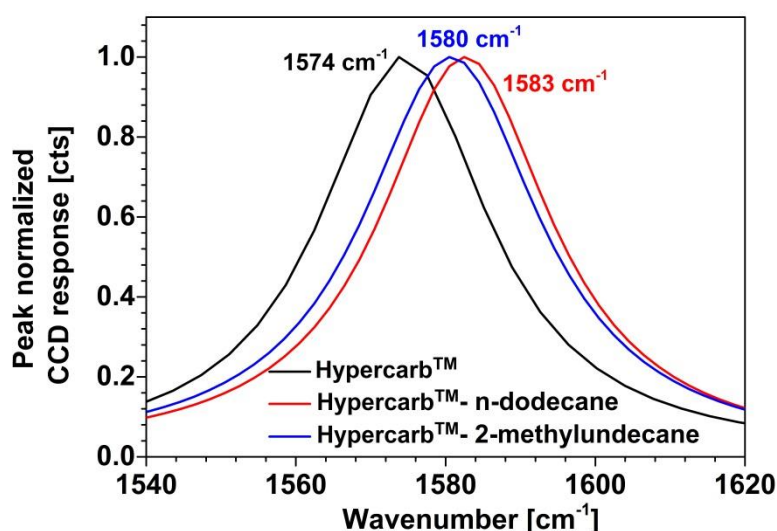


Figure 71 G-band of Hypercarb™/n-dodecane at 20 °C

The δ in HypercarbTM/2-methylundecane to lower wavenumber by 3 cm⁻¹ compared to that of the linear analogue (Figure 71). These results are in line with the behavior in HT-HPLC i.e., more branching results in a reduced interaction. The existence of a δ of 6 cm⁻¹ for HypercarbTM/2-methylundecane signifies the interaction of 2-methylundecane with HypercarbTM.

7.4.4. Interaction of PE with Graphite using Raman Spectroscopy

Considering this as proof of concept, the concept was then applied to the system HypercarbTM/PE/adsorli at high temperature (155 °C). N-decane was chosen as adsorli, as its Raman spectrum doesn't show a band in the region of the G-band of graphite (Figure 68). First the Raman spectrum of HypercarbTM was recorded at 155 °C (Figure 72) to mark the characteristic bands as temperature can influence the band position [303].

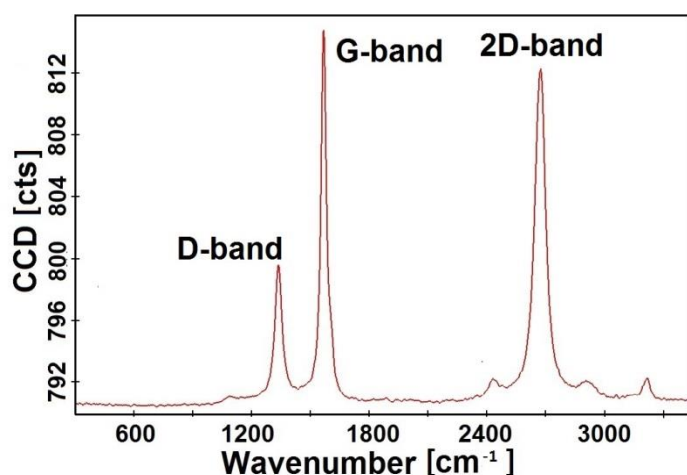


Figure 72 Raman spectrum of HypercarbTM at 155 °C

Figure 72 is very similar to Figure 67, both at room temperature and high temperature, with the 3 characteristics graphite bands G, D, and 2D. Yet, each of these experiences a shift to a lower wavenumber at high temperature (for example G-band of HypercarbTM at 20 °C is 1574 cm⁻¹ and at 155 °C is 1567 cm⁻¹), which is in agreement with [303]. This can be explained by the fact that an increase in temperature reduces the interaction between the graphene layers and results in a shift to a lower wavenumber.

Then the system HypercarbTM/n-decane was studied at 155 °C using a heatable microscopic stage. The Brownian movement of the HypercarbTM particles in n-decane at 155 °C made it difficult to obtain interpretable spectra. Therefore, the ratio HypercarbTM/n-decane was varied (from 0.5 mg/1 mL to 0.5 mg/0.5 mL). This resulted however in dominant spectra of HypercarbTM. Thus the measurement temperature was reduced to 60 °C, which turned out to be the upper limit for obtaining reproducible spectra. The G-band of HypercarbTM/n-decane at these conditions is shown in Figure 73.

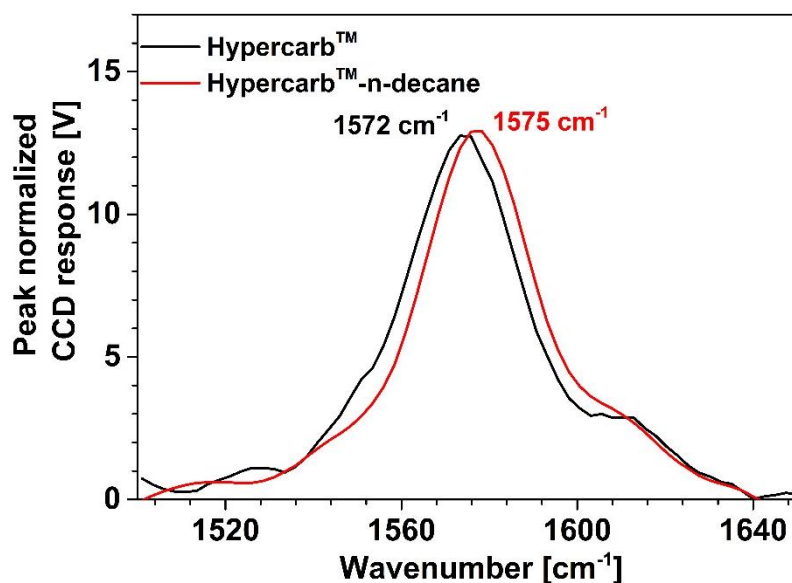


Figure 73 G-band of HypercarbTM/n-decane at 60 °C

From Figure 73 it can be noticed that the system HypercarbTM/n-decane exhibits a δ to a higher wavenumber by 3 cm⁻¹ which indicates an interaction between HypercarbTM and n-decane at 60 °C. Yet, at the same time δ decreased from 7 cm⁻¹ to 3 cm⁻¹ in comparison with the measurement at 20 °C (Figure 70a), which proves that an increase in temperature reduces the interaction between the graphitic surface and n-decane as expected.

Then the measurements were carried out at 155 °C for the individual components as well as the suspension HypercarbTM/PE/n-decane (Figure 74). Optimum conditions for recording Raman spectra were identified at a ratio HypercarbTM/PE/n-decane of 0.5 mg/1 mg/1 mL at which spectra of all compounds could be obtained with quality adequate for interpretation. The G and 2D band are shown in Figure 74b and c.

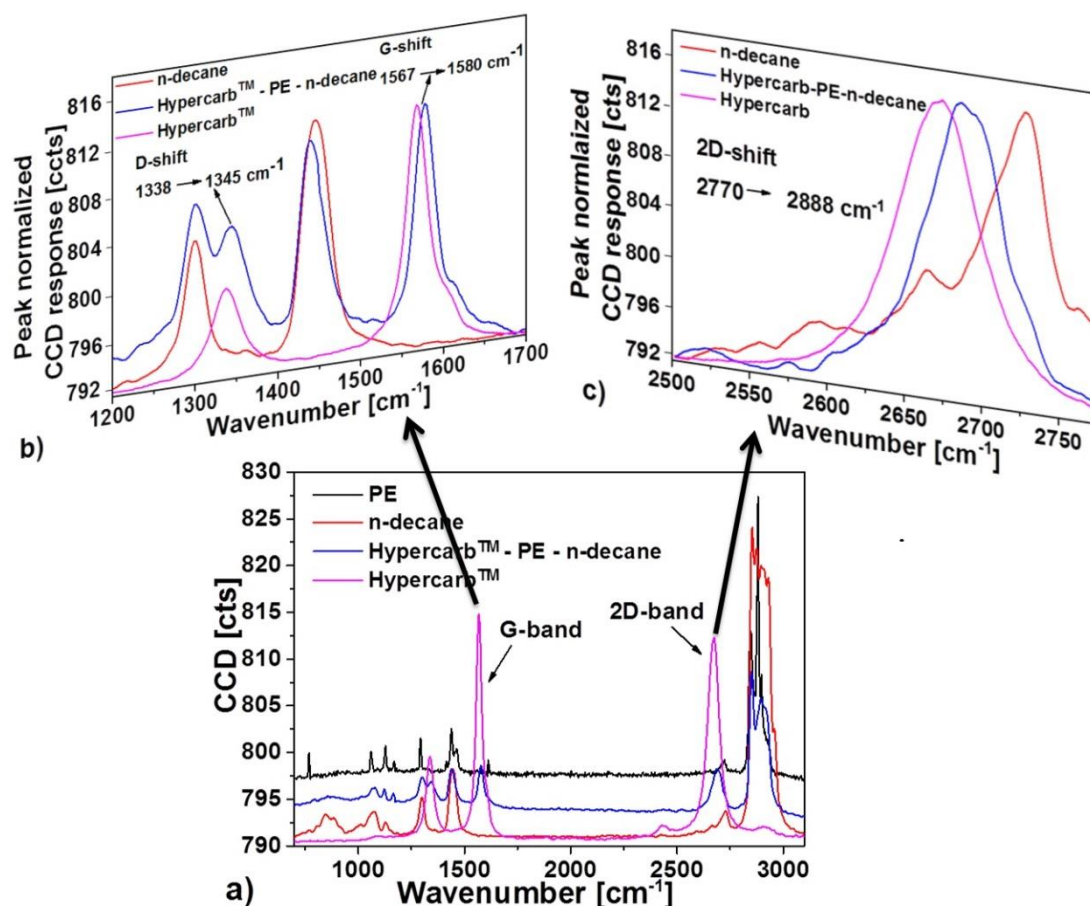


Figure 74 Raman spectrum of PE in n-decane with Hypercarb™ a) G- shift and b) 2D shift at 155 °C

In the spectrum Hypercarb™/PE/n-decane (Figure 74) all 3 individual components are evident. Figure 74b shows a δ of 13 cm^{-1} between pure Hypercarb™ and the mixture Hypercarb™/PE/n-decane, while the 2D band experiences a shift (Δ) of 18 cm^{-1} (Figure 74c) [172]. These significant values for δ and Δ for Hypercarb™/PE/n-decane indicate a van der Waals interaction between PE and Hypercarb™ [172,175,176,299-301].

For comparison, all values for δ are tabulated (Table 10).

Table 10 δ for Hypercarb™ with alkanes, branched alkanes and PE at RT and HT

Samples	Temperature	$\delta \text{ [cm}^{-1}\text{]}$
Hypercarb™/n-dodecane	RT (20 °C)	9
Hypercarb™/2-methylundecane	RT (20 °C)	6
Hypercarb™/n-decane	RT (20 °C)	7
Hypercarb™/n-decane	HT (60 °C)	3

Hypercarb TM /n-decane/PE	HT (155 °C)	13
--------------------------------------	-------------	----

Increasing the temperature leads to a decrease in the interaction between the analyte and the surface [304]. As a consequence the observed δ at higher temperature can be predominantly attributed to the interaction of HypercarbTM with PE. In summa, alkanes, branched alkanes, and PE exhibit a van der Waals interaction [172,175,176,299-301] with HypercarbTM.

7.4.5. Conclusion

Interface plays a vital role in interaction based chromatography. To understand the separation selectivity and mechanism and use this knowledge to improve the resolution in separation in HT-HPLC of polymers, it is important to gain insight into the nature of interaction between polymer and sorbent. Raman spectroscopy, which is sensitive to the morphology of carbon materials, was utilized for the first time to provide direct evidence for the interaction between the hydrocarbon and the surface of porous graphite (HypercarbTM) at room and high temperature. The characteristic bands of graphite (G- and 2D-band) were probed with regard to their sensitivity towards the interaction between hydrocarbons and the surface of HypercarbTM. The essential criteria for choosing the analyte/solvent were low volatility and absence of solvent bands in the G-band region. N-decane, n-dodecane and 2-methylundecane were selected as model analytes as they are low molecular weight homologues of polyethylene (PE) and liquid at room temperature. It was observed that an increase in chain length led to an increased shift of the G-band i.e., stronger interactions (HypercarbTM/n-decane vs. n-dodecane). Analogously, the introduction of short alkyl branches reduces the interactions (HypercarbTM/n-decane vs. 2-methylundecane). The approach was then extended to the system HypercarbTM/n-decane/PE at 155 °C. It was not possible to obtain the spectra of HypercarbTM/n-decane at this temperature due to the high Brownian movement of the HypercarbTM particles. At 60 °C interpretable spectra could be recorded, showing a reduced shift in the G-band position from 7 (20 °C) to 3 cm^{-1} (60 °C). The Raman spectrum of HypercarbTM/n-decane/PE at 155 °C in solution shows a shift in both the G and 2D band position of 13 cm^{-1} and 19 cm^{-1} respectively. This shift confirms the existence of van der Waals interactions between the analyte (PE) and HypercarbTM. This same principle holds good potential to understand and rank the interactions between sorbent/solvent systems in the future. The long term perspective would be to use Raman spectroscopy as a fast screening tool to select the most suitable mobile phase for separations of analytes with porous graphite by interaction based chromatographic techniques.

8. Summary and Conclusions

Developments in polyolefin catalysis during the last 50 years made it possible to synthesize polymer with a vastly improved control of regio- and stereo-selectivity, branching (their number and length) and the order, in which the monomers are incorporated into a polymer chain. At the same time, this created the need to develop appropriate and more comprehensive analytical methodologies for their molecular characterization. The molecular heterogeneities in polyolefins can to a large extent be defined by the molecular mass distribution (MMD), chemical composition distribution (CCD) and stereo-regularity distribution (SRD). Recently, HT-HPLC in the form of High Temperature Solvent Gradient Interaction Chromatography (HT-SGIC) has become an emerging technique to determine the CCD of polyolefins. The interrelationship between the distributions with regard to composition and molar mass can be studied by hyphenating HT-LAC and HT-SEC. The aim of the work presented in this thesis was to develop improved quantitative methodologies to separate complex polymer, which are broadly distributed with regard to both composition and molar mass using HT 2D-LC. The research presented in this thesis is divided into four parts. Upon giving a concise synopsis on the state of the art and the results, the conclusions will be summarized for each part separately.

In the first part a methodology was developed to separate bimodal high density polyethylene (BiHDPE) (non-polar polyolefins) into its constituents, HDPE and LLDPE, by using HT-SGIC. A stepwise optimization of the HT-HPLC chromatographic parameters, comprising gradient slope and temperature was carried out using model homo- and copolymers of ethylene. The goal was to minimize the impact of the molar mass on the composition separation. Then separation achieved by the developed HT-HPLC was further optimized via hyphenation with HT-SEC. The effects of column temperature, the volume of the HT-HPLC fractions injected into the HT-SEC and the separation efficiency of the HT-SEC were investigated. Bimodality was observed for the first time in both HT-HPLC and HT-SEC dimension for BiHDPE in HT 2D-LC. This was achieved by using a low transfer volume of 100 μ L, a HT-SEC column with high theoretical plate number (N_{11000}) and by providing sufficient time for one HT-SEC analysis.

To achieve quantitative information the evaporative light scattering detector (ELSD) was replaced by an infrared (IR) detector and BiHDPE was analyzed by HT 2D-LC. Yet, to fully use the potential of IR detection for HT 2D-LC in the case of BiHDPE several chromatographic parameters had to be carefully optimized. With each fraction transfer from the HT-HPLC into the HT-SEC dimension in HT 2D-LC, a small amount of 1-decanol (solvent plug) is injected, with the amount depending on the gradient. Since the IR detector used here is tuned to the stretching vibration of the methyl and methylene groups, 1-decanol causes an intense broad peak in the chromatograms which may significantly overlap with the polymer peak when a column of low plate number (N_{4500}) is used. Thus, to separate the solvent peak from the polymer fractions over the entire range of molar mass a HT-SEC column of high theoretical plate number, (N_{11000}) was required. Also, an optimum transfer volume between HT-HPLC and HT-SEC dimension and volume for an individual HT-SEC analysis was identified. By employing these conditions the solvent peak and the polymer peak were baseline separated in all HT-SEC traces of BiHDPE. As a result the contour plot from HT 2D-LC \rightarrow IR exhibited a two spot regime, reflecting the HDPE and LLDPE component of BiHDPE. A comprehensive calibration with regard to molar mass, composition, and concentration of the HT 2D-LC system was carried out, which revealed the presence of oligomers (down to 500 g/mol) originating from HDPE and the presence of polymer fractions ranging over a 1-butene content from 0 to 6.5 mol %.

To gain a comprehensive knowledge of the molecular heterogeneities present in polyolefins chromatographic separation (HT-HPLC/HT-SEC) can be off-line hyphenated with ^{13}C NMR (off-flow HT-HPLC/HT-SEC \rightarrow ^{13}C NMR). For the case of BiHDPE, the comonomer content is very low. This might make on-flow HT-LC \rightarrow ^{13}C NMR complicated, due to solvent suppression, and is an almost stringent argument to work off-flow. To achieve this for the first time a portable automatic fraction collector (PAFC) was designed which enables to work over a wide temperature range (20 – 220 $^{\circ}\text{C}$) and can be plugged in at a series of HT-LC instruments. Using the PAFC fractions were

collected from HT-SEC of BiHDPE and analyzed off-line by ^1H NMR. The fractions obtained using the PAFC from HT-SEC exhibited a narrow dispersity of 1.08 – 1.5. ^1H NMR investigation on the fractions showed that the comonomer content is enriched in the medium and high molar mass region. This PAFC can be customized for a wide range of operating conditions with regard to temperature and number of fractions. The long term perspective would be to use the designed PAFC (working temperature 20 – 220 °C) for off-flow hyphenation of LC techniques (SGIC, TGIC, 2D-LC) \rightarrow ^{13}C NMR for in depth analysis of structural heterogeneities in polyolefins.

Polyolefins impose a limit on several applications due to their low surface energy and poor compatibility/reactivity with other polar polymers. Analogously, their adhesion to materials like wood, metals, or reinforcing fibers requires special attention. Most of these difficulties can be resolved by introducing polar functionalities or by grafting suitable polar monomers to polyolefins. The chemical modification of polypropylene using reactive extrusion has been an area of intense interest and the grafting of maleic anhydride (MA) on polypropylene (PP) is of high commercial relevance. The application properties of these products are, for a given overall composition, determined by their molar mass distribution (MMD) and chemical composition distribution (CCD). Despite the fact that various analytical techniques have been applied in the past to characterize functionalized polyolefins, the challenge of determining the bivariate distribution of such reaction products remained unsolved. This creates the need for an analytical technique which can separate functionalized polyolefins according to their degree of functionalization. Two samples of polypropylene grafted with maleic anhydride, PP-g-MA¹ and PP-g-MA^{1.7} with an average MA content of 1 and 1.7 mol %, respectively, were chosen for the investigations. By using HT-SEC \rightarrow FTIR via the LC-Transform interface it could be shown that the grafting of maleic anhydride (MA) occurred primarily in the low molar mass part of the polypropylene (PP) for both PP-g-MA samples. Although a compositional separation could be achieved via CRYSTAF, the selectivity of such a crystallization based approach is not sufficient for both PP-g-MA samples. Yet, using HT-HPLC with silica gel as stationary phase and a solvent gradient decalin \rightarrow cyclohexanone^{G-10 min} at 140 °C both PP-g-MA samples could be separated into a functionalized and a non-functionalized portion. The separation was confirmed by analyzing the fractions with FTIR spectroscopy.

HT 2D-LC \rightarrow IR enabled for the first time to investigate the bivariate distribution of PP-g-MA. The obtained contour plot exhibited a baseline-separated two spot regime, reflecting the grafted and non-grafted component. From the contour plots it could be shown that the two PP-g-MA samples are comparable with regard to the amount of grafted material in them. Yet, a higher degree of grafting is accompanied by a lower molar mass of the grafted portion. Contrary to that the MMD of the polypropylene of both samples was similar i.e., hardly affected by the graft reaction. The developed analytical methodology may be highly useful for developing more efficient processes of functionalization, and the analytical information can be applied to derive structure \leftrightarrow property relationships for functionalized polyolefins.

All of the above studies on HT-SGIC and HT 2D-LC focused on controlling the separation of the macromolecules using porous graphitic carbon as stationary phase and applying a solvent gradient at a constant temperature. To understand the separation selectivity and mechanism and to use this knowledge to improve the resolution in separation in HPLC of polymers, it is important to gain insight into the nature of interaction between polymer and sorbent. Raman spectroscopy, which is sensitive to the morphology of carbon materials, was utilized for the first time to provide direct evidence for the interaction between the hydrocarbon and the surface of porous graphite (HypercarbTM) at room and high temperature. The characteristic bands of graphite (G-, D- and 2D-band) were probed with regard to their sensitivity towards the interaction between hydrocarbons and the surface of HypercarbTM. The essential criteria for choosing the analyte/solvent were low volatility, and absence of solvent bands in the G-band region. Alkanes (n-decane, n-dodecane and 2-methylundecane) were chosen as model analytes as they are oligomers of PE and dissolvable at room temperature. It was observed that an increase in chain length led to an increased shift of the G-band i.e., stronger interactions (HypercarbTM/n-decane vs. n-dodecane). Analogously, the

introduction of short alkyl branches reduced the interactions (HypercarbTM/n-decane vs. 2-methylundecane).

The approach was extended to the system HypercarbTM/n-decane/PE at 155 °C. The Raman spectrum of HypercarbTM/n-decane/PE at 155 °C in solution shows a shift in both the G and 2D band position of 13 cm⁻¹ and 19 cm⁻¹ respectively. This shift confirms the existence of van der Waals interactions between the analyte (PE) and HypercarbTM. This same principle holds good potential to understand and rank the interactions between sorbent/solvent systems in the future. The long term perspective would be to use Raman spectroscopy as a fast screening tool to select the most suitable mobile phase for separations of analytes with porous graphite by interaction based chromatographic techniques.

The above work augments the understanding of the compositional separation of macromolecules with the help of HT-HPLC and opens new possibilities for the compositional separation of complex macromolecules. The development of a separation of bimodal HDPE using HT 2D-LC→IR aids in determining the molecular heterogeneity of BiHDPE. The development of a PAFC (working temperature window 20 – 220 °C) extends the application potential of chromatography in elucidating the structure of the complex polymer materials. The newly developed HT-SGIC separations for functionalized PP could be further extended to other functionalized polyolefins for achieving separations based on grafting and non-grafting. The Raman study increased the understanding of interactions in the system PE/graphite/solvent in solution at high temperature (155 °C). This knowledge could be utilized to better control the separations by interaction based chromatography techniques.

9. Bibliography

- [1] T. Nowlin, J. Wiley & Sons, New York (2014).
- [2] (Plastic News, August 30, 2012).
- [3] G. Lappin, Alpha olefins applications handbook, CRC Press, 1989.
- [4] O. Olabisi, K. Adewale, Handbook of Thermoplastics, Taylor & Francis, 1997.
- [5] D.B. Malpass, Introduction to Industrial Polyethylene: Properties, Catalysts, and Processes, Wiley, 2010.
- [6] <http://www.newworldencyclopedia.org/entry/Polyethylene>, in.
- [7] Z. Guan, P. Cotts, E. McCord, S. McLain, Science 283 (1999) 2059.
- [8] S. Gupta, Current Science 56 (1987) 979.
- [9] F. Reding, J. Faucher, R. Whitman, Journal of Polymer Science 57 (1962) 483.
- [10] D. Yan, W.-J. Wang, S. Zhu, Polymer 40 (1999) 1737.
- [11] K. Ziegler, E. Holzkamp, H. Breil, H. Martin, Angewandte Chemie 67 (1955) 426.
- [12] A. W. Anderson, G.S. Stamatoff, Hydrocarbon interpolymer compositions, US4076698 A, 1957.
- [13] H.J. Paul, R.L. Banks, Polymers and production thereof, US2825721 A, 1958.
- [14] D.B. Malpass, E. Band, Introduction to Industrial Polypropylene: Properties, Catalysts Processes, Wiley, 2012.
- [15] J.P. Hogan, R.L. Banks, Purification of olefin-rich feed prior to polymerization, US2837587 A, 1958.
- [16] H. Sinn, W. Kaminsky, Advances Organometallic Chemistry 18 (1980) 99.
- [17] F. Aftalion, A History of the International Chemical Industry, Chemical Heritage Press, 2001.
- [18] D.S. Breslow, N.R. Newburg, Journal of the American Chemical Society 79 (1957) 5072.
- [19] A. Andresen, H.G. Cordes, J. Herwig, W. Kaminsky, A. Merck, R. Mottweiler, J. Pein, H. Sinn, H.J. Vollmer, Angewandte Chemie International Edition in English 15 (1976) 630.
- [20] W. Kaminsky, Journal of Polymer Science Part A: Polymer Chemistry 42 (2004) 3911.
- [21] L. Johnson, Journal of the American Chemical Society 117 (1995) 6414.
- [22] B.L. Small, M. Brookhart, A.M. Bennett, Journal of the American Chemical Society 120 (1998) 4049.
- [23] G.J. Britovsek, V.C. Gibson, S.J. McTavish, G.A. Solan, A.J. White, D.J. Williams, B.S. Kimberley, P.J. Maddox, Chemical Communications (1998) 849.
- [24] L.L. Böhm, Angewandte Chemie International Edition 42 (2003) 5010.
- [25] Y. Yu, E. Schwerdtfeger, M. McDaniel, Journal of Polymer Science Part A: Polymer Chemistry 50 (2012) 1166.
- [26] J. Boor, Ziegler-Natta catalyst and polymerizations, Academic Press New York, 1979.
- [27] T. Erik, J.A.W. Langer, Polymerization catalyst, US3032510 A, 1962.
- [28] A. Schallis, Process and apparatus for the activation of catalysts, US3688992 A, 1972.
- [29] E.J. Arlman, P. Cossee, Journal of Catalysis 3 (1964) 99.
- [30] T.F.L. McKenna, A. Di Martino, G. Weickert, J.B.P. Soares, Macromolecular Reaction Engineering 4 (2010) 40.
- [31] H.-H. Brintzinger, D. Fischer, R. Mülhaupt, B. Rieger, R.M. Waymouth, (1995).
- [32] D. Steinborn, Fundamentals of Organometallic Catalysis, Wiley, 2012.
- [33] W. Kaminsky, A. Funck, H. Hahnsen, Dalton Transactions (2009) 8803.
- [34] J.A. Ewen, Journal of the American Chemical Society 106 (1984) 6355.
- [35] H.S. Zijlstra, S. Harder, European Journal of Inorganic Chemistry 2015 (2015) 19.
- [36] <http://pslc.ws/macrog/level4.htm>
- [37] G. Odian, Principles of Polymerization, Wiley, 2004.

- [38] J.B. Soares, T.F. McKenna, Polyolefin Reaction Engineering, John Wiley & Sons, 2013.
- [39] A. Winter, M. Antberg, V. Dolle, J. Rohrmann, W. Spaleck, Process for the preparation of an olefin polymer using metallocenes having specifically substituted indenyl ligands, US5304614 A, 1994.
- [40] P. Kübler, PhD thesis, Cyclopentadienyliden-Phosphoran-Komplexe des Eisens und Rutheniums: Von Katalysatoren für CC-Knüpfungen zu redoxaktiven ionischen Flüssigkeiten, Philipps-Universität Marburg, 2014.
- [41] W. Spaleck, M. Aulbach, B. Bachmann, F. Küber, A. Winter, in Macromolecular Symposia, Wiley Online Library, 1995, p. 237.
- [42] W. Kaminsky, A. Laban, Applied Catalysis A: General 222 (2001) 47.
- [43] G.W. Coates, ChemInform, Encyclopedia of analytical chemistry 31 (2000) 42.
- [44] W. Liu, J.M. Malinoski, M. Brookhart, Organometallics 21 (2002) 2836.
- [45] L.K. Johnson, S. Mecking, M. Brookhart, Journal of the American Chemical Society 118 (1996) 267.
- [46] W. Liu, J.M. Malinoski, M. Brookhart, Organometallics 21 (2002) 2836.
- [47] E.Y.X. Chen, Chemical Reviews 109 (2009) 5157.
- [48] A. Nakamura, S. Ito, K. Nozaki, Chemical Reviews 109 (2009) 5215.
- [49] A.M.A. Bennett, WO 98/27124 (DuPont), Using iron cobalt or complex catalyst, 1998.
- [50] L.K. Johnson, S. Mecking, M. Brookhart, Journal of the American Chemical Society 118 (1996) 267.
- [51] D.J. Arriola, E.M. Carnahan, P.D. Hustad, R.L. Kuhlman, T.T. Wenzel, Science 312 (2006) 714.
- [52] E.M. Carnahan, P.D. Hustad, R.L. Kuhlman, T.T. Wenzel, Catalytic olefin block copolymers with controlled block sequence distribution, US8053529 B2, 2011.
- [53] L.L. Böhm, J. Berthold, H.F. Enderle, M. Fleissner, in W. Kaminsky (Editor), Metalorganic Catalysts for Synthesis and Polymerization, Springer Berlin Heidelberg, 1999, p. 3.
- [54] N. Brown, S. Bhattacharya, Journal of materials science 20 (1985) 4553.
- [55] X. Lu, N. Brown, Polymer Testing 11 (1992) 309.
- [56] X. Lu, Z. Zhou, N. Brown, Polymer Engineering & Science 37 (1997) 1896.
- [57] http://www.ineos.com/globalassets/ineos-group/businesses/ineos-olefins-and-polymers-usa/products/technical-information--patents/aga_escr.pdf
- [58] L. Kurelec, M. Teeuwen, H. Schoffeleers, R. Deblieck, Polymer 46 (2005) 6369.
- [59] E.F. Palermo, D. Chang, Increasing Importance of Rapid Crack Propagation (RCP) for Gas Piping Applications-Industry Status, In *AGA Operations Conference*, 2010.
- [60] Plastics piping and ducting systems – determination of the long-term hydrostatic strength of thermoplastics materials in pipe form by extrapolation, DIN EN ISO 9080, 2003.
- [61] F.M. Peres, C.G. Schön, Journal of Materials Science 43 (2008) 1844.
- [62] K. Al-Bani, Bimodal innovation of pressure pipe applications, SABIC
- [63] P.J. DesLauriers, M.P. McDaniel, D.C. Rohlfing, R.K. Krishnaswamy, S.J. Secora, E.A. Benham, P.L. Maeger, A.R. Wolfe, A.M. Sukhadia, B.B. Beaulieu, Polymer Engineering & Science 45 (2005) 1203.
- [64] F.P. Alt, L.L. Böhm, H.-F. Enderle, J. Berthold, Macromolecular Symposia 163 (2001) 135.
- [65] T.C. Chung, Progress in Polymer Science 27 (2002) 39.
- [66] R.T. Swiger, L.A. Mango, Polyamide and modified polyethylene binary mixtures with high melt viscosity, DE 2,722,270 A1, 1977.

- [67] M.D. Purgett, O. Vogl, *Journal of Polymer Science Part A: Polymer Chemistry* 26 (1988) 677.
- [68] T.C. Chung, *Functionalization of Polyolefins*, Academic Press, 2002.
- [69] M.M. Marques, S.G. Correia, J.R. Ascenso, A.F. Ribeiro, P.T. Gomes, A.R. Dias, P. Foster, M.D. Rausch, J.C. Chien, *Journal of Polymer Science-A-Polymer Chemistry Edition* 37 (1999) 2457.
- [70] G. Xu, S. Lin, *Journal of Macromolecular Science, Part C: Polymer Reviews* 34 (1994) 555.
- [71] M.K. Naqvi, M.S. Choudhary, *Journal of Macromolecular Science, Part C: Polymer Reviews* 36 (1996) 601.
- [72] P. Burchill, D. Pinkerton, R. Stacewicz, in *Journal of Polymer Science: Polymer Symposia*, Wiley Online Library, 1976, p. 303.
- [73] T.C. Chung, Method for preparing functional alpha-olefin polymers and copolymers, U.S. 4734472 A, 1989.
- [74] T.C. Chung and H. Lu, Alpha-olefin/para-alkylstyrene copolymers and functionalized copolymers thereof, WO1996016096 A1, 1996.
- [75] T.C. Chung, H. Lu, Functionalized alpha-olefin/para-alkylstyrene terpolymers, US6015862 A, 2000.
- [76] L. Wild, T.R. Ryle, D.C. Knobloch, I.R. Peat, *Journal of Polymer Science: Polymer Physics Edition* 20 (1982) 441.
- [77] B. Monrabal, *Encyclopedia of Analytical Chemistry*, Meyers, RA, Ed.; John Wiley & Sons, Inc.: New York 14 (2000) 1.
- [78] B. Monrabal, J. Sancho-Tello, N. Mayo, L. Romero, *Macromolecular Symposia* 257 (2007) 71.
- [79] B. Monrabal, N. Mayo, R. Cong, in *Macromolecular Symposia*, Wiley Online Library, 2012, p. 115.
- [80] P.J. Flory, *The Journal of Chemical Physics* 17 (1949) 223.
- [81] R. Brüll, V. Grumel, H. Pasch, H.G. Raubenheimer, R. Sanderson, U.M. Wahner, *Macromolecular Symposia* 178 (2002) 81.
- [82] L. Mandelkern, F.A. Quinn, P.J. Flory, *Journal of Applied Physics* 25 (1954) 830.
- [83] J. Nieto, T. Oswald, F. Blanco, J.B.P. Soares, B. Monrabal, *Journal of Polymer Science Part B: Polymer Physics* 39 (2001) 1616.
- [84] B. Monrabal, in K.N. Takeshi Shiono, T. Minoru (Editors), *Studies in Surface Science and Catalysis*, Elsevier, 2006, p. 35.
- [85] S. Anantawaraskul, J.B.P. Soares, P.M. Wood-Adams, *Journal of Polymer Science Part B: Polymer Physics* 41 (2003) 1762.
- [86] V. Desreux, M. Spiegels, *Bulletin des Societes Chimiques Belges* 59 (1950) 476.
- [87] B. Monrabal, in *Encyclopedia of Analytical Chemistry*, John Wiley & Sons, Ltd, 2006.
- [88] L. Wild, *Advances in Polymer Science* 98 (1991) 1.
- [89] G. Glöckner, *Journal of Applied Polymer Science* 45 (1990) 1.
- [90] I.R.H. C. A. Fonseca, in E. R. A. Pethrick (Editor), 1999, p. 1.
- [91] A.E.H. J. B. P. Soares, in E. R. A. Pethrick (Editor), 1999, p. 15.
- [92] S. Anantawaraskul, J.B.P. Soares, P.M. Wood-Adams, B. Monrabal, *Polymer* 44 (2003) 2393.
- [93] B. Monrabal, in R.A. Meyers (Editor), *Encyclopedia of Analytical Chemistry*, Wiley, New York, 2000, p. 8074
- [94] B. Monrabal, *Journal of applied polymer science* 52 (1994) 491.
- [95] W.H. Stockmayer, *The Journal of Chemical Physics* 13 (1945) 199.

- [96] B. Monrabal, in US Patent 5, 390 (Editor), 1991.
- [97] B. Monrabal, Journal of Applied Polymer Science 52 (1994) 491.
- [98] R. Brüll, H. Pasch, H.G. Raubenheimer, R. Sanderson, A.J. van Reenen, U.M. Wahner, Macromolecular Chemistry and Physics 202 (2001) 1281.
- [99] D.M. Sarzotti, J.B.P. Soares, A. Penlidis, Journal of Polymer Science Part B: Polymer Physics 40 (2002) 2595.
- [100] H. Pasch, R. Brüll, U. Wahner, B. Monrabal, Macromolecular Materials and Engineering 279 (2000) 46.
- [101] B. Monrabal, J. Sanhco-Tello, N. Mayo, L. Romero, Macromolecular Symposia 257 (2007) 71.
- [102] B. Monrabal, L. Romero, N. Mayo, J. Sanhco-Tello, Macromolecular Symposia 282 (2009) 14.
- [103] B. Monrabal, Analytical and Bioanalytical Chemistry 407 (2015) 3269.
- [104] A. Ortín, J. Montesinos, E. López, P. del Hierro, B. Monrabal, J.R. Torres-Lapasió, M.C. García-Álvarez-Coque, Macromolecular Symposia 330 (2013) 63.
- [105] H. Pasch, in Polymer Analysis Polymer Physics, Springer, 1997, p. 1.
- [106] H. Pasch, B. Trathnigg, Springer, Berlin, 1999.
- [107] A. Skvortsov, B. Trathnigg, Journal of Chromatography A 1015 (2003) 31.
- [108] D. Mekap, T. Macko, R. Brüll, R. Cong, A. Parrott, P. Cools, W. Yau, Polymer 54 (2013) 5518.
- [109] S.S. Bhati, T. Macko, R. Brüll, D. Mekap, Macromolecular Chemistry and Physics (2015).
- [110] A. Striegel, W.W. Yau, J.J. Kirkland, D.D. Bly, Modern size-exclusion liquid chromatography: practice of gel permeation and gel filtration chromatography, John Wiley & Sons, 2009.
- [111] P.J. Wyatt, Instrumentation science & technology 25 (1997) 1.
- [112] P. Tackx, S. Bremmers, Polymeric Materials: Science and Engineering 78 (1998) 50.
- [113] P.J. DesLauriers, D.C. Rohlfing, E.T. Hsieh, Polymer 43 (2002) 159.
- [114] K. Ute, R. Niimi, K. Hatada, A.C. Kolbert, International Journal of Polymer Analysis and Characterization 5 (1999) 47.
- [115] W. Hiller, H. Pasch, T. Macko, M. Hofmann, J. Ganz, M. Spraul, U. Braumann, R. Streck, J. Mason, F.A. Van Damme, Journal of Magnetic Resonance 183 (2006) 290.
- [116] T. Macko, U. Schulze, R. Brüll, A. Albrecht, H. Pasch, T. Fónagy, L. Häussler, B. Iván, Macromolecular Chemistry and Physics 209 (2008) 404.
- [117] S.J. Kok, C.A. Wold, T. Hankemeier, P.J. Schoenmakers, Journal of Chromatography A 1017 (2003) 83.
- [118] C. Piel, A. Albrecht, C. Neubauer, C. Klampfl, J. Reussner, Analytical and Bioanalytical Chemistry 400 (2011) 2607.
- [119] A. Ortín, B. Monrabal, J. Montesinos, P. del Hierro, Macromolecular Symposia 282 (2009) 65.
- [120] I. Suárez, M.J. Caballero, B. Coto, Polymer Engineering & Science 51 (2011) 317.
- [121] T. Macko, U. Schulze, R. Brüll, A. Albrecht, H. Pasch, T. Fónagy, L. Häussler, B. Iván, Macromolecular Chemistry and Physics 209 (2008) 404.
- [122] C. Piel, A. Albrecht, C. Neubauer, C.W. Klampfl, J. Reussner, Analytical and bioanalytical chemistry 400 (2011) 2607.
- [123] G. Glöckner, Gradient HPLC and Chromatographic Cross-Fractionation, Springer, Berlin, Heidelberg, New York, 1991.
- [124] T. Chang, Advances in Polymer Science 163 (2003) 1.
- [125] H.T. Pasch, B. HPLC of Polymers, Springer: Berlin, 1997

- [126] T. Macko, H. Pasch, J.F. Denayer, *Journal of Chromatography A* 1002 (2003) 55.
- [127] T. Macko, H. Pasch, Y.V. Kazakevich, A.Y. Fadeev, *Journal of Chromatography A* 988 (2003) 69.
- [128] T. Macko, R. Brüll, H. Pasch, *Chromatographia* 57 (2003) S39.
- [129] T. Macko, J.F. Denayer, H. Pasch, G.V. Baron, *Journal of separation science* 26 (2003) 1569.
- [130] L.C. Heinz, H. Pasch, *Polymer* 46 (2005) 12040.
- [131] L.C. Heinz, S. Graef, T. Macko, R. Brull, S. Balk, H. Keul, H. Pasch, *E-Polymers* (2005) 1.
- [132] L.C. Heinz, T. Macko, H. Pasch, M.S. Weiser, R. Mulhaupt, *International Journal of Polymer Analysis and Characterization* 11 (2006) 47.
- [133] T. Macko, R. Brull, R.G. Alamo, F.J. Stadler, S. Losio, *Analytical and Bioanalytical Chemistry* 399 (2011) 1547.
- [134] T. Macko, R. Brull, C. Brinkmann, H. Pasch, *Journal of Automated Methods & Management in Chemistry* (2009).
- [135] T. Macko, H. Pasch, *Macromolecules* 42 (2009) 6063.
- [136] L.-C. Heinz, H. Pasch, *Polymer* 46 (2005) 12040.
- [137] H.J. Möckel, A. Braedikow, H. Melzer, G. Aced, *Journal of Liquid Chromatography* 14 (1991) 2477.
- [138] G. Kalies, U. Messow, P. Bräuner, K. Quitzs, *Adsorption* 4 (1998) 35.
- [139] G.H. Findenegg, M. Liphard, *Carbon* 25 (1987) 119.
- [140] S. Yin, C. Wang, X. Qiu, B. Xu, C. Bai, *Surface and Interface Analysis* 32 (2001) 248.
- [141] T. Macko, H. Pasch, *Macromolecules* 42 (2009) 6063.
- [142] J.H. Knox, B. Kaur, G.R. Millward, *Journal of Chromatography A* 352 (1986) 3.
- [143] T. Macko, R. Brüll, R.G. Alamo, Y. Thomann, V. Grumel, *Polymer* 50 (2009) 5443.
- [144] R. Chitta, T. Macko, R. Brüll, C. Boisson, E. Cossoul, O. Boyron, *Macromolecular Chemistry and Physics* 216 (2015) 721.
- [145] A. Ginzburg, T. Macko, V. Dolle, R. Brüll, *Journal of Applied Polymer Science* 129 (2013) 1897.
- [146] R. Chitta, T. Macko, R. Brull, M. Miller, R. Cong, W. deGroot, *J Sep Sci* 36 (2013) 2063.
- [147] T. Macko, R. Brüll, Y. Zhu, Y. Wang, *Journal of Separation Science* 33 (2010) 3446.
- [148] R. Chitta, T. Macko, R. Brüll, G. Van Doremaele, L.C. Heinz, *Journal of Polymer Science Part A: Polymer Chemistry* 49 (2011) 1840.
- [149] J. Arndt, T. Macko, R. Brüll, *Journal of Chromatography A* 1310 (2013) 1.
- [150] J.N. Fairchild, K. Horváth, G. Guiochon, *Journal of Chromatography A* 1216 (2009) 6210.
- [151] F. Rittig, H. Pasch, in *Multidimensional Liquid Chromatography*, John Wiley & Sons, Inc., 2008, p. 385.
- [152] K. Im, H.-w. Park, S. Lee, T. Chang, *Journal of Chromatography A* 1216 (2009) 4606.
- [153] H. Pasch, P. Kilz, *Macromolecular Rapid Communications* 24 (2003) 104.
- [154] P.J. Schoenmakers, G. Vivó-Truyols, W.M.C. Decrop, *Journal of Chromatography A* 1120 (2006) 282.
- [155] A. van der Horst, P.J. Schoenmakers, *Journal of Chromatography A* 1000 (2003) 693.
- [156] X. Jiang, A. van der Horst, P.J. Schoenmakers, *Journal of Chromatography A* 982 (2002) 55.
- [157] A. Ginzburg, T. Macko, V. Dolle, R. Brüll, *Journal of Chromatography A* 1217 (2010) 6867.

- [158] A. Roy, M.D. Miller, M.D. Meunier, W. deGroot, W.L. Winniford, F.A. Van Damme, R.J. Pell, J.W. Lyons, *Macromolecules* 43 (2010) 3710.
- [159] A. Ginzburg, T. Macko, V. Dolle, R. Brüll, *European Polymer Journal* 47 (2011) 319.
- [160] D. Lee, M.D. Miller, D.M. Meunier, J.W. Lyons, J.M. Bonner, R.J. Pell, C. Li Pi Shan, T. Huang, *Journal of Chromatography A* 1218 (2011) 7173.
- [161] F. Rittig, H. Pasch, *Multidimensional Liquid Chromatography: Theory and Applications in Industrial Chemistry and the Life Sciences* (2008) 385.
- [162] A. Ortin, B. Monrabal, J. Sancho-Tello, *Macromolecular Symposia* 257 (2007) 13.
- [163] W.W. Yau, D. Gillespie, *Polymer* 42 (2001) 8947.
- [164] J. Adrian, E. Esser, G. Hellmann, H. Pasch, *Polymer* 41 (2000) 2439.
- [165] J. Gerber, W. Radke, *Polymer* 46 (2005) 9224.
- [166] H. Malerod, E. Lundanes, T. Greibrokk, *Analytical Methods* 2 (2010) 110.
- [167] A. Ginzburg, T. Macko, V. Dolle, R. Brüll, *Journal of Chromatography A* 1217 (2010) 6867.
- [168] A. Roy, M.D. Miller, D.M. Meunier, A.W. Degroot, W.L. Winniford, F.A. Van Damme, R.J. Pell, J.W. Lyons, *Macromolecules* 43 (2010) 3710.
- [169] J. Hodkiewicz, *Thermofischer Scientific Application note: 51946* (2012).
- [170] Y. Wang, D.C. Alsmeyer, R.L. McCreery, *Chemistry of Materials* 2 (1990) 557.
- [171] S. Reich, C. Thomsen, *Philosophical Transactions of the Royal Society of London A: Mathematical, Physical and Engineering Sciences* 362 (2004) 2271.
- [172] J. Hodkiewicz, *Thermofischer Scientific Application note: 51901* (2012).
- [173] A. Sanoria, T. Schuster, R. Brüll, *Analytical Methods* (2015).
- [174] A.C. Ferrari, *Solid state communications* 143 (2007) 47.
- [175] H. Kreyenschulte, S. Richter, T. Götze, D. Fischer, D. Steinhauser, M. Klüppel, G. Heinrich, *Carbon* 50 (2012) 3649.
- [176] K. Subramaniam, A. Das, G. Heinrich, *Composites Science and Technology* 71 (2011) 1441.
- [177] J.P. RABE, S. BUCHHOLZ, *Science* 253 (1991) 424.
- [178] R. Hentschke, B.L. Schürmann, J.P. Rabe, *The Journal of Chemical Physics* 96 (1992) 6213.
- [179] L. Askadskaya, J.P. Rabe, *Physical Review Letters* 69 (1992) 1395.
- [180] G. Parshall, G. Pearson, T. Inch, E. Becker, R.K. Harris, E.D. Becker, S.M.C. de Menezes, R. Goodfellow, P. Granger, J. Durig, *Pure Appl. Chem* 32 (1972) 51.
- [181] F. Malz, H. Jancke, *Journal of pharmaceutical and biomedical analysis* 38 (2005) 813.
- [182] A. Albrecht, R. Brüll, T. Macko, F. Malz, H. Pasch, *Macromolecular Chemistry and Physics* 210 (2009) 1319.
- [183] Z. Zhou, R. Cong, Y. He, M. Paradkar, M. Demirors, M. Cheatham, A.W. deGroot, in *Macromolecular Symposia*, Wiley Online Library, 2012, p. 88.
- [184] V. Busico, R. Cipullo, N. Friederichs, H. Linssen, A. Segre, V. Van Axel Castelli, G. van der Velden, *Macromolecules* 38 (2005) 6988.
- [185] Z. Zhou, J.C. Stevens, J. Klosin, R. Kümmerle, X. Qiu, D. Redwine, R. Cong, A. Taha, J. Mason, B. Winniford, *Macromolecules* 42 (2009) 2291.
- [186] J.C. Randall, *Journal of Macromolecular Science—Reviews in Macromolecular Chemistry and Physics* 29 (1989) 201.
- [187] X. Qiu, Z. Zhou, G. Gobbi, O.D. Redwine, *Analytical chemistry* 81 (2009) 8585.
- [188] P.M. Wood-Adams, J.M. Dealy, A.W. Degroot, O.D. Redwine, *Macromolecules* 33 (2000) 7489.
- [189] R. Shroff, H. Mavridis, *Macromolecules* 32 (1999) 8454.
- [190] R. Shroff, H. Mavridis, *Macromolecules* 34 (2001) 7362.

- [191] X. Qiu, D. Redwine, G. Gobbi, A. Nuamthanom, P.L. Rinaldi, *Macromolecules* 40 (2007) 6879.
- [192] J. Sühm, in, University of A. Lugwigs, Freiburg, Germany, 1998.
- [193] S. de Goede, R. Brüll, H. Pasch, N. Marshall, in *Macromolecular Symposia*, Wiley Online Library, 2003, p. 35.
- [194] H. Pasch, M.I. Malik, *Advanced Separation Techniques for Polyolefins*, Springer International Publishing, 2014.
- [195] Å. Björck, *Linear Algebra and Its Applications* 197 (1994) 297.
- [196] T. Beesley, B. Buglio, *Quantitative Chromatographic Analysis*, Taylor & Francis, 2000.
- [197] E. de Goede, P. Mallon, H. Pasch, *Macromolecular Materials and Engineering* 295 (2010) 366.
- [198] T.G. Scholte, N.L.J. Meijerink, H.M. Schoffeleers, A.M.G. Brands, *Journal of Applied Polymer Science* 29 (1984) 3763.
- [199] P.J. DesLauriers, D.C. Rohlffing, *Macromolecular Symposia* 282 (2009) 136.
- [200] L. Verdurmen-Noël, L. Baldo, S. Bremmers, *Polymer* 42 (2001) 5523.
- [201] S. Anantawaraskul, J.B.P. Soares, P.M. Wood-Adams, *Macromolecular Chemistry and Physics* 205 (2004) 771.
- [202] K. Suriya, S. Anantawaraskul, J.B.P. Soares, *Journal of Polymer Science Part B: Polymer Physics* 49 (2011) 678.
- [203] L. Mandelkern, *Crystallization of polymers*, McGraw-Hill, 1964.
- [204] J. Pak, B. Wunderlich, *Macromolecules* 34 (2001) 4492.
- [205] M.J. Galante, L. Mandelkern, R.G. Alamo, *Polymer* 39 (1998) 5105.
- [206] K. Tashiro, K. Imanishi, Y. Izumi, M. Kobayashi, K. Kobayashi, M. Satoh, R.S. Stein, *Macromolecules* 28 (1995) 8477.
- [207] R.A. García, A. Carrero, C. Martín, C. Domínguez, *Journal of Applied Polymer Science* 121 (2011) 3269.
- [208] J.G. Fatou, *Encyclopedia of Polymer Science and Engineering*, 2nd ed., , Wiley, New York, 1989.
- [209] J. Fatou, C. Marco, L. Mandelkern, *Polymer* 31 (1990) 1685.
- [210] D.M. Sarzotti, J.B.P. Soares, L.C. Simon, L.J.D. Britto, *Polymer* 45 (2004) 4787.
- [211] J. Tacx, H. Linssen, A. German, *Journal of Polymer Science Part A: Polymer Chemistry* 26 (1988) 61.
- [212] J.C.J.F. Tacx, J.L. Ammerdorffer, A.L. German, *Polymer* 29 (1988) 2087.
- [213] J.K. Swadesh, *HPLC: Practical and Industrial Applications*, Second Edition, Taylor & Francis, 2000.
- [214] J.H. Arndt, T. Macko, R. Brüll, in *Macromolecular Symposia*, Wiley Online Library, 2015, p. 34.
- [215] D. Mekap, T. Macko, R. Brüll, R. Cong, A. deGroot, A. Parrott, W. Yau, *Macromolecules* 46 (2013) 6257.
- [216] R.E. Murphy, M.R. Schure, J.P. Foley, *Analytical Chemistry* 70 (1998) 1585.
- [217] S.A. Cohen, M.R. Schure, *Multidimensional Liquid Chromatography: Theory and Applications in Industrial Chemistry and the Life Sciences*, Wiley, 2008.
- [218] A. Brüll, H. Pasch, M. Bashir, *e-Polymers* 6 (2006) 610.
- [219] C. Wu, *Column Handbook for Size Exclusion Chromatography*, Elsevier Science, 1999.
- [220] J.-A. Raust, A. Brüll, C. Moire, C. Farcet, H. Pasch, *Journal of Chromatography A* 1203 (2008) 207.

- [221] B. Mathews, P. Higginson, R. Lyons, J. Mitchell, N. Sach, M. Snowden, M. Taylor, A. Wright, *Chromatographia* 60 (2004) 625.
- [222] P. Kilz, W. Radke, *Anal Bioanal Chem* 407 (2015) 193.
- [223] B. Monrabal, J. Sancho-Tello, (2009).
- [224] B. Monrabal, E. López, L. Romero, in *Macromolecular Symposia*, Wiley Online Library, 2013, p. 9.
- [225] N. WATANABE, E. NIKI, *Proceedings of the Japan Academy. Ser. B: Physical and Biological Sciences* 54 (1978) 194.
- [226] K. Hatada, K. Ute, Y. Okamoto, M. Imanari, N. Fujii, *Polymer Bulletin* 20 (1988) 317.
- [227] W. Hiller, M. Hehn, P. Sinha, J.-A. Raust, H. Pasch, *Macromolecules* 45 (2012) 7740.
- [228] J.A. Raust, A. Bruell, P. Sinha, W. Hiller, H. Pasch, *Journal of separation science* 33 (2010) 1375.
- [229] K. Albert, M. Dachtler, T. Glaser, H. Händel, T. Lackner, G. Schlotterbeck, S. Strohschein, L.H. Tseng, U. Braumann, *Journal of High Resolution Chromatography* 22 (1999) 135.
- [230] W. Hiller, H. Pasch, T. Macko, M. Hofmann, J. Ganz, M. Spraul, U. Braumann, R. Streck, J. Mason, F. Van Damme, *Journal of Magnetic Resonance* 183 (2006) 290.
- [231] W. Hiller, P. Sinha, M. Hehn, H. Pasch, *Progress in Polymer Science* 39 (2014) 979.
- [232] Z. Zhou, M. Miller, D. Lee, R. Cong, C. Klinker, T. Huang, C. Li Pi Shan, B. Winniford, A. deGroot, L. Fan, *Macromolecules* (2015).
- [233] H. Kovacs, D. Moskau, M. Spraul, *Progress in Nuclear Magnetic Resonance Spectroscopy* 46 (2005) 131.
- [234] A. Peyrouset, R. Panaris, *Journal of Applied Polymer Science* 16 (1972) 315.
- [235] A. Peyrouset, R. Prechner, R. Panaris, H. Benoit, *Journal of Applied Polymer Science* 19 (1975) 1363.
- [236] H.-S. Kim, B.-H. Lee, S.-W. Choi, S. Kim, H.-J. Kim, *Composites Part A: Applied Science and Manufacturing* 38 (2007) 1473.
- [237] M. Sclavons, M. Laurent, J. Devaux, V. Carlier, *Polymer* 46 (2005) 8062.
- [238] S.H.P. Bettini, J.A.M. Agnelli, *Journal of Applied Polymer Science* 85 (2002) 2706.
- [239] M. Sclavons, P. Franquinet, V. Carlier, G. Verfaillie, I. Fallais, R. Legras, M. Laurent, F.C. Thyron, *Polymer* 41 (2000) 1989.
- [240] S.H.P. Bettini, J.A.M. Agnelli, *Polymer Testing* 19 (2000) 3.
- [241] L. Yang, F. Zhang, T. Endo, T. Hirotsu, *Macromolecules* 36 (2003) 4709.
- [242] K.T.H.K. R.T., *Proceedings of the 49th Annual TEchnical Conference*, Montreal 3 (1991) 1570.
- [243] S.H.P. Bettini, J.A.M. Agnelli, *Journal of Applied Polymer Science* 74 (1999) 247.
- [244] G. Chen, J. Yang, J.J. Liu, *Journal of Applied Polymer Science* 71 (1999) 2017.
- [245] D. Jia, Y. Luo, Y. Li, H. Lu, W. Fu, W.L. Cheung, *Journal of Applied Polymer Science* 78 (2000) 2482.
- [246] C. Li, Y. Zhang, Y. Zhang, *Polymer Testing* 22 (2003) 191.
- [247] Y. Göldoğan, S. Eğri, Z.M.O. Rzaev, E. Pişkin, *Journal of Applied Polymer Science* 92 (2004) 3675.
- [248] M.Z. L. L. Hou, *eXPRESS Polymer Letters* 2 (2008) 19.
- [249] Q. Cheng, Z. Lü, H.J. Byrne, *Journal of Applied Polymer Science* 114 (2009) 1820.
- [250] Z.M. Rzaev, *arXiv preprint arXiv:1105.1260* (2011).
- [251] M. Zhang, R.H. Colby, S.T. Milner, T.C.M. Chung, T. Huang, W. deGroot, *Macromolecules* 46 (2013) 4313.

- [252] W. Heinen, M. van Duin, C.H. Rosenmöller, C.B. Wenzel, H.J.M. De Groot, J. Lugtenburg, *Macromolecular Symposia* 129 (1998) 119.
- [253] Y. Minoura, M. Ueda, S. Mizunuma, M. Oba, *Journal of Applied Polymer Science* 13 (1969) 1625.
- [254] N.G. Gaylord, M.K. Mishra, *Journal of Polymer Science: Polymer Letters Edition* 21 (1983) 23.
- [255] B. De Roover, M. Sclavons, V. Carlier, J. Devaux, R. Legras, A. Momtaz, *Journal of Polymer Science Part A: Polymer Chemistry* 33 (1995) 829.
- [256] M. Sclavons, V. Carlier, B. De Roover, P. Franquinet, J. Devaux, R. Legras, *Journal of Applied Polymer Science* 62 (1996) 1205.
- [257] M. FUJIYAMA, T. WAKINO, H. WACHI, K. TANI, *KOBUNSHI RONBUNSHU* 49 (1992) 97.
- [258] R.G. Alamo, R.H. Glaser, L. Mandelkern, *Journal of Polymer Science Part B: Polymer Physics* 26 (1988) 2169.
- [259] A. Albrecht, R. Brüll, T. Macko, P. Sinha, H. Pasch, *Macromolecular Chemistry and Physics* 209 (2008) 1909.
- [260] A. Albrecht, R. Brüll, T. Macko, H. Pasch, *Macromolecules* 40 (2007) 5545.
- [261] A. Albrecht, R. Brüll, T. Macko, P. Sinha, H. Pasch, *Macromolecular Chemistry and Physics* 209 (2008) 1909.
- [262] S. Cheruthazhekatt, T.F. Pijpers, G.W. Harding, V.B. Mathot, H. Pasch, *Macromolecules* 45 (2012) 2025.
- [263] G. Lamberti, V. Brucato, *Journal of Polymer Science Part B: Polymer Physics* 41 (2003) 998.
- [264] T. Schuster, K. Rode, R. Brüll, J. Heinemann, H. Haupt, *Journal of Applied Polymer Science* 130 (2013) 4182.
- [265] S. Damodaran, T. Schuster, K. Rode, A. Sanoria, R. Brüll, M. Wenzel, M. Bastian, *Polymer Degradation and Stability* 111 (2015) 7.
- [266] I. Noda, A. Dowrey, J. Haynes, C. Marcott, in *Physical Properties of Polymers Handbook*, Springer, 2007, p. 395.
- [267] A. Ginzburg, T. Macko, F. Malz, M. Schroers, I. Troetsch-Schaller, J. Strittmatter, R. Brüll, *Journal of Chromatography A* 1285 (2013) 40.
- [268] K. Prabhu, R. Brüll, T. Macko, K. Remerie, J. Tacx, P. Garg, A. Ginzburg, *Journal of Chromatography A* (2015).
- [269] T. Macko, A. Ginzburg, K. Remerie, R. Bruell, *Macromolecular Chemistry and Physics* 213 (2012) 937.
- [270] B. Monrabal, P. del Hierro, *Anal Bioanal Chem* 399 (2011) 1557.
- [271] J. Kříž, E. Adamcová, J.H. Knox, J. Hora, *Journal of Chromatography A* 663 (1994) 151.
- [272] Q.-h. Wan, P.N. Shaw, M.C. Davies, D.A. Barrett, *Journal of Chromatography A* 786 (1997) 249.
- [273] N. Tanaka, T. Tanigawa, K. Kimata, K. Hosoya, T. Arai, *Journal of Chromatography A* 549 (1991) 29.
- [274] N. Tanaka, K. Kimata, K. Hosoya, H. Miyanishi, T. Araki, *Journal of Chromatography A* 656 (1993) 265.
- [275] J.L. Gundersen, *Journal of Chromatography A* 914 (2001) 161.
- [276] L. Pereira, *Journal of Liquid Chromatography & Related Technologies* 31 (2008) 1687.
- [277] H. Colin, G. Guiochon, *Journal of Chromatography A* 126 (1976) 43.
- [278] C. Elfakir, M. Lafosse, *Journal of Chromatography A* 782 (1997) 191.

- [279] K. Gaudin, P. Chaminade, A. Baillet, *Journal of Chromatography A* 973 (2002) 69.
- [280] R. Cong, W. deGroot, A. Parrott, W. Yau, L. Hazlitt, R. Brown, M. Miller, Z. Zhou, *Macromolecules* 44 (2011) 3062.
- [281] G.C. McGonigal, R.H. Bernhardt, D.J. Thomson, *Applied Physics Letters* 57 (1990) 28.
- [282] S. Buchholz, J.P. Rabe, *Angewandte Chemie International Edition in English* 31 (1992) 189.
- [283] J.P. Rabe, S. Buchholz, L. Askadskaya, *Physica Scripta* 1993 (1993) 260.
- [284] H.E. Kern, A. Piechocki, U. Brauer, G.H. Findenegg, in G. Lagaly, F.H. Müller, A. Weiss (Editors), *Progress in Colloid & Polymer Science*, Steinkopff, 1978, p. 118.
- [285] F. Thibaudau, G. Watel, J. Cousty, *Surface Science* 281 (1993) L303.
- [286] J.A. Lavelle, A.C. Zettlemoyer, *The Journal of Physical Chemistry* 71 (1967) 414.
- [287] C. West, C. Elfakir, M. Lafosse, *Journal of Chromatography A* 1217 (2010) 3201.
- [288] A. Wawkuszewski, H.J. Cantow, S.N. Magonov, *Langmuir* 9 (1993) 2778.
- [289] T. Yang, S. Berber, J.-F. Liu, G.P. Miller, D. Tománek, *The Journal of Chemical Physics* 128 (2008) 124709.
- [290] J.S. Foster, J.E. Frommer, *Nature* 333 (1988) 542.
- [291] G.M. Florio, J.E. Klare, M.O. Pasamba, T.L. Werblowsky, M. Hyers, B.J. Berne, M.S. Hybertsen, C. Nuckolls, G.W. Flynn, *Langmuir* 22 (2006) 10003.
- [292] D.M. Cyr, B. Venkataraman, G.W. Flynn, *Chemistry of Materials* 8 (1996) 1600.
- [293] H. Taub, *NATO Advanced Study Institutes, Series C: Mathematical and Physical Sciences*, Kluwer Academic Publishers, Dordrecht, The Netherlands.
- [294] D. Mekap, F. Malz, R. Brüll, Z. Zhou, R. Cong, A.W. deGroot, A.R. Parrott, *Macromolecules* 47 (2014) 7939.
- [295] A. Jorio, M. Pimenta, A. Souza Filho, R. Saito, G. Dresselhaus, M. Dresselhaus, *New Journal of Physics* 5 (2003) 139.
- [296] R. Chitta, T. Macko, R. Brüll, G. Kalies, *Journal of Chromatography A* 1217 (2010) 7717.
- [297] T. Macko, R. Brüll, R.G. Alamo, F.J. Stadler, S. Losio, *Analytical and bioanalytical chemistry* 399 (2011) 1547.
- [298] D. Mekap, T. Macko, R. Brüll, R. Cong, A.W. deGroot, A.R. Parrott, *Industrial & Engineering Chemistry Research* 53 (2014) 15183.
- [299] N.L. Allinger, D.W. Rogers, *Molecular Structure: Understanding Steric and Electronic Effects from Molecular Mechanics*, Wiley, 2010.
- [300] J.A. Schwarz, C.I. Contescu, K. Putyera, *Dekker Encyclopedia of Nanoscience and Nanotechnology*, M. Dekker, 2004.
- [301] R.J. K. N. Prabhu, K. W. Stöckelhuber, A. Das, A. Leuteritz, G. Heinrich, B. Adhikari, in, *WO*, 2012.
- [302] T. Macko, H. Pasch, Y. Wang, *Macromolecular Symposia* 282 (2009) 93.
- [303] I. Calizo, A.A. Balandin, W. Bao, F. Miao, C.N. Lau, *Nano Letters* 7 (2007) 2645.
- [304] S.A. Arrhenius, *Z. Physik. Chem* 4 (1889) 96.

10. Copyrights and Permissions

For Figure 1:

11/22/2015

RightsLink Printable License

JOHN WILEY AND SONS LICENSE TERMS AND CONDITIONS

Nov 22, 2015

This Agreement between Prabhu Kavimani Nagar ("You") and John Wiley and Sons ("John Wiley and Sons") consists of your license details and the terms and conditions provided by John Wiley and Sons and Copyright Clearance Center.

License Number	3754181094254
License date	Nov 22, 2015
Licensed Content Publisher	John Wiley and Sons
Licensed Content Publication	Wiley eBooks
Licensed Content Title	Chromium Catalysts
Licensed Content Author	Dennis B. Malpass
Licensed Content Date	Jul 16, 2010
Pages	10
Type of use	Dissertation/Thesis
Requestor type	University/Academic
Format	Print and electronic
Portion	Figure/table
Number of figures/tables	1
Original Wiley figure/table number(s)	Figure 5.2
Will you be translating?	No
Title of your thesis / dissertation	Development of Novel Methodologies to Characterize Polyolefins using Multi-Dimensional High Temperature Two Dimensional Liquid Chromatography
Expected completion date	Feb 2016
Expected size (number of pages)	120
Requestor Location	Prabhu Kavimani Nagar schlossgartenstrasse 6 Darmstadt, Germany 64289 Attn: Prabhu Kavimani Nagar
Billing Type	Invoice
Billing Address	Prabhu Kavimani Nagar schlossgartenstrasse 6 Darmstadt, Germany 64289 Attn: Prabhu Kavimani Nagar
Total	0.00 EUR
Terms and Conditions	

TERMS AND CONDITIONS

This copyrighted material is owned by or exclusively licensed to John Wiley & Sons, Inc. or

<https://s100.copyright.com/AppPrintableLicenseFrame.jsp?publisherID=140&publisherName=Wiley&publication=oBook&publicationID=37887&rightID=1...> 1/5

For Figure 2:

11/22/2015

RightsLink Printable License

**JOHN WILEY AND SONS LICENSE
TERMS AND CONDITIONS**

Nov 22, 2015

This Agreement between Prabhu Kavimani Nagar ("You") and John Wiley and Sons ("John Wiley and Sons") consists of your license details and the terms and conditions provided by John Wiley and Sons and Copyright Clearance Center.

License Number	3754180709765
License date	Nov 22, 2015
Licensed Content Publisher	John Wiley and Sons
Licensed Content Publication	Wiley eBooks
Licensed Content Title	Ziegler-Natta Catalysts
Licensed Content Author	Dennis B. Malpass
Licensed Content Date	Jul 16, 2010
Pages	12
Type of use	Dissertation/Thesis
Requestor type	University/Academic
Format	Print and electronic
Portion	Figure/table
Number of figures/tables	2
Original Wiley figure/table number(s)	Equation 3.4, Equation 3.5
Will you be translating?	No
Title of your thesis / dissertation	Development of Novel Methodologies to Characterize Polyolefins using Multi-Dimensional High Temperature Two Dimensional Liquid Chromatography
Expected completion date	Feb 2016
Expected size (number of pages)	120
Requestor Location	Prabhu Kavimani Nagar schlossgartenstrasse 6 Darmstadt, Germany 64289 Attn: Prabhu Kavimani Nagar
Billing Type	Invoice
Billing Address	Prabhu Kavimani Nagar schlossgartenstrasse 6 Darmstadt, Germany 64289 Attn: Prabhu Kavimani Nagar
Total	0.00 EUR
Terms and Conditions	

TERMS AND CONDITIONS

This copyrighted material is owned by or exclusively licensed to John Wiley & Sons, Inc. or

<https://s100.copyright.com/AppPrintableLicenseFrame.jsp?publisherID=1408&publisherName=Wiley&publication=oBook&publicationID=37887&rightID=1...> 1/5

For Figure 3:

11/22/2015

RightsLink Printable License

**JOHN WILEY AND SONS LICENSE
TERMS AND CONDITIONS**

Nov 22, 2015

This Agreement between Prabhu Kavimani Nagar ("You") and John Wiley and Sons ("John Wiley and Sons") consists of your license details and the terms and conditions provided by John Wiley and Sons and Copyright Clearance Center.

License Number	3754180840341
License date	Nov 22, 2015
Licensed Content Publisher	John Wiley and Sons
Licensed Content Publication	Wiley eBooks
Licensed Content Title	Ziegler-Natta Catalysts
Licensed Content Author	Dennis B. Malpass
Licensed Content Date	Jul 16, 2010
Pages	12
Type of use	Dissertation/Thesis
Requestor type	University/Academic
Format	Print and electronic
Portion	Figure/table
Number of figures/tables	2
Original Wiley figure/table number(s)	Equation 3.6, Equation 3.7
Will you be translating?	No
Title of your thesis / dissertation	Development of Novel Methodologies to Characterize Polyolefins using Multi-Dimensional High Temperature Two Dimensional Liquid Chromatography
Expected completion date	Feb 2016
Expected size (number of pages)	120
Requestor Location	Prabhu Kavimani Nagar schlossgartenstrasse 6 Darmstadt, Germany 64289 Attn: Prabhu Kavimani Nagar
Billing Type	Invoice
Billing Address	Prabhu Kavimani Nagar schlossgartenstrasse 6 Darmstadt, Germany 64289 Attn: Prabhu Kavimani Nagar
Total	0.00 EUR
Terms and Conditions	

TERMS AND CONDITIONS

This copyrighted material is owned by or exclusively licensed to John Wiley & Sons, Inc. or
<https://s100.copyright.com/App/PrintableLicenseFrame.jsp?publisherID=140&publisherName=Wiley&publication=oBook&publicationID=37887&rightID=1...> 1/5

For Figure 4 and 5:

11/22/2015

RightsLink Printable License

JOHN WILEY AND SONS LICENSE TERMS AND CONDITIONS

Nov 22, 2015

This Agreement between Prabhu Kavimani Nagar ("You") and John Wiley and Sons ("John Wiley and Sons") consists of your license details and the terms and conditions provided by John Wiley and Sons and Copyright Clearance Center.

License Number	3754181175970
License date	Nov 22, 2015
Licensed Content Publisher	John Wiley and Sons
Licensed Content Publication	Wiley eBooks
Licensed Content Title	Single Site Catalysts
Licensed Content Author	Dennis B. Malpass
Licensed Content Date	Jul 16, 2010
Pages	14
Type of use	Dissertation/Thesis
Requestor type	University/Academic
Format	Print and electronic
Portion	Figure/table
Number of figures/tables	3
Original Wiley figure/table number(s)	Figure 6.1, Equation 6.5 & Equation 6.6
Will you be translating?	No
Title of your thesis / dissertation	Development of Novel Methodologies to Characterize Polyolefins using Multi-Dimensional High Temperature Two Dimensional Liquid Chromatography
Expected completion date	Feb 2016
Expected size (number of pages)	120
Requestor Location	Prabhu Kavimani Nagar schlossgartenstrasse 6 Darmstadt, Germany 64289 Attn: Prabhu Kavimani Nagar
Billing Type	Invoice
Billing Address	Prabhu Kavimani Nagar schlossgartenstrasse 6 Darmstadt, Germany 64289 Attn: Prabhu Kavimani Nagar
Total	0.00 EUR
Terms and Conditions	

TERMS AND CONDITIONS

This copyrighted material is owned by or exclusively licensed to John Wiley & Sons, Inc. or

<https://ls100.copyright.com/App/PrintableLicenseFrame.jsp?publisherID=140&publisherName=Wiley&publication=oBook&publicationID=37887&rightID=1...> 1/5

For Figure 6 and 7:

11/22/2015

RightsLink Printable License

**JOHN WILEY AND SONS LICENSE
TERMS AND CONDITIONS**

Nov 22, 2015

This Agreement between Prabhu Kavimani Nagar ("You") and John Wiley and Sons ("John Wiley and Sons") consists of your license details and the terms and conditions provided by John Wiley and Sons and Copyright Clearance Center.

License Number	3754170941265
License date	Nov 22, 2015
Licensed Content Publisher	John Wiley and Sons
Licensed Content Publication	Wiley eBooks
Licensed Content Title	Polymerization Catalysis and Mechanism
Licensed Content Author	João B. P. Soares, Timothy F. L. McKenna
Licensed Content Date	Aug 23, 2012
Pages	34
Type of use	Dissertation/Thesis
Requestor type	University/Academic
Format	Print and electronic
Portion	Figure/table
Number of figures/tables	2
Original Wiley figure/table number(s)	Figure 3.7 and Figure 3.8
Will you be translating?	No
Title of your thesis / dissertation	Development of Novel Methodologies to Characterize Polyolefins using Multi-Dimensional High Temperature Two Dimensional Liquid Chromatography
Expected completion date	Feb 2016
Expected size (number of pages)	120
Requestor Location	Prabhu Kavimani Nagar schlossgartenstrasse 6 Darmstadt, Germany 64289 Attn: Prabhu Kavimani Nagar
Billing Type	Invoice
Billing Address	Prabhu Kavimani Nagar schlossgartenstrasse 6 Darmstadt, Germany 64289 Attn: Prabhu Kavimani Nagar
Total	0.00 EUR
Terms and Conditions	

TERMS AND CONDITIONS

This copyrighted material is owned by or exclusively licensed to John Wiley & Sons, Inc. or

<https://s100.copyright.com/AppPrintableLicenseFrame.jsp?publisherID=1408&publisherName=Wiley&publication=eBook&publicationID=37887&rightID=1...> 1/5

For Figure 9:

11/22/2015

RightsLink Printable License

**JOHN WILEY AND SONS LICENSE
TERMS AND CONDITIONS**

Nov 22, 2015

This Agreement between Prabhu Kavimani Nagar ("You") and John Wiley and Sons ("John Wiley and Sons") consists of your license details and the terms and conditions provided by John Wiley and Sons and Copyright Clearance Center.

License Number	3754180333433
License date	Nov 22, 2015
Licensed Content Publisher	John Wiley and Sons
Licensed Content Publication	Wiley eBooks
Licensed Content Title	Introduction to Polymers of Ethylene
Licensed Content Author	Dennis B. Malpass
Licensed Content Date	Jul 16, 2010
Pages	22
Type of use	Dissertation/Thesis
Requestor type	University/Academic
Format	Print and electronic
Portion	Figure/table
Number of figures/tables	1
Original Wiley figure/table number(s)	Figure 1.1
Will you be translating?	No
Title of your thesis / dissertation	Development of Novel Methodologies to Characterize Polyolefins using Multi-Dimensional High Temperature Two Dimensional Liquid Chromatography
Expected completion date	Feb 2016
Expected size (number of pages)	120
Requestor Location	Prabhu Kavimani Nagar schlossgartenstrasse 6 Darmstadt, Germany 64289 Attn: Prabhu Kavimani Nagar
Billing Type	Invoice
Billing Address	Prabhu Kavimani Nagar schlossgartenstrasse 6 Darmstadt, Germany 64289 Attn: Prabhu Kavimani Nagar
Total	0.00 EUR
Terms and Conditions	

TERMS AND CONDITIONS

This copyrighted material is owned by or exclusively licensed to John Wiley & Sons, Inc. or

<https://s100.copyright.com/AppPrintableLicenseFrame.jsp?publisherID=1408&publisherName=Wiley&publication=eBook&publicationID=37887&rightID=1...> 1/5

For Figure 10:

11/20/2015

RightsLink Printable License

**JOHN WILEY AND SONS LICENSE
TERMS AND CONDITIONS**

Nov 20, 2015

This Agreement between Prabhu Kavimani Nagar ("You") and John Wiley and Sons ("John Wiley and Sons") consists of your license details and the terms and conditions provided by John Wiley and Sons and Copyright Clearance Center.

License Number	3752951280664
License date	Nov 20, 2015
Licensed Content Publisher	John Wiley and Sons
Licensed Content Publication	Wiley Books
Licensed Content Title	Introduction to Industrial Polypropylene: Properties, Catalysts Processes
Licensed Content Author	Dennis B. Malpass, Elliot Band
Licensed Content Date	Jul 1, 2012
Pages	360
Type of use	Dissertation/Thesis
Requestor type	University/Academic
Format	Print and electronic
Portion	Figure/table
Number of figures/tables	1
Original Wiley figure/table number(s)	Figure 1.1
Will you be translating?	No
Title of your thesis / dissertation	Development of Novel Methodologies to Characterize Polyolefins using Multi-Dimensional High Temperature Two Dimensional Liquid Chromatography
Expected completion date	Feb 2016
Expected size (number of pages)	120
Requestor Location	Prabhu Kavimani Nagar schlossgartenstrasse 6 Darmstadt, Germany 64289 Attn: Prabhu Kavimani Nagar
Billing Type	Invoice
Billing Address	Prabhu Kavimani Nagar schlossgartenstrasse 6 Darmstadt, Germany 64289 Attn: Prabhu Kavimani Nagar
Total	0.00 EUR
Terms and Conditions	

TERMS AND CONDITIONS

<https://s100.copyright.com/App/PrintableLicenseFrame.jsp?publisherID=140&publisherName=wiley&publication=Book&publicationID=39725&rightID=1&...> 1/5

For Figure 11:

11/22/2015

RightsLink Printable License

**JOHN WILEY AND SONS LICENSE
TERMS AND CONDITIONS**

Nov 22, 2015

This Agreement between Prabhu Kavimani Nagar ("You") and John Wiley and Sons ("John Wiley and Sons") consists of your license details and the terms and conditions provided by John Wiley and Sons and Copyright Clearance Center.

License Number	3754190571868
License date	Nov 22, 2015
Licensed Content Publisher	John Wiley and Sons
Licensed Content Publication	Angewandte Chemie International Edition
Licensed Content Title	The Ethylene Polymerization with Ziegler Catalysts: Fifty Years after the Discovery
Licensed Content Author	Ludwig L. Böhm
Licensed Content Date	Oct 22, 2003
Pages	21
Type of use	Dissertation/Thesis
Requestor type	University/Academic
Format	Print and electronic
Portion	Figure/table
Number of figures/tables	1
Original Wiley figure/table number(s)	Figure 27
Will you be translating?	No
Title of your thesis / dissertation	Development of Novel Methodologies to Characterize Polyolefins using Multi-Dimensional High Temperature Two Dimensional Liquid Chromatography
Expected completion date	Feb 2016
Expected size (number of pages)	120
Requestor Location	Prabhu Kavimani Nagar schlossgartenstrasse 6 Darmstadt, Germany 64289 Attn: Prabhu Kavimani Nagar
Billing Type	Invoice
Billing Address	Prabhu Kavimani Nagar schlossgartenstrasse 6 Darmstadt, Germany 64289 Attn: Prabhu Kavimani Nagar
Total	0.00 EUR
Terms and Conditions	

TERMS AND CONDITIONS

<https://s100.copyright.com/App/PrintableLicenseFrame.jsp?publisherID=1408&publisherName=Wiley&publication=ANIE&publicationID=31635&rightID=1&...> 1/5

For Figure 13 and 14:

11/20/2015

RightsLink Printable License

ELSEVIER ORDER DETAILS

Nov 20, 2015

This is an Agreement between Prabhu Kavimani Nagar ("You") and Elsevier ("Elsevier"). It consists of your order details, the terms and conditions provided by Elsevier ("Elsevier"), and the payment terms and conditions.

Order Number	501082652
Order Date	Nov 20, 2015
Licensed content publisher	Elsevier
Licensed content publication	Elsevier Books
Licensed content title	Functionalization of Polyolefins
Licensed content author	T.C. Mike Chung
Licensed content date	2002
Number of pages	1
Start Page	xi
End Page	xii
Type of Use	reuse in a thesis/dissertation
Intended publisher of new work	other
Portion	figures/tables/illustrations
Number of figures/tables/illustrations	3
Format	both print and electronic
Are you the author of this Elsevier chapter?	No
Will you be translating?	No
Original figure numbers	Equation 3.1, Equation 5.2 and Equation 6.1
Title of your thesis/dissertation	Development of Novel Methodologies to Characterize Polyolefins using Multi-Dimensional High Temperature Two Dimensional Liquid Chromatography
Expected completion date	Feb 2016
Estimated size (number of pages)	
Elsevier VAT number	GB 494 6272 12
Permissions price	Not Available
VAT/Local Sales Tax	Not Available
Total	Not Available

<https://s100.copyright.com/App/PrintableOrderFrame.jsp?publisherID=70&orderNumber=&publisherName=ELS&publication=Elsevier%20Books&publica...> 1/1

For Section 5.1 and 5.2

Creative Commons Legal Code

<http://creativecommons.org/licenses/by-nc-nd/2.5/legalcode>

[Creative Commons](#)



Attribution-NonCommercial-NoDerivs 2.5

CREATIVE COMMONS CORPORATION IS NOT A LAW FIRM AND DOES NOT PROVIDE LEGAL SERVICES. DISTRIBUTION OF THIS LICENSE DOES NOT CREATE AN ATTORNEY-CLIENT RELATIONSHIP. CREATIVE COMMONS PROVIDES THIS INFORMATION ON AN "AS-IS" BASIS. CREATIVE COMMONS MAKES NO WARRANTIES REGARDING THE INFORMATION PROVIDED, AND DISCLAIMS LIABILITY FOR DAMAGES RESULTING FROM ITS USE.

License

THE WORK (AS DEFINED BELOW) IS PROVIDED UNDER THE TERMS OF THIS CREATIVE COMMONS PUBLIC LICENSE ("CCPL" OR "LICENSE"). THE WORK IS PROTECTED BY COPYRIGHT AND/OR OTHER APPLICABLE LAW. ANY USE OF THE WORK OTHER THAN AS AUTHORIZED UNDER THIS LICENSE OR COPYRIGHT LAW IS PROHIBITED.

BY EXERCISING ANY RIGHTS TO THE WORK PROVIDED HERE, YOU ACCEPT AND AGREE TO BE BOUND BY THE TERMS OF THIS LICENSE. THE LICENSOR GRANTS YOU THE RIGHTS CONTAINED HERE IN CONSIDERATION OF YOUR ACCEPTANCE OF SUCH TERMS AND CONDITIONS.

1. Definitions

- a. **"Collective Work"** means a work, such as a periodical issue, anthology or encyclopedia, in which the Work in its entirety in unmodified form, along with a number of other contributions, constituting separate and independent works in themselves, are assembled into a collective whole. A work that constitutes a Collective Work will not be considered a Derivative Work (as defined below) for the purposes of this License.
- b. **"Derivative Work"** means a work based upon the Work or upon the Work and other pre-existing works, such as a translation, musical arrangement, dramatization, fictionalization, motion picture version, sound recording, art reproduction, abridgment, condensation, or any other form in which the Work may be recast, transformed, or adapted, except that a work that constitutes a Collective Work will not be considered a Derivative Work for the purpose of this License. For the avoidance of doubt, where the Work is a musical composition or sound recording, the synchronization of the Work in timed-relation with a moving image ("synching") will be considered a Derivative Work for the purpose of this License.
- c. **"Licensor"** means the individual or entity that offers the Work under the terms of this License.
- d. **"Original Author"** means the individual or entity who created the Work.
- e. **"Work"** means the copyrightable work of authorship offered under the terms of this License.
- f. **"You"** means an individual or entity exercising rights under this License who has not previously violated the terms of this License with respect to the Work, or who has received express permission from the Licensor to exercise rights under this License despite a previous violation.

2. Fair Use Rights. Nothing in this license is intended to reduce, limit, or restrict any rights arising from fair use, first sale or other limitations on the exclusive rights of the copyright owner under copyright law or other applicable laws.

3. License Grant. Subject to the terms and conditions of this License, Licensor hereby grants You a worldwide, royalty-free, non-exclusive, perpetual (for the duration of the applicable

Kavimani Nagar Prabhu
Schlossgartenstrasse 6
64289 Darmstadt

08. April 2016

Declaration

Ich erkläre hiermit, dass ich meine Dissertation selbstständig und nur mit den angegebenen Hilfsmitteln angefertigt habe.

Kavimani Nagar Prabhu

Kavimani Nagar Prabhu
Schlossgartenstrasse 6
64289 Darmstadt

08. April 2016

Declaration

Ich erkläre hiermit, noch keinen Promotionsversuch unternommen zu haben.

Kavimani Nagar Prabhu

Kavimani Nagar, Prabhu

Address: SABIC Innovative Plastics B.V.,
Plasticslaan 1, 4612 PX Bergen op Zoom, The Netherlands

Email: prabhu.kavimani.nagar@sabic.com

Phone: +31 6465 288 98

Date of Birth: 1st April, 1989

Nationality: Indian

EDUCATION

From January 2016

Scientist at SABIC

Molecular Characterization of Polyolefins
T & I, Analytical Technology
SABIC, Bergen op Zoom, The Netherlands

2012-15

Research Associate

Characterization of polyolefins using multidimensional high temperature liquid chromatographic techniques (**PhD thesis**)
Fraunhofer Institute LBF, Darmstadt, Germany

2010-12

Master of Technology (M. Tech)

Ionic liquid assisted dispersion of graphite nanoplatelets in Bromobutyl elastomer (**Master thesis**)
Indian Institute of Technology, Kharagpur (IIT KGP), India

2006-10

Bachelor of Technology (B. Tech)

Developed polyethylene-polyethylene terephthalate (PE-PET) microfibrillar composite by using a compatibilizer PE-g-maleic anhydride (**Bachelor thesis**)
Amrita University, Coimbatore, India

POSTER PRESENTATIONS

2014

“Improving resolution in high temperature gradient liquid chromatography of polyolefins” in *International conference on Polyolefin Characterization*, Valencia, Spain

2013

“Multidimensional liquid chromatography of bimodal high density polyethylene” in *International Symposium on High performance Liquid Chromatography*, Amsterdam, The Netherlands

2012

“Two dimensional liquid chromatography of LLDPE” in *Chemelot International Polyolefins Symposium*, Maastricht, The Netherlands

PATENT

Development of bromobutyl rubber nanocomposite with substantially low gas permeability property (Elastomeric materials and their use)

Europe DE102012212422 A1

World WO2014012819 A1

<https://www.google.de/patents/WO2014012819A1?cl=en>

ACHIEVEMENTS

- 2012 Department 3rd with 9.33 CGPA in M.Tech in IIT KGP
2011 DAAD scholarship holder. Selected to carry out Master thesis in Leibniz Institute for Polymer Research in Dresden, Germany
2010 Cleared Graduate Aptitude Test in Engineering with 99.8 percentile
2010 Best outgoing student and gold medallist with 8.53 CGPA, polymer engineering in B.Tech
2009 Awarded Plast India scholarship

SKILLS

TECHNICAL	<ul style="list-style-type: none">• HT-HPLC• HT-SEC• HT 2D-LC	<ul style="list-style-type: none">• TREF• CRYSTAF• TGIC	<ul style="list-style-type: none">• Polymer processing• Polymer composite• DMA• TGA• Mechanical testing• XRD• SEM• Gas permeability
SOFTWARE	<ul style="list-style-type: none">• Auto CAD• Origin• Endnote• PolymerChar Softwares• WinGPC	<ul style="list-style-type: none">• Microsoft tools• Windows• Mac OS	
LANGUAGES	English (Fluent), Tamil (mother tongue), German (basic)		
HOBBIES	Dancing, gym, swimming, yoga		

Kavimani Nagar, Prabhu